PHYSICAL REVIEW B **83**, 115132 (2011)

Projective ribbon permutation statistics: A remnant of non-Abelian braiding in higher dimensions

Michael Freedman,[1] Matthew B. Hastings,[1] Chetan Nayak,[1,2] Xiao-Liang Qi,[1,3] Kevin Walker,[1] and Zhenghan Wang[1]

[1]*Microsoft Research, Station Q, Elings Hall, University of California, Santa Barbara, California 93106, USA*

[2]*Department of Physics, University of California, Santa Barbara, California 93106, USA*

[3]*Department of Physics, Stanford University, Stanford, California 94305, USA*

(Received 10 October 2010; revised manuscript received 11 January 2011; published 23 March 2011)

In a recent paper, Teo and Kane [Phys. Rev. Lett. **104**, 046401 (2010)] proposed a three-dimensional (3D) model in which the defects support Majorana fermion zero modes. They argued that exchanging and twisting these defects would implement a set $\mathcal{R}$ of unitary transformations on the zero-mode Hilbert space which is a "ghostly" recollection of the action of the braid group on Ising anyons in two dimensions. In this paper, we find the group $\mathcal{T}_{2n}$, which governs the statistics of these defects by analyzing the topology of the space K_{2n} of configurations of $2n$ defects in a slowly spatially varying gapped free-fermion Hamiltonian: $\mathcal{T}_{2n} \equiv \pi_1(K_{2n})$. We find that the group $\mathcal{T}_{2n} = \mathbb{Z} \times \mathcal{T}^r_{2n}$, where the "ribbon permutation group" $\mathcal{T}^r_{2n}$ is a mild enhancement of the permutation group S_{2n}: $\mathcal{T}^r_{2n} \equiv \mathbb{Z}_2 \times E((\mathbb{Z}_2)^{2n} \rtimes S_{2n})$. Here, $E((\mathbb{Z}_2)^{2n} \rtimes S_{2n})$ is the "even part" of $(\mathbb{Z}_2)^{2n} \rtimes S_{2n}$, namely, those elements for which the total parity of the element in $(\mathbb{Z}_2)^{2n}$ added to the parity of the permutation is even. Surprisingly, $\mathcal{R}$ is only a projective representation of $\mathcal{T}_{2n}$, a possibility proposed by Wilczek [e-print arXiv:hep-th/9806228]. Thus, Teo and Kane's defects realize projective ribbon permutation statistics," which we show to be consistent with locality. We extend this phenomenon to other dimensions, codimensions, and symmetry classes. We note that our analysis applies to 3D networks of quantum wires supporting Majorana fermions; thus, these networks are not required to be planar. Because it is an essential input for our calculation, we review the topological classification of gapped free-fermion systems and its relation to Bott periodicity.

DOI: 10.1103/PhysRevB.83.115132 PACS number(s): 73.20.−r, 73.43.−f, 71.10.Pm

I. INTRODUCTION

In two dimensions (2D), the configuration space of n pointlike particles $\mathcal{C}^{2D}_n$ is multiply connected. Its first homotopy group, or *fundamental group*, is the n-particle braid group, $\pi_1(\mathcal{C}^{2D}_n) = \mathcal{B}_n$. The braid group $\mathcal{B}_n$ is generated by counterclockwise exchanges σ_i of the ith and $(i+1)$th particles satisfying the defining relations

$$\begin{aligned} \sigma_i\sigma_j &= \sigma_j\sigma_i \quad \text{for } |i-j| \geqslant 2, \\ \sigma_i\sigma_{i+1}\sigma_i &= \sigma_{i+1}\sigma_i\sigma_{i+1} \quad \text{for } 1 \leqslant i \leqslant n-2. \end{aligned} \tag{1}$$

This is an infinite group, even for only two particles, because $(\sigma_i)^m$ is a nontrivial element of the group for any $m > 0$. In fact, even if we consider distinguishable particles, the resulting group, called the "pure Braid group," is nontrivial. (For two particles, the pure braid group consists of all even powers of σ_1.)

In quantum mechanics, the equation $\pi_1(\mathcal{C}^{2D}_n) = \mathcal{B}_n$ opens the door to the possibility of anyons.[1,2] Higher-dimensional representations of the braid group give rise to non-Abelian anyons.[3–5] Recently there has been intense effort directed toward observing non-Abelian anyons owing, in part, to their potential use for fault-tolerant quantum computation.[6,7] One of the simplest models of non-Abelian anyons is called *Ising anyons*. They arise in theoretical models of the $\nu = 5/2$ fractional quantum Hall state[8–11] (see also Ref. 12), chiral p-wave superconductors,[13,14] a solvable model of spins on the honeycomb lattice,[15] and interfaces between superconductors and either three-dimensional (3D) topological insulators[16] or spin-polarized semiconductors with strong spin-orbit coupling.[17] A special feature of Ising anyons, which makes them relatively simple and connects them to BCS superconductivity, is that they can be understood in a free-fermion picture.

A collection of $2n$ Ising anyons has a 2^{n-1}-dimensional Hilbert space (assuming a fixed boundary condition). This can be understood in terms of $2n$ Majorana fermion operators $\gamma_i = \gamma_i^\dagger$, $i = 1,2,\ldots,n$, one associated to each Ising anyon, satisfying the anticommutation rules

$$\{\gamma_i, \gamma_j\} = 2\delta_{ij}. \tag{2}$$

The Hilbert space of $2n$ Ising anyons with a fixed boundary condition furnishes a representation of this Clifford algebra; by restricting to fixed boundary condition, we obtain a representation of products of an even number of γ matrices, which has a minimal dimension 2^{n-1}. When the ith and $(i+1)$th anyons are exchanged in a counterclockwise manner, a state of the system is transformed according to the action of

$$\rho(\sigma_i) = e^{i\pi/8} e^{-\pi\gamma_i\gamma_{i+1}/4}. \tag{3}$$

[There is a variant of Ising anyons, associated with $SU(2)_2$ Chern-Simons theory, for which the phase factor $e^{i\pi/8}$ is replaced by $e^{-i\pi/8}$. In the fractional quantum Hall effect, Ising anyons are tensored with Abelian anyons to form more complicated models with more particle species; the phase factor depends on the model.] A key property, essential for applications to quantum computing, is that *a pair* of Ising anyons forms a two-state system. The two states correspond to the two eigenvalues ± 1 of $\gamma_i\gamma_j$. No local degree of freedom can be associated with each anyon; if we insisted on doing so, we would have to say that each Ising anyon has $\sqrt{2}$ internal states. In superconducting contexts, the γ_i's are the Bogoliubov-de Gennes operators for zero-energy modes (or, simply, "zero modes") in vortex cores; the vortices themselves are Ising anyons if they possess a single such zero mode γ_i.

Although the Hilbert space is nonlocal in the sense that it cannot be decomposed into the tensor product of local Hilbert spaces associated with each anyon, the system is perfectly compatible with locality and arises in local lattice models and quantum-field theories.

In three or more dimensions, the configuration space of n pointlike particles is simply connected if the particles are distinguishable. If the particles are indistinguishable, it is multiply connected, $\pi_1(\mathcal{C}_n^{3D}) = S_n$. The generators of the permutation group satisfy the relations (1) and one more, $\sigma_i^2 = 1$. As a result of this last relation, the permutation group is finite. The one-dimensional (1D) representations of S_n correspond to bosons and fermions. One might have hoped that higher-dimensional representations of S_n would give rise to interesting 3D analogs of non-Abelian anyons. However, this is not the case, as shown in Refs. 18 and 19: Any higher-dimensional representation of S_n, which is compatible with locality, can be decomposed into the tensor product of local Hilbert spaces associated with each particle. For instance, suppose we had $2n$ spin-1/2 particles but ignored their spin values. Then we would have 2^{2n} states that would transform into each other under permutations. Clearly, if we discovered such a system, we would simply conclude that we were missing some quantum number and set about trying to measure it. This would simply lead us back to bosons and fermions with additional quantum numbers. (The color quantum number of quarks was conjectured by essentially this kind of reasoning.) The quantum information contained in these 2^{2n} states would not have any special protection.

The preceding considerations point to the following tension. The Clifford algebra (2) of Majorana fermion zero modes is not special to 2D. One could imagine a 3D (or higher) system with topological defects supporting such zero modes. But the Hilbert space of these topological defects would be 2^{n-1} dimensional, which manifestly cannot be decomposed into the tensor product of local Hilbert spaces associated with each particle, seemingly in contradiction with the results of Refs. 18 and 19 on higher-dimensional representations of the permutation group described above. However, as long as no one had a 3D or higher system in hand with topological defects supporting Majorana fermion zero modes, one could, perhaps, sweep this worry under the rug. Recently, however, Teo and Kane[20] have shown that a 3D system that is simultaneously a superconductor and a topological insulator[21–24] (which, in many but not all examples, is arranged by forming superconductor-topological insulator heterostructures) supports Majorana zero modes at pointlike topological defects.

To make matters worse, Teo and Kane[20] further showed that exchanging these defects enacts unitary operations on this 2^{n-1}-dimensional Hilbert space, which are essentially equal to (3). But we know that these unitary matrices form a representation of the braid group, which is not the relevant group in 3D. One would naively expect that the relevant group is the permutation group, but S_n has no such representation (and even if it did, its use in this context would contradict locality, according to Refs. 18 and 19 and arguments in Ref. 25). So this begs the question: What is the group $\mathcal{T}_{2n}$ for which Teo and Kane's unitary transformations form a representation?

With the answer to this question in hand, we could address questions such as the following. We know that a 3D incarnation of Ising anyons is one possible representation of $\mathcal{T}_{2n}$; is a 3D version of other anyons another representation of $\mathcal{T}_{2n}$?

Attempts to generalize the braiding of anyons to higher dimensions sometimes start with extended objects, whose configuration space may have a fundamental group that is richer than the permutation group. Obviously, if one has linelike defects in 3D that are all oriented in the same direction, then one is essentially back to the 2D situation governed by the braid group. This is too trivial, but it is not clear what kinds of extended objects in higher dimensions would be the best starting point. What is clear, however, is that Teo and Kane's topological defects must really be some sort of extended objects. This is clear from the above-noted contradiction with the permutation group. It also follows from the "order parameter" fields, which must deform as the defects are moved, as we will discuss.

In this paper, we show that Teo and Kane's defects are properly viewed as pointlike defects connected pairwise by ribbons. We call the resulting $2n$-particle configuration space K_{2n}. We compute its fundamental group $\pi_1(K_{2n})$, which we denote by $\mathcal{T}_{2n}$ and find that $\mathcal{T}_{2n} = \mathbb{Z} \times \mathcal{T}_{2n}^r$. Here, $\mathcal{T}_{2n}^r$ is the "ribbon permutation group," defined by $\mathcal{T}_{2n}^r \equiv \mathbb{Z}_2 \times E((\mathbb{Z}_2)^{2n} \rtimes S_{2n})$. The group $E((\mathbb{Z}_2)^{2n} \rtimes S_{2n})$ is a nonsplit extension of the permutation group S_{2n} by $\mathbb{Z}_2^{2n-1}$, which is defined as follows: It is the subgroup of $(\mathbb{Z}_2)^{2n} \rtimes S_{2n}$ composed of those elements for which the total parity of the element in $(\mathbb{Z}_2)^{2n}$ added to the parity of the permutation is even. The ribbon permutation group for $2n$ particles, by $\mathcal{T}_{2n}^r$, is the fundamental group of the reduced space of $2n$-particle configurations.

Our analysis relies on the topological classification of gapped free fermion Hamiltonians[26,27]—band insulators and superconductors—which is the setting in which Teo and Kane's 3D defects and their motions are defined. The starting point for this classification is reducing the problem from classifying gapped Hamiltonians defined on a lattice to classifying Dirac equations with a spatially varying mass term. One can motivate the reduction to a Dirac equation as Teo and Kane do: They start from a lattice Hamiltonian and assume that the parameters in the Hamiltonian vary smoothly in space, so that the Hamiltonian can be described as a function of both the momentum k and the position r. Near the minimum of the band gap, the Hamiltonian can be expanded in a Dirac equation, with a position-dependent mass term. In fact, Kitaev[27] has shown that the reduction to the Dirac equation with a spatially varying mass term can be derived much more generally: Gapped lattice Hamiltonians, even if the parameters in the Hamiltonian do not vary smoothly in space, are *stably equivalent* to Dirac Hamiltonians with a spatially varying mass term. Here, equivalence of two Hamiltonians means that one can be smoothly deformed into the other while preserving locality of interactions and the spectral gap, while stable equivalence means that one can add additional "trivial" degrees of freedom (additional sites that have vanishing hopping matrix elements) to the original lattice Hamiltonian to obtain a Hamiltonian that is equivalent to a lattice discretization of the Dirac Hamiltonian.

Because this classification of Dirac Hamiltonians is essential for the definition of K_{2n}, we give a self-contained review,

following Kitaev's analysis.[27] Our exposition parallels the discussion of Bott periodicity in Milnor's book.[28] The basic idea is that each additional discrete symmetry that squares to -1, which we impose on the system, is encapsulated by an antisymmetric matrix that defines a complex structure on $\mathbb{R}^N$, where $N/2$ is the number of bands (or, equivalently, N is the number of bands of Majorana fermions). For any given system, these are chosen and fixed. This leads to a progression of symmetric spaces $O(N) \to O(N)/U(N/2) \to U(N/2)/\mathrm{Sp}(N/4) \to \cdots$ as the number of such symmetries is increased. Following Kitaev,[27] we view the Hamiltonian as a final antisymmetric matrix that must be chosen (and thus put almost on the same footing as the symmetries); it is defined by a choice of an arbitrary point in the next symmetric space in the progression. The space of such Hamiltonians is topologically equivalent to that symmetric space. However, as the spatial dimension is increased, γ matrices squaring to $+1$ must be chosen in order to expand the Hamiltonian in the form of the Dirac equation in the vicinity of a minimum of the band gap. These halve the dimension of subspaces of $\mathbb{R}^N$ by separating it into their $+1$ and -1 eigenspaces and thereby lead to the opposite progression of symmetric spaces. Thus, taking into account both the symmetries of the system and the spatial dimension, we conclude that the space of gapped Hamiltonians with no symmetries in $d = 3$ is topologically equivalent to $U(N)/O(N)$. (However, by the preceding considerations, the same symmetric space also, for instance, classifies systems with time-reversal symmetry in $d = 4$.) All such Hamiltonians can be continuously deformed into each other without closing the gap, $\pi_0(U(N)/O(N)) = 0$. However, there are topologically stable pointlike defects classified by $\pi_2(U(N)/O(N)) = \mathbb{Z}_2$. These are the defects whose multidefect configuration space we study in order to see what happens when they are exchanged.

The second key ingredient in our analysis is a 1950's-vintage homotopy theory, which we use to compute $\pi_1(K_{2n})$. We apply the Pontryagin-Thom construction to show that K_{2n}, which includes not only the particle locations but also the full field configuration around the particles [i.e., the way in which the gapped free-fermion Hamiltonian of the system explores $U(N)/O(N)$], is topologically equivalent to a much simpler space, namely, pointlike defects connected pairwise by ribbons. In order to then calculate $\pi_1(K_{2n})$, we rely on the long exact sequence of homotopy groups,

$$\cdots \to \pi_i(E) \to \pi_i(B) \to \pi_{i-1}(F) \to \pi_{i-1}(E) \to \cdots, \quad (4)$$

associated to a fibration defined by $F \to E \to B$. (In an exact sequence, the kernel of each map is equal to the image of the previous map. If the exact sequence has only five terms, $1 \to A \to B \to C \to 1$, then it is called a short exact sequence. If the sequence is infinite, it is called a long exact sequence.) This exact sequence may be familiar to some readers from Mermin's review of the topological theory of defects,[29] where a symmetry associated with the group G is spontaneously broken to H, thereby leading to topological defects classified by homotopy groups $\pi_n(G/H)$. These can be computed by (4) with $E = G, F = H, B = G/H$, e.g., if $\pi_1(G) = \pi_0(G) = 0$, then $\pi_1(G/H) = \pi_0(H)$.

The ribbon permutation group is a rather weak enhancement of the permutation group and, indeed, we conclude that Teo and Kane's unitary operations are *not* a representation of the ribbon permutation group. However, they are a *projective* representation of the ribbon permutation group. In a *projective* representation, the group multiplication rule is only respected up to a phase, a possibility allowed in quantum mechanics. A representation ρ (sometimes called a linear representation) of some group G is a map from the group to the group of linear transformations of some vector space such that the group multiplication law is reproduced:

$$\rho(gh) = \rho(g) \cdot \rho(h), \quad (5)$$

if $g,h \in G$. Particle statistics arising as a projective representation of some group realizes a proposal of Wilczek's,[30] albeit for the ribbon permutation group rather than the permutation group itself. This difference allows us to sidestep a criticism of Read[25] based on locality, which Teo and Kane's projective representation respects. The group $(\mathbb{Z}_2)^{2n-1}$ is generated by $2n-1$ generators $x_1, x_2, \ldots, x_{2n-1}$, satisfying

$$\begin{aligned} x_i^2 &= 1, \\ x_i x_j &= x_j x_i. \end{aligned} \quad (6)$$

However, the projective representation of $(\mathbb{Z}_2)^{2n-1}$, which gives a subgroup of Teo and Kane's transformations, is an ordinary linear representation of a $\mathbb{Z}_2$-central extension, called the extra special group E^1_{2n-1}:

$$\begin{aligned} x_i^2 &= 1, \\ x_i x_j = x_j x_i \quad &\text{for} \quad |i-j| \geqslant 2, \\ x_i x_{i+1} &= z x_{i+1} x_i, \\ z^2 &= 1. \end{aligned} \quad (7)$$

Here, z generates the central extension, which we may take to be $z = -1$. The operations generated by the x_i's were dubbed "braidless operations" by Teo and Kane[20] because they could be enacted without moving the defects. While these operations form an Abelian subgroup of $\mathcal{T}_{2n}$, their representation on the Majorana zero-mode Hilbert space is *not* Abelian—two such operations that twist the same defect *anticommute* (e.g., x_i and x_{i+1}).

The remaining sections of this paper will be as follows. In Sec. II, we rederive Teo and Kane's zero modes and unitary transformations by simple pictorial and counting arguments in a "strong-coupling" limit of their model. In Sec. III, we review the topological classification of free-fermion Hamiltonians, including topological insulators and superconductors. From this classification, we obtain the classifying space relevant to Teo and Kane's model and, in turn, the topological classification of defects and their configuration space. In Sec. IV, we use a toy model to motivate a simple picture for the defects used by Teo and Kane and give a heuristic construction of the ribbon permutation group. In Sec. V, we give a full homotopy theory calculation. In Sec. VI, we compare the ribbon permutation group to Teo and Kane's unitary transformations and conclude that the latter form a projective, rather than a linear, representation of the former.

Finally, in Sec. VII, we review and discuss our results. Several appendixes contain technical details.

II. STRONG-COUPLING LIMIT OF THE TEO-KANE MODEL

In this section, we present a lattice model in d dimensions that has, as its continuum limit in $d = 3$, the model discussed by Teo and Kane.[20] In the limit that the mass terms in this model are large (which can be viewed as a strong-coupling limit), a simple picture of topological defects ("hedgehogs") emerges. Here, a hedgehog is simply a pointlike defect that is topologically stable. We show by a counting argument that hedgehogs possess Majorana zero modes that evolve as the hedgehogs are adiabatically moved. This adiabatic evolution is the 3D non-Abelian statistics, which it is the main purpose of this paper to explain.

The strong-coupling limit that we describe is the simplest way to derive the existence of Majorana zero modes and the unitary transformations of their Hilbert space that results from exchanging them. This section does not require the reader to be *au courant* with the topological classification of insulators and superconductors.[26,27] (In the next section, we will review that classification in order to make our exposition self-contained.)

We use a hypercubic lattice in d dimensions, with a single Majorana degree of freedom at each site. That is, for $d = 1$ we use a chain, in $d = 2$ we use a square lattice, in $d = 3$ we use a cubic lattice, and so on. We first construct a lattice model whose continuum limit is the Dirac equation with 2^d-dimensional γ matrices to reproduce the Dirac equation considered by Teo and Kane; we then show how to perturb this model to open a mass gap. We begin by considering only nearest-neighbor couplings. The Hamiltonian H is an antisymmetric Hermitian matrix. In $d = 1$, we can take the linear chain to give a lattice model with the Dirac equation as its continuum limit. That is, $H_{j,j+1} = i$ and $H_{j+1,j} = -i$. To describe this state in pictures, we draw these bonds as oriented lines, as shown in Fig. 1(a), with the orientation indicating the sign of the bond. The continuum limit of this Hamiltonian is described by a Dirac equation with 2D γ matrices. While this system can be described by a unit cell of a single site, we instead choose to describe it by a unit cell of two sites for convenience when adding mass terms later. In $d = 2$, we can take a π-flux state to obtain the Dirac equation in the continuum limit. A convenient gauge to take to describe the π-flux state is shown in Fig. 1(b), with all the vertical bonds having the same orientation, and the orientation of the horizontal bonds alternating from row to row. The continuum limit here has 4D γ matrices and we use a four-site unit cell.

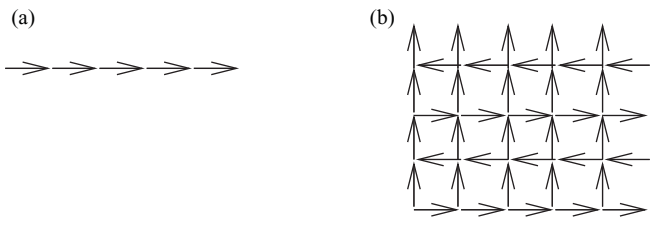

FIG. 1. (a) A lattice model giving the Dirac equation in $d = 1$. (b) A lattice model in $d = 2$.

FIG. 2. Dimerization in $d = 1$.

In general, in d dimensions, we can obtain a Dirac equation with 2^d-dimensional γ matrices by the following iterative procedure. Let the "vertical" direction refer to the direction of the dth basis vector. Having constructed the lattice Hamiltonian in $d - 1$ dimensions, we stack these Hamiltonians vertically on top of each other, with alternating signs in each layer. Then we take all the vertical bonds to be oriented in the same direction. This Hamiltonian is invariant under translation in the vertical direction by distance 2. Thus, if H_{d-1} is the Hamiltonian in $d - 1$ dimensions, the Hamiltonian H_d is given by

$$H_d = \begin{pmatrix} H_{d-1} & 2\sin(k/2)I \\ 2\sin(k/2)I & -H_{d-1} \end{pmatrix}, \tag{8}$$

where I is the identity matrix and k is the momentum in the vertical direction. Near $k = 0$, this is

$$H_d \approx H_{d-1} \otimes \sigma_z + k \otimes \sigma_x. \tag{9}$$

This iterative construction corresponds to an iterative construction of γ matrices. Having constructed $d - 1$ different 2^{d-1}-dimensional γ matrices $\gamma_1, \ldots, \gamma_{d-1}$, we construct d different 2^d-dimensional γ matrices, $\tilde{\gamma}_1, \ldots, \tilde{\gamma}_d$, by $\tilde{\gamma}_i = \gamma_i \otimes \sigma_z$ for $i = 1, \ldots, d-1$, and $\tilde{\gamma}_d = I \otimes \sigma_x$.

In 1D, dimerization of bonds corresponds to alternately strengthening and weakening the bonds as shown in Fig. 2. In 2D, we can dimerize in either the horizontal or vertical directions. In d dimensions, we have d different directions to dimerize. Dimerizing in the "vertical" direction gives, instead of (9), the result

$$H_d \approx H_{d-1} \otimes \sigma_z + k \otimes \sigma_x + m_d \otimes \sigma_y, \tag{10}$$

where m_d is the dimerization strength. This corresponds to an iterative construction of mass matrices, M_i, as follows. In 1D, we have $M_1 = i\sigma_y$. Given $d - 1$ different mass matrices in $d - 1$ dimensions, M_i, we construct $\tilde{M}_i$ in d dimensions by $\tilde{M}_i = M_i \otimes \sigma_z$, for $i = 1 \ldots d - 1$, and $\tilde{M}_d = iI \otimes \sigma_y$.

If the dimerization is nonzero, and constant, we can increase the dimerization strength without closing the gap until a strong-coupling limit is reached. In 1D, by increasing the dimerization strength, we eventually reach a fully dimerized configuration, in which each site has one nonvanishing bond connected to it. In two or more dimensions, the dimerization can be a combination of dimerization in different directions. However, if the dimerization is completely in one direction, for example the vertical direction, we increase the dimerization strength until the vertical bonds are fully dimerized. Simultaneously, we reduce the strength of the other bonds to zero without closing the gap. This is again a fully dimerized state, the columnar state, with each site having one nonvanishing bond. Any configuration with uniform, small dimerization can be deformed into this pattern without closing the gap by rotating the direction of dimerization, increasing the strength of dimerization, and then setting the bonds in the other directions to zero.

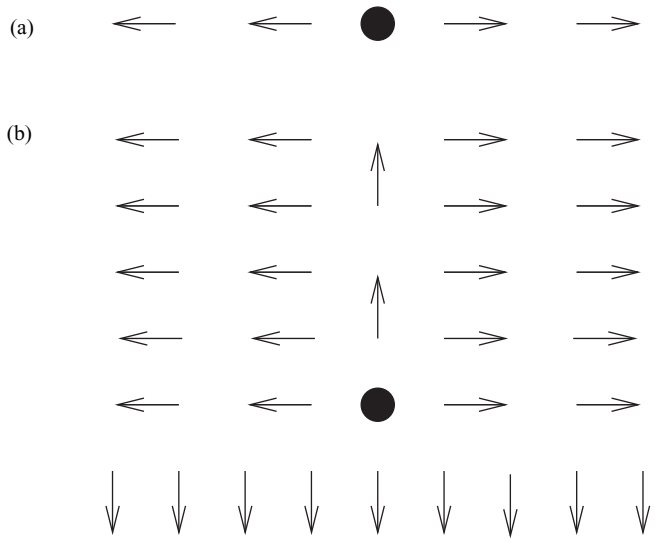

FIG. 3. (a) A 1D hedgehog. (b) A 2D hedgehog.

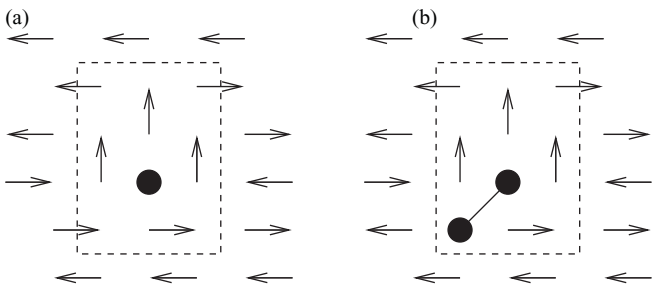

FIG. 4. (a) Defect acting as a source of $U(1)$ flux. Bonds are oriented from the A to B sublattice. There is a net flux of one leaving the region defined by the dashed line. (b) Configuration with diagonal bond added, indicated by the undirected line connecting the two circles; either orientation of this line, corresponding to different choices of the sign of the term in the Hamiltonian, would lead to the same result. There is a net of flux of 2 leaving the region defined by the dashed line.

It is important to understand that the ability to reach such a strong-coupling limits depends on the perturbation of the Dirac equation that we consider; for dimerization, it is possible to reach a strong-coupling limit, while if we had instead chosen to open a mass gap by adding, for example, diagonal bonds with imaginary coupling to the 2D Dirac equations, we would open a mass gap by perturbing the Hamiltonian with the term $i\gamma_1\gamma_2$, and such a perturbation cannot be continued to the strong-coupling limit owing to topological obstruction.

Further, if the dimerization is nonuniform then it may not be possible to reach a fully dimerized state without having defect sites. Consider the configurations in Fig. 3(a) in $d = 1$ and in Fig. 3(b) in $d = 2$. These are the strong-coupling limits of the hedgehog configuration, and each contains a zero mode, a single unpaired site. This is one of the central results of the strong-coupling limit: *Topological defects have unpaired sites that, in turn, support Majorana zero modes*.

Such strong-coupling hedgehog configurations can be constructed by the following iterative process in any dimension d. Let x_d correspond to the coordinate in the vertical direction. For $x_d \geqslant 0$, stack $(d-1)$-dimensional hedgehog configurations. Along the half-line given by $x_d > 0$ and $x_i = 0$ for $1 \leqslant i \leqslant d-1$, arrange vertical bonds, oriented to connect the site with $x_d = 2k-1$ to that with $x_d = 2k$, for $k \geqslant 1$. Along the lower half-plane, given by $x_d < 0$, arrange vertical bonds oriented to connect a site with $x_d = -(2k-1)$ to that with $-2k$, for $k \geqslant 1$. This procedure gives the $d = 2$ hedgehog in Fig. 3(b) from the $d = 1$ hedgehog in Fig. 3(a), and gives a strong-coupling limit of the Teo-Kane hedgehog in $d = 3$. That is, the Teo-Kane hedgehog can be deformed into this configuration, without closing the gap.

As long as we consider only nearest-neighbor bonds, there is an integer index ν describing different dimerization patterns in the strong-coupling limit. This index, which is present in any dimension, arises from the sublattice symmetry of the system, and is closely related to the $U(1)$ symmetry of dimer models of spin systems.[31] Label the two sublattices by A and B. Consider any set of sites, such that every site in that set has exactly one bond connected to it. (Recall that, in the strong-coupling limit, every bond has strength 0 or 1 and every site has exactly one bond connected to it, except for defect sites.) Then, the number of bonds going from A sites in this set to B sites outside the set is exactly equal to the number of bonds going from B sites in this set to A sites outside the set. On the other hand, if there are defect sites in the set, then this rule is broken. Consider the region defined by the dashed line in Fig. 4(a). We define the "flux" crossing, the dashed line, to be the number of bonds crossing that boundary, which leave starting on an A site, minus the number that leave starting on a B site. The flux is nonzero in this case, but is unchanging as we increase the size of the region. This flux is the index ν. By the argument given above for the existence of zero modes, ν computed for any region is equal to the number of Majorana zero modes contained within the region.

The index ν can be defined beyond the strong-coupling limit. Consider, for the sake of concreteness, $d = 3$. There are three possible dimerizations, one for each dimension, as we concluded in Eq. (10). In weak coupling, the square of the gap is equal to the sum of the squares of the dimerizations. Thus, if we assume a fixed gap, we can model these dimerizations by a unit vector. The integer index discussed above is simply the total winding number of this unit vector on the boundary of any region.

However, once diagonal bonds are allowed, the integer index ν no longer counts zero modes. Instead, there is a $\mathbb{Z}_2$ index, equal to $\nu(\mathrm{mod}2)$, which counts zero modes modulo 2. To see this in the strong-coupling limit, consider the configuration in Fig. 4(b). This is a configuration with $\nu = 2$ but no Majorana zero modes. However, a $\nu = 1$ configuration must still have a zero mode and, thus, any configuration with odd ν must have at least one zero mode.

In Fig. 4, we have chosen to orient the bonds from the A to B sublattice to make it easier to compute ν. However, the ν and its residue modulo 2, defined above, are independent of the orientation of the bonds (that indicate the sign of terms in the Hamiltonian) and depend only on which sites are connected by bonds (that indicate which terms in the Hamiltonian are nonvanishing).

The $\nu(\mathrm{mod}2)$ with diagonal bonds is the same as Kitaev's "Majorana number."[15] We can use this to show the existence

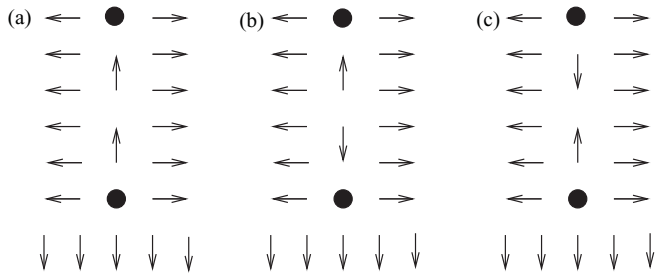

FIG. 5. (a) Pairs of defects connected by a string. (b) First rotation applied to the configuration in (a). The open circle replaces the filled circle to indicate a sign change of the Majorana mode on the site. (c) After rotating along the string. (d) Rotating the last site and restoring the string to its original configuration.

of zero modes in the Teo-Kane hedgehog even outside the strong-coupling limit. Consider a hedgehog configuration. Outside some large distance R from the center of the hedgehog, deform to the strong-coupling limit without closing the gap. Then, outside a distance R, we can count $\nu(\mathrm{mod}2)$ by counting bonds leaving the region, and we find a nonvanishing result relative to a reference configuration: If there is an even number of sites in the region then there is an odd number of bonds leaving in a hedgehog configuration, and if there is an odd number of sites then there is an even number of bonds leaving. However, because this implies a nonvanishing Majorana number, there must be a zero mode inside the region, regardless of what the Hamiltonian inside is. We note that this is a highly nontrivial result in the weak-coupling limit, where the addition of weak diagonal bonds, all oriented the same direction, to the configuration of Fig. 1(b) corresponds to adding the term $i\gamma_1\gamma_2$ to the Hamiltonian in $d = 2$. By the argument given above, even this Hamiltonian has a zero mode in the presence of a defect with nonzero $\nu(\mathrm{mod}2)$.

Given any two zero modes, corresponding to defect sites in the strong-coupling limit, we can identify a string of sites connecting them. If we have a pair of defect sites on opposite sublattices, corresponding to opposite hedgehogs, then one particular string corresponds to the north pole of the order parameter, as in Fig. 5(a). However, we can simply choose *any* arbitrary string. Let γ_i, γ_j be the Majorana operators at the two defect sites. The operation $\gamma_i \to -\gamma_i, \gamma_j \to -\gamma_j$ can be implemented as follows. We begin with an adiabatic operation on one of the defect sites and the nearest two sites on the line. The Hamiltonian on those three sites is an antisymmetric, Hermitian matrix. That is, it corresponds to an oriented plane in 3D. We can adiabatically perform orthogonal rotations of this plane. Thus, by rotating by π in the plane corresponding to the defect site and the first site on the string, we can change the sign of the mode on the defect and the orientation of the bond, as shown in Fig. 5(b). This rotation is an adiabatic transformation of the three-site Hamiltonian,

$$\begin{pmatrix} 0 & 0 & i\sin(\theta) \\ 0 & 0 & i\cos(\theta) \\ -i\sin(\theta) & -i\cos(\theta) & 0 \end{pmatrix}, \tag{11}$$

along the path $\theta = 0 \to \pi$. We then perform rotations on consecutive triples of sites along the defect line, which changes the orientation of pairs of neighboring bonds, arriving at the configuration in Fig. 5(c). Finally, we rotate by π in the plane containing the other defect site and the last site. This returns the system to the original configuration, having effected the desired operation.

Because we only consider adiabatic transformation, we can only perform orthogonal rotations with a unit determinant. Thus, any transformation that swaps two defects and returns the bonds to their original configuration must change the sign of one of the zero modes: $\gamma_i \to \gamma_j, \gamma_j \to -\gamma_i$. Indeed, any orthogonal transformation with a determinant equal to -1 would change the sign of the fermion parity in the system, as the fermion parity operator is equal to the product of the γ_i operators.

We used the ability to change the orientation of a pair of bonds in this construction. The fact that one can only change the orientation of bonds in pairs, and not the orientation of a single bond, is related to a global Z_2 invariant: The Hamiltonian is an antisymmetric matrix and the sign of its Pfaffian cannot be changed without closing the gap. Changing the direction of a single bond changes the sign of this Pfaffian and so is not possible.

The above discussion left open the question of which zero changes its sign, i.e., is the effect of the exchange $\gamma_i \to \gamma_j, \gamma_j \to -\gamma_i$ or $\gamma_i \to -\gamma_j, \gamma_j \to \gamma_i$? The answer is that it depends on how the bonds are returned to their original configuration after the exchange is completed (which is a clue that the defects must be understood as extended objects, not pointlike ones). For the bonds to be restored, one of the defects must be rotated by 2π; the corresponding zero mode acquires a minus sign. We will discuss this in greater detail in a later section. The salient point here is that the effect of an exchange is a unitary transformation generated by the operator $e^{\pm\pi\gamma_i\gamma_j/4}$. This is reminiscent of the representation of braid group generators for non-Abelian quasiparticles in the quantum Hall effect[9] and vortices in chiral p-wave superconductors,[14] namely, the braid group representation realized by Ising anyons.[7] But, of course, in 3D the braid group is not relevant, and the permutation group, which is associated with pointlike particles in $d > 2$, does not have nontrivial higher-dimensional representations consistent with locality.[18,19] As noted in the Introduction, this begs the question: What group are the unitary matrices $e^{\pm\pi\gamma_i\gamma_j/4}$ representing?

III. TOPOLOGICAL CLASSIFICATION OF GAPPED FREE-FERMION HAMILTONIANS

A. Setup of the problem

In this section, we will briefly review the topological classification of translationally invariant or slowly spatially varying free-fermion Hamiltonians following Kitaev's analysis in Ref. 27. (For a different perspective, see Schnyder *et al.*'s approach in Ref. 26.) The 3D Hamiltonian of the previous section is a specific example that fits within the general scheme and, by implication, the 3D non-Abelian statistics that we derived at the end of the previous section also holds for an entire class of models into which it can be deformed

without closing the gap. Our discussion will follow the logic of Milnor's treatment of the Bott periodicity in Ref. 28.

Consider a system of N flavors of electrons $c_j(\mathbf{k})$ in d dimensions. The flavor index j accounts for spin as well as the possibility of multiple bands. Because we will not be assuming charge conservation, it is convenient to express the complex fermion operators $c_j(\mathbf{k})$ in terms of real fermionic operators (Majorana fermions), $c_j(\mathbf{k}) = [a_{2j-1}(\mathbf{k}) + ia_{2j}(\mathbf{k})]/2$ (the index j now runs from 1 to $2N$). The momentum $\mathbf{k}$ takes values in the Brillouin zone, which has the topology of the d-dimensional torus T^d. The Hamiltonian may be written in the form

$$H = \sum_{i,j,\mathbf{p}} i A_{ij}(\mathbf{p}) a_i(\mathbf{p}) a_j(-\mathbf{p}), \tag{12}$$

where, by Fermi statistics, $A_{ij}(\mathbf{p}) = -A_{ji}(-\mathbf{p})$. Let us suppose that the Hamiltonian (12) has an energy gap 2Δ, by which we mean that its eigenvalues $E_\alpha(p)$ (α is an index labeling the eigenvalues of H) satisfy $|E_\alpha(p)| \geqslant \Delta$. The basic question that we address in this section is the following: What topological obstructions prevent us from continuously deforming one such gapped Hamiltonian into another?

Such an analysis can apply, as we will see, not only to free-fermion Hamiltonians, but also to those interacting fermion Hamiltonians that, deep within ordered phases, are well approximated by free-fermion Hamiltonians. (This can include rather nontrivial phases such as Ising anyons, but not Fibonacci anyons.) In such settings, the fermions may be emergent fermionic quasiparticles; if the interactions between these quasiparticles are irrelevant in the renormalization-group sense, then an analysis of free-fermion Hamiltonians can shed light on the phase diagrams of such systems. Thus, the analysis of free-fermion Hamiltonians is equivalent to the analysis of *interacting fermion ground states* whose low-energy quasiparticle excitations are free fermions.

Let us begin by considering a few concrete examples, in order of increasing complexity.

B. Zero-dimensional systems

First, we analyze a zero-dimensional (0D) system that we will not assume to have any special symmetry. The Hamiltonian (12) takes the simpler form

$$H = \sum_{i,j} i A_{ij} a_i a_j, \tag{13}$$

where A_{ij} is a $2N \times 2N$ antisymmetric matrix, $A_{ij} = -A_{ji}$. Any real antisymmetric matrix can be written in the form

$$A = O^T \begin{pmatrix} 0 & -\lambda_1 & & & \\ \lambda_1 & 0 & & & \\ & & 0 & -\lambda_2 & \\ & & \lambda_2 & 0 & \\ & & & & \ddots \end{pmatrix} O, \tag{14}$$

where O is an orthogonal matrix and the λ_i's are positive. The eigenvalues of A come in pairs $\pm i\lambda_i$; thus, the *absence of charge conservation* can also be viewed as the *presence of a particle-hole symmetry*. By assumption, $\lambda_i \geqslant \Delta$ for all i. Clearly, we can continuously deform A_{ij} without closing the gap so that $\lambda_i = \Delta$ for all i. (This is usually called "spectrum flattening.") Then, we can write

$$A = \Delta \cdot O^T J O, \tag{15}$$

where

$$J = \begin{pmatrix} 0 & -1 & & & \\ 1 & 0 & & & \\ & & 0 & -1 & \\ & & 1 & 0 & \\ & & & & \ddots \end{pmatrix}. \tag{16}$$

The possible choices of A_{ij} correspond to the possible choices of $O \in O(2N)$, modulo O, which commute with the matrix J. But the set of $O \in O(2N)$ satisfying $O^T J O = J$ is $U(N) \subset O(2N)$. Thus, the space of all possible 0D free-fermionic Hamiltonians with N single-particle energy levels is topologically equivalent to the symmetric space $O(2N)/U(N)$.

This can be restated in more geometrical terms as follows. Let us here and henceforth take units in which $\Delta = 1$. Then the eigenvalues of A are $\pm i$. If we view the $2N \times 2N$ matrix A as a linear transformation on $\mathbb{R}^{2N}$, then it defines a complex structure. Consequently, we can view $\mathbb{R}^{2N}$ as $\mathbb{C}^N$ because multiplication of $\vec{v} \in \mathbb{R}^{2N}$ by a complex scalar can be defined as $(a + ib)\vec{v} \equiv a\vec{v} + bA\vec{v}$. The set of complex structures on $\mathbb{R}^{2N}$ is given by performing an arbitrary $O(2N)$ rotation on a fixed complex structure, modulo the rotations of $\mathbb{C}^N$ that respect the complex structure, namely, $U(N)$. Thus, once again, we conclude that the desired space of Hamiltonians is topologically equivalent to $O(2N)/U(N)$.

What are the consequences of this equivalence? Consider the simplest case, $N = 1$. Then the space of 0D Hamiltonians is topologically equivalent to $O(2)/U(1) = \mathbb{Z}_2$: There are two classes of Hamiltonians, those in which the single fermionic level is unoccupied in the ground state, $c^\dagger c = (1 + ia_1a_2)/2 = 0$, and those in which it is occupied. For larger N, $O(2N)/U(N)$ is a more complicated space, but it still has two connected components, $\pi_0(O(2N)/U(N)) = \mathbb{Z}_2$, so that there are two classes of free-fermion Hamiltonians, corresponding to even or odd numbers of occupied fermionic levels in the ground state.

Suppose now that we restrict ourselves to time-reversal-invariant systems and, furthermore, to those time-reversal-invariant systems that satisfy $T^2 = -1$, where T is the antiunitary operator generating time reversal. Then, following Ref. 27, we write $T a_i T^{-1} = (J_1)_{ij} a_j$. The matrix J_1 is antisymmetric and satisfies $J_1^2 = -1$. T invariance of the Hamiltonian requires

$$J_1 A = -A J_1. \tag{17}$$

Because J_1 is antisymmetric and satisfies $J_1^2 = -1$, its eigenvalues are $\pm i$. Therefore, J_1 defines a complex structure on $\mathbb{R}^{2N}$ that may, consequently, be viewed as $\mathbb{C}^N$. Now consider A, which is also antisymmetric and satisfies $A^2 = -1$, in addition to anticommuting with J_1. It defines a quaternionic structure on $\mathbb{C}^N$ that may, consequently, be viewed as $\mathbb{H}^{N/2}$. Multiplication of $\vec{v} \in \mathbb{R}^{2N}$ by a quaternion can be defined

as $(a+bi+cj+dk)\vec{v} \equiv a\vec{v} + bJ_1\vec{v} + cA\vec{v} + dJ_1A\vec{v}$. The possible choices of A can be obtained from a fixed one by performing rotations of $\mathbb{C}^N$, modulo those rotations that respect the quaternionic structure, namely, $\mathrm{Sp}(N/2)$. Thus, the set of time-reversal-invariant 0D free-fermionic Hamiltonians with $T^2 = -1$ is topologically equivalent to $U(N)/\mathrm{Sp}(N/2)$. Because $\pi_0(U(N)/\mathrm{Sp}(N/2)) = 0$, any such Hamiltonian can be continuously deformed into any other. This can be understood as a result of Kramers doubling: There must be an even number of fermions in the ground state so the division into two classes of the previous case does not exist here.

C. 2D systems: *T*-breaking superconductors

Now, let us consider systems in more than 0D. Once again, we will assume that charge is not conserved, and we will also assume that time-reversal symmetry is not preserved. For the sake of concreteness, let us consider a single band of spin-polarized electrons on a 2D lattice. Let us suppose that the electrons condense into a (fully spin-polarized) p_x-wave superconductor. For a fixed superconducting order parameter, the low-energy theory is a free-fermion Hamiltonian for gapless fermionic excitations at the nodal points $\pm\vec{k}_F \equiv (0, \pm p_F)$. We now ask the question, what other order parameters could develop that would fully gap the fermions? For fixed values of these order parameters, we have a free-fermion Hamiltonian. Thus, these different possible order parameters correspond to different possible gapped free-fermion Hamiltonians.

The low-energy Hamiltonian of a fully spin-polarized p_x-wave superconductor can be written in the form

$$H = \psi^\dagger(i v_\Delta \partial_x \tau_x + i v_F \partial_y \tau_z)\psi, \tag{18}$$

where v_F, v_Δ are, respectively, the Fermi velocity and slope of the gap near the node. The Pauli matrices τ act in the particle-hole space:

$$\psi(k) \equiv \begin{pmatrix} c_{\vec{k}_F+\vec{k}} \\ c^\dagger_{-\vec{k}_F+\vec{k}} \end{pmatrix}. \tag{19}$$

This Hamiltonian is invariant under the $U(1)$: $\psi \to e^{i\theta}\psi$, which corresponds to conservation of momentum in the p_y direction (not to charge conservation). Because we will be considering perturbations that do not respect this symmetry, it is convenient to introduce Majorana fermions χ_1, χ_2 according to $\psi = \chi_1 + i\chi_2$. Then

$$H = i\chi_a(v_\Delta \partial_x \tau_x + v_F \partial_y \tau_z)\chi_a, \tag{20}$$

with $a = 1,2$. Note that we have suppressed the particle-hole index on which the Pauli matrices τ act. Because χ_1, χ_2 are each a two-component real spinor, this model has four real Majorana fields.

We now consider the possible mass terms that we could add to make this Hamiltonian fully gapped:

$$H = i\chi_a(v_\Delta \partial_x \tau_x + v_F \partial_y \tau_z)\chi_a + i\chi_a M_{ab}\chi_b. \tag{21}$$

If we consider the possible order parameters that could develop in this system, it is clear that there are only two choices: an imaginary superconducting order parameter ip_y (which breaks time-reversal symmetry) and charge-density-wave order (CDW). These take the form

$$M^{ip_y}_{ab} = \Delta_{ip_y} i\tau^y \delta_{ab} \tag{22}$$

and

$$M^{\mathrm{CDW}}_{ab} = \rho_{2k_F}\tau^y\left(\cos\theta\,\mu^z_{ab} + \sin\theta\,\mu^x_{ab}\right), \tag{23}$$

where $\mu^{x,z}$ are Pauli matrices and θ is an arbitrary angle. For an analysis of the possible mass terms in the more complex situation of graphenelike systems, see, for instance, Ref. 32.

Let us consider the space of mass terms with a fixed energy gap Δ, which is the same for all four of the Majorana fermions in the model (i.e., a flattened mass spectrum). An arbitrary gapped Hamiltonian can be continuously deformed to one that satisfies this condition. Then we can have $\Delta_{ip_y} = \pm\Delta$, $\rho_{2k_F} = 0$ or $\rho_{2k_F} = \Delta$, $\Delta_{ip_y} = 0$ (in the latter case, arbitrary θ is allowed). If both order parameters are present, then the energy gap is not the same for all fermions. It is not that there is anything wrong with such a Hamiltonian—indeed, one can imagine a system developing both kinds of order. Rather, it is that such a Hamiltonian can be continuously deformed to one with either $\Delta_{ip_y} = 0$ or $\rho_{2k_F} = 0$ without closing the gap. For instance, if $\Delta_{ip_y} > \rho_{2k_F}$, then the Hamiltonian can be continuously deformed to one with $\rho_{2k_F} = 0$. (However, if we try to deform it to a Hamiltonian with $\Delta_{ip_y} = 0$, the gap will close at $\Delta_{ip_y} = \rho_{2k_F}$.) Hence, we conclude that the space of possible mass terms is topologically equivalent to the disjoint union $U(1) \cup \mathbb{Z}_2$: a single one-parameter family and two disjoint points.

Because $\pi_0(U(1) \cup \mathbb{Z}_2) = \mathbb{Z}_3$, there are three distinct classes of quadratic Hamiltonians for four flavors of Majorana fermions in 2D. The one-parameter family of CDW-ordered Hamiltonians counts as a single class because they can be continuously deformed into each other. The parameter θ is the phase of the CDW, which determines whether the density is maximum at the sites, the midpoints of the bonds, or somewhere in between. It is important to keep in mind, however, that, although there is no topological obstruction to continuously deforming one θ into another, there may be an energetic penalty that makes it costly. For instance, the coupling of the system to the lattice may prefer some particular value of θ. The classification discussed here accounts only for topological obstructions; the possibility of energetic barriers must be analyzed by different methods.

We can restate the preceding analysis in the following, more abstract language. This formulation will make it clear that we have not overlooked a possible mass term and will generalize to more complicated free-fermion models. Let us write $\gamma_1 = \tau_x\delta_{ab}$, $\gamma_2 = \tau_z\delta_{ab}$. Then

$$\{\gamma_i, \gamma_j\} = 2\delta_{ij}. \tag{24}$$

The Dirac Hamiltonian for $N = 4$ Majorana fermion fields takes the form

$$H = i\chi(\gamma_i\partial_i + M)\chi. \tag{25}$$

The matrix M plays the role that the matrix A did in the 0D case. As in that case, we assume a flattened spectrum that here means that each Majorana fermion field has the same gap and that this gap is equal to 1. (It does *not* mean that the energy is

independent of the momentum **k**.) In order to satisfy this, we must require that

$$\{\gamma_i, M\} = 0 \quad \text{and} \quad M^2 = -1. \tag{26}$$

Note that it is customary to write the Dirac Hamiltonian in a slightly different form,

$$H = \overline{\psi}(i\gamma_i \partial_i + m)\psi, \tag{27}$$

which can be massaged into the form of (25) using $\overline{\psi} = \psi^\dagger \gamma_0$:

$$\begin{aligned} H &= \psi^\dagger (i\gamma_0\gamma_i \partial_i + m\gamma_0)\psi \\ &= \psi^\dagger (i\alpha_i \partial_i + m\beta)\psi \\ &= i\psi^\dagger (\alpha_i \partial_i - im\beta)\psi, \end{aligned} \tag{28}$$

where $\alpha_i = \gamma_0\gamma_i$ and $\beta = \gamma_0$. Thus, if we write $\gamma_i \equiv \alpha_i$ and $M \equiv -im\beta$ and consider Majorana fermions (or decompose Dirac fermions into Majoranas), we recover (25). We have used the form (25) so that it is analogous to (13), with $(\gamma_i \partial_i + M)$ replacing A_{ij} and the i pulled out front. Then, the matrix M determines the gaps of the various modes in the same way as A does in the 0D case. Similarly, assuming a "flattened" spectrum leads to the condition $M^2 = -1$.

How many ways can we choose such an M? Because $\gamma_2^2 = 1$, its eigenvalues are ± 1. Hence, viewed as a linear map from $\mathbb{R}^4$ to itself, this matrix divides $\mathbb{R}^4$ into two 2D subspaces $\mathbb{R}^4 = X_+ \oplus X_-$ with eigenvalue ± 1 under γ_2, respectively. For $\gamma_2 = \tau_z \delta_{ab}$, this is trivial:

$$X_+ = \text{span}\left\{ \begin{pmatrix} 1 \\ 0 \end{pmatrix} \otimes \begin{pmatrix} 1 \\ 0 \end{pmatrix}, \begin{pmatrix} 1 \\ 0 \end{pmatrix} \otimes \begin{pmatrix} 0 \\ 1 \end{pmatrix} \right\}, \tag{29}$$

where τ_z acts on the first spinor and the second spinor is indexed by $a = 1,2$, i.e., is acted on by the Pauli matrices $\mu^{x,z}$ in (23). This construction generalizes straightforwardly to arbitrary numbers N of Majorana fermions, which is why we use it now.

Now $\gamma_1 M$ commutes with γ_2 and satisfies $(\gamma_1 M)^2 = 1$. Thus, it maps X_+ to itself and defines subspaces X_+^1, X_+^2 with eigenvalue ± 1 under $\gamma_1 M$ (and equivalently for X_-). X_+ can decomposed into $X_+^1 \oplus X_+^2 = X_+$. Choosing M is thus equivalent to choosing a linear subspace X_+^1 of X_+.

This can be divided into three cases. If $\gamma_1 M$ has one positive eigenvalue and one negative one when acting on X_+ then the space of possible choices of $\gamma_1 M$ is equal to the space of 1D linear subspaces of $\mathbb{R}^2$, which is simply $U(1)$. If, on the other hand, $\gamma_1 M$ has two positive eigenvalues, then there is a unique choice, which is simply $M = \gamma_1\gamma_2$. If $\gamma_1 M$ has two negative eigenvalues, then there is again a unique choice, $M = -\gamma_1\gamma_2$. Therefore, the space of possible M's is topologically equivalent to $U(1) \cup \mathbb{Z}_2$.

Now, suppose that we have $2N$ Majorana fermions. Then γ_2 defines N-dimensional eigenspaces X_+, X_- such that $\mathbb{R}^{2N} = X_+ \oplus X_-$ and $\gamma_1 M$ defines eigenspaces of X_+: $X_+^1 \oplus X_+^2 = X_+$. If $\gamma_1 M$ has k positive eigenvalues and $N - k$ negative ones, then the space of possible choices of $\gamma_1 M$ is $O(N)/O(k) \times O(N-k)$, i.e., we can take the restriction of $\gamma_1 M$ to X_+ to be of the form

$$\gamma_1 M = O^T \begin{pmatrix} 1 & & & & & \\ & \ddots & & & & \\ & & 1 & & & \\ & & & -1 & & \\ & & & & \ddots & \\ & & & & & -1 \end{pmatrix} O, \tag{30}$$

with k diagonal entries equal to $+1$ and $N - k$ entries equal to -1. Thus, the space of Hamiltonians for N flavors of free Majorana fermions is topologically equivalent to

$$\mathcal{M}_{2N} = \bigcup_{k=0}^{N} O(N)/[O(k) \times O(N-k)]. \tag{31}$$

However, because $\pi_0(O(N)/[O(k) \times O(N-k)]) = 0$, independent of k (note that 0 is the group with a single element, not the empty set $\emptyset$), $\pi_0(\mathcal{M}_{2N}) = \mathbb{Z}_{N+1}$.

In the model analyzed above, we had only a single spin-polarized band of electrons. By increasing the number of bands and allowing both spins, we can increase the number of flavors of Majorana fermions. In principle, the number of bands in a solid is infinity. Usually, we can introduce a cutoff and restrict attention to a few bands near the Fermi energy. However, for a purely topological classification, we can ignore energetics and consider all bands on equal footing. Then we can take $N \to \infty$, so that $\pi_0(\mathcal{M}_\infty) = \mathbb{Z}$. This classification permits us to deform Hamiltonians into each other as long as there is no topological obstruction, with no regard to how energetically costly the deformation may be. Thus, the $2N = 4$ classification that we discussed above can perhaps be viewed as a "hybrid" classification, which looks for topological obstructions in a class of models with a fixed set of bands close to the Fermi energy.

But even this point of view is not really natural. The discussion above took as its starting point an expansion about a p_x superconductor; the p_x superconducting order parameter was assumed to be large and fixed while the ip_y and CDW order parameters were assumed to be small. In other words, we assumed that the system was at a point in parameter space at which the gap, though nonzero, was small at two points in the Brillouin zone (the intersection points of the nodal line in the p_x superconducting order parameter with the Fermi surface). This allowed us to expand the Hamiltonian about these points in the Brillouin zone and write it in Dirac form. And this may, indeed, be reasonable in a system in which p_x superconducting order is strong (i.e., highly energetically favored) and other orders are weak. However, a topological classification should allow us to take the system into regimes in which p_x superconductivity is small and other orders are large. Suppose, for instance, that we took our model of spin-polarized electrons (which we assume, for simplicity, to be at half-filling on the square lattice) and went into a regime in which there was a large $d_{x^2-y^2}$ density-wave (or "staggered flux") order parameter[33] $\langle c^\dagger_{\mathbf{k}+\mathbf{Q}} c_{\mathbf{k}} \rangle = i\Phi(\cos k_x a - \cos k_y a)$, where a is the lattice constant and Φ is the magnitude of the order parameter. With nearest-neighbor hopping only, the energy spectrum is $E_{\mathbf{k}}^2 = (2t)^2(\cos k_x a + \cos k_y a)^2 + \Phi^2(\cos k_x a - \cos k_y a)^2$.

Thus, the gap vanishes at four points, $(\pm\pi/2, \pm\pi/2)$ and $(\mp\pi/2, \pm\pi/2)$. The Hamiltonian can be linearized in the vicinity of these points:

$$H = \psi_1^\dagger (i v_\Delta \partial_x \tau_x + i v_F \partial_y \tau_z)\psi_1 + \psi_2^\dagger (i v_\Delta \partial_y \tau_x + i v_F \partial_x \tau_z)\psi_2, \quad (32)$$

where v_F, v_Δ are, respectively, the Fermi velocity and slope of the gap near the nodes; the subscripts 1,2 refer to the two sets of nodes $(\pm\pi/2, \pm\pi/2)$ and $(\mp\pi/2, \pm\pi/2)$; and ψ_A, $A = 1,2$ are defined by

$$\psi_{1,2}(k) \equiv \begin{pmatrix} c_{(\pi/2,\pm\pi/2)+\vec{k}} \\ c_{(-\pi/2,\mp\pi/2)+\vec{k}} \end{pmatrix}. \quad (33)$$

If we introduce Majorana fermions $\psi_A = \chi_{A1} + i\chi_{A2}$, then we can write this Hamiltonian with possible mass terms as

$$H = i\chi_{1a}(v_\Delta \partial_x \tau_x + v_F \partial_y \tau_z)\chi_{1a} + i\chi_{2a}(v_\Delta \partial_y \tau_x + v_F \partial_x \tau_z)\chi_{2a} + i\chi_{Aa} M_{Aa,Bb}\chi_{Bb}. \quad (34)$$

We have suppressed the spinor indices (e.g., χ_{11} is a two-component spinor); with these indices included, $M_{Aa,Bb}$ is an 8×8 matrix. However, in order for the gap to be the same for all flavors, the mass matrix must anticommute with $\tau_{x,z}$. Thus, $M_{Aa,Bb} = \tau_y \tilde{M}_{Aa,Bb}$. The matrix $\tilde{M}_{Aa,Bb}$ can have 0,1,2,3, or 4 eigenvalues equal to $+1$ (with the rest being -1). The spaces of such mass terms are, respectively, 0, $O(4)/[O(1) \times O(3)]$, $O(4)/[O(2) \times O(2)]$, $O(4)/[O(3) \times O(1)]$, and 0. Mass terms with 0 or 4 eigenvalues equal to $+1$ correspond physically to $\pm id_{xy}$ density-wave order, $\langle c^\dagger_{\mathbf{k}+\mathbf{Q}} c_{\mathbf{k}}\rangle = \pm \sin k_x a \sin k_y a$. Mass terms with 2 eigenvalues equal to $+1$ correspond physically to superconductivity, to $Q' = (\pi,0)$ CDW order, and to linear combinations of the two. Mass terms with 1 or 3 eigenvalues equal to $+1$ correspond to (physically unlikely) hybrid orders with, for instance, superconductivity at $(\pm\pi/2, \pm\pi/2)$ and $\pm id_{xy}$ density-wave order at $(\pm\pi/2, \mp\pi/2)$. Clearly, this is the $2N = 8$ case of the general classification discussed above. Thus, the same underlying physical degrees of freedom—a single band of spin-polarized electrons on a square lattice—can correspond to either $2N = 4$ or $2N = 8$, depending on where the system is in parameter space. One can imagine regions of parameter space where the gap is small at an arbitrary number N of points. Thus, if we restrict ourselves to systems with a single band, then different regions of the parameter space (with different numbers of points at which the gap is small) will have very different topologies. Although such a classification may be a necessary evil in some contexts, it is far preferable, given the choice, to allow topology to work unfettered by energetics. Then we can consider a large number n of bands. Suppose that the gap becomes small at r points in the Brillouin zone in each band. Then, the low-energy Hamiltonian takes the Dirac form for $2N = 2rn$ Majorana fermion fields. As we will see below, if N is sufficiently large, the topology of the space of possible mass terms will be independent of N. Consequently, for n sufficiently large, the topology of the space of possible mass terms will be independent of r. In other words, we are in the good situation in which the topology of the space of Hamiltonians will be the same in the vicinity of any gap closing. But any gapped Hamiltonian can be continuously deformed so that the gap becomes small at some points in the Brillouin zone. Thus, the problem of classifying gapped free-fermion Hamiltonians in d dimensions is equivalent to the problem of classifying possible mass terms in a generic d-dimensional Dirac Hamiltonian as long as the number of bands is sufficiently large.[27] This statement can be made more precise and put on more solid mathematical footing by using ideas that we discuss in Appendix B.

D. Classification of topological defects

The topological classification described above holds not only for classes of translationally invariant Hamiltonians such as (25), but also for topological defects within a class. Suppose, for instance, that we consider (25) with a mass that varies slowly as the origin is encircled at a great distance. We can ask whether such a Hamiltonian can be continuously deformed into a uniform one. In a system in which the mass term is understood as arising as a result of some kind of underlying ordering such as superconductivity or CDW order, we are simply talking about topological defects in an ordered media, but with the caveat that the order parameter is allowed to explore a very large space that may include many physically distinct or unnatural orders, subject only to the condition that the gap does not close.

Let us, for the sake of concreteness, assume that we have a mass term with $N/2$ positive eigenvalues when restricted to the $+1$ eigenspace of γ_2. [For N large, the answer obviously cannot depend on the number of positive eigenvalues k so long as k scales with N. Thus, we will denote the space $\mathcal{M}_{2N}$ defined in Eq. (31) by $\mathbb{Z} \times O(N)/[O(N/2) \times O(N/2)]$, where the integers in $\mathbb{Z}$ correspond to the number of positive eigenvalues of the mass term when restricted to the $+1$ eigenspace of γ_2.] Then $M(r = \infty,\theta)$ defines a loop in $O(N)/[O(N/2) \times O(N/2)]$ that cannot be continuously unwound if it corresponds to a nontrivial element of $\pi_1(O(N)/[O(N/2) \times O(N/2)])$.

To compute $\pi_1(O(N)/[O(N/2) \times O(N/2)])$, we parametrize $O(N)/[O(N/2) \times O(N/2)]$ by symmetric matrices K that satisfy $K^2 = 1$ and $\mathrm{tr}(K) = 0$. [Such matrices decompose $\mathbb{R}^N$ into their $+1$ and -1 eigenspaces: $\mathbb{R}^N = V_+ \oplus V_-$. K can be written in the form $K = O^T K_0 O$, where K_0 has $N/2$ diagonal entries equal to $+1$ and $N/2$ equal to -1, i.e., $K_0 = \mathrm{diag}(1, \ldots, 1, -1, \ldots, -1)$.] Note that any such K is itself an orthogonal matrix, i.e., an element of $O(N)$; thus $O(N)/[O(N/2) \times O(N/2)]$ can be viewed as a submanifold of $O(N)$ in a canonical way. Consider a curve $L(\lambda)$ in $O(N)/[O(N/2) \times O(N/2)]$ with $L(0) = K$ and $L(\pi) = -K$. We will parametrize it as $L(\lambda) = Ke^{\lambda A}$, where A is in the Lie algebra of $O(N)$. In order for this loop to remain in $O(N)/[O(N/2) \times O(N/2)]$, we need $(Ke^{\lambda A})^2 = 1$. Because $(Ke^{\lambda A})^2 = Ke^{\lambda A}Ke^{i\lambda A} = e^{i\lambda KAK}e^{\lambda A}$, this condition implies that $KA = -AK$. In order to have $L(\pi) = -K$, we need $A^2 = -1$. Such a curve is, in fact, a minimal geodesic from K to $-K$. Each such geodesic can be represented by its midpoint $L(\pi/2) = KA$, so the space of such geodesics is equivalent to the space of matrices A satisfying $A^2 = -1$ and $KA = -AK$. As discussed in Ref. 28, the space of minimal geodesics is a good enough approximation to the entire space

of loops (essentially because an arbitrary loop can be deformed to a geodesic) that we can compute π_1 from the space of minimal geodesics just as well as from the space of loops. Thus, the loop space of $O(N/2)/[O(k)\times O(N/2-k)]$ is homotopically equivalent to the space of matrices A satisfying $A^2=-1$ and $KA=-AK$. Because it anticommutes with K, KA maps the $+1$ eigenspace of K to the -1 eigenspace. It is clearly a length-preserving map because $(KA)^2=1$ and, because the ±1 eigenspaces of K are isomorphic to $\mathbb{R}^{N/2}$, KA defines an element of $O(N/2)$. Thus a loop in $O(N)/[O(N/2)\times O(N/2)]$ corresponds to an element of $O(N/2)$ or, in other words,

$$\pi_1(O(N)/[O(N/2)\times O(N/2)])=\pi_0(O(N/2)). \quad (35)$$

The latter group is simply $\mathbb{Z}_2$ because $O(N/2)$ has two connected components: (1) pure rotations and (2) rotations combined with a reflection.

It might come as a surprise that we find a $\mathbb{Z}_2$ classification for pointlike defects in 2D. Indeed, if we require that the superconducting order parameter has a fixed amplitude at infinity, then the vortices of an arbitrary winding number are stable and we have a $\mathbb{Z}$ classification. However, in the classification discussed here, we require a weaker condition be satisfied: that the fermionic gap remain constant. Consequently, a vortex configuration of an even winding number can be unwound without closing the free-fermion gap by, for instance, "rotating" superconductivity into CDW order.

E. 3D systems with no symmetry

With these examples under our belts, we now turn to the case that is of primary interest in this paper: free-fermion systems in 3D without time-reversal or charge-conservation symmetry. We consider the Dirac Hamiltonian in 3D for an $2N$-component Majorana fermion field χ:

$$H=i\chi\left(\partial_1\gamma_1+\partial_2\gamma_2+\partial_3\gamma_3\right)\chi+i\chi M\chi. \quad (36)$$

In the previous section, we discussed a lattice model that realizes (36) in its continuum limit with $2N=8$. Different mass terms correspond to different quadratic perturbations of this model that open a gap (which can be viewed as order parameters that we are turning on at the mean-field level). We could classify such terms by considering, from a physical perspective, all such ways of opening a gap. However, we will instead determine the topology of the space of mass terms (and, thereby, the space of gapped free-fermion Hamiltonians) by the same mathematical methods by which we analyzed the 2D case.

Because $\gamma_1^2=1$ and has a vanishing trace, this matrix decomposes $\mathbb{R}^{2N}$ into its ±1 eigenspaces: $\mathbb{R}^{2N}=X_+\oplus X_-$. Now $(\gamma_2\gamma_3)^2=-1$ and $[\gamma_1,\gamma_2\gamma_3]=0$. Therefore, $\gamma_2\gamma_3$ is a complex structure on X_+ (and also on X_-), i.e., we can define multiplication of vectors $\vec{v}\in X_+$ by complex scalars according to $(a+bi)\vec{v}\equiv a\vec{v}+\gamma_2\gamma_3\vec{v}$. (Consequently, we can view X_+ as $\mathbb{C}^{N/2}$.) Now, consider a possible mass term M, with $M^2=-1$. $(\gamma_2M)^2=1$, and $[\gamma_1,\gamma_2M]=0$. Let Y be the subspace of X_+ with eigenvalue $+1$ under γ_2M. Because $\{\gamma_2M,\gamma_2\gamma_3\}=0$, $\gamma_2\gamma_3Y$ is the subspace of X_+ with eigenvalue -1 under γ_2M. In other words, $X_+=Y\oplus\gamma_2\gamma_3Y$, i.e., Y is a real subspace of X_+. Hence, the space of choices of M is the space of real subspaces $Y\subset X_+$ (or, equivalently, of real subspaces $\mathbb{R}^{N/2}\subset\mathbb{C}^{N/2}$). Given any fixed real subspace $Y\subset X_+$, we can obtain all others by performing $U(N/2)$ rotations of X_+, but two such rotations give the same real subspace if they differ only by an $O(N/2)$ rotation of Y. Thus, the space of gapped Hamiltonians for $2N$ free Majorana fermion fields in 3D with no symmetry is topologically equivalent to $U(N/2)/O(N/2)$. In the remaining sections of this paper, we will be discussing topological defects in such systems and their motions. Our focus will be on hedgehogs, which are pointlike defects of such systems; by the preceding analysis, they are classified by $\pi_2(U(N/2)/O(N/2))$.

F. General classification and Bott periodicity

Before doing so, we pause to consider the classification in other dimensions and in the presence of symmetries such as time-reversal and charge conservation. We have seen that systems with no symmetry in $d=0,2,3$ are classified by the spaces $O(2N)/U(N)$, $\mathbb{Z}\times\frac{O(N)}{O(N/2)\times O(N/2)}$, and $U(N/2)/O(N/2)$. By similar methods, it can be shown that the $d=1$ case is classified by $O(N)$. As we have seen, increasing the spatial dimension increases the number of γ matrices by 1. The problem of choosing $\gamma_1,\ldots,\gamma_d$ satisfying $\{\gamma_i,\gamma_j\}=2\delta_{ij}$ and M, which anticommutes with the γ_i's and squares to -1 leads us to subspaces of $\mathbb{R}^{2N}$ of increasingly smaller dimension, isometries between these spaces, or complex of quaternionic structures on these spaces. This leads the progression of spaces in the top row of Table I.

At the same time, we have seen that a time-reversal-invariant system in $d=0$ is classified by $U(N)/\mathrm{Sp}(N/2)$. Suppose that we add a discrete antiunitary symmetry $SiS^{-1}=-i$ defined by

$$Sa_iS^{-1}=(J)_{ij}a_j, \quad (37)$$

which squares to $J^2=-1$. It must anticommute with the mass term

$$\{J,M\}=0 \quad (38)$$

in order to ensure invariance under the symmetry, so choosing a J amounts to adding a complex structure, which leads to the *opposite* progression of classifying spaces. Consider, as an example of the preceding statements, a time-reversal invariant system in $d=3$. Then time-reversal symmetry T is an example of a symmetry generator J discussed in the previous paragraph. We define a real subspace $Y\subset X_+$, in a similar manner as above, but now as the subspace of X_+ with eigenvalue $+1$ under γ_2T, rather than under γ_2M. Once again, $X_+=Y\oplus\gamma_2\gamma_3Y$. Now, $\{\gamma_3M,\gamma_2T\}=0$, and $(\gamma_3M)^2=1$, so the $+1$ eigenspace of γ_3M is a linear subspace of Y. The set of all such linear subspaces is $\mathbb{Z}\times\frac{O(N/2)}{O(N/4)\times O(N/4)}$. But this is the same classifying space as for a system with no symmetry in $d=2$ (apart from a reduction of N by a factor of 2). Thus, we are led to the list of classifying spaces for gapped free-fermion Hamiltonians in Table I. After the present paper was submitted to the arXiv, Bott periodicity was discussed from a similar perspective by M. Stone *et al.*[34]

In Table I, Q refers to charge-conservation symmetry. Charge conservation is owing to the invariance of the Hamiltonian of a system under the $U(1)$ symmetry $c_i\to e^{i\theta}c_i$.

TABLE I. The period-8 (in both dimension and number of symmetries) table of classifying spaces for free-fermion Hamiltonians for N complex $= 2N$ real (Majorana) fermion fields in dimensions $d = 0,1,2,3,\ldots$ with no symmetries; time-reversal symmetry (T) only; time-reversal and charge-conservation symmetries (T and Q); time-reversal, charge-conservation, and sublattice symmetries (T, Q, and χ); and the latter two cases with $SU(2)$ symmetry. As a result of the period-8 nature of the table, the top two rows could equally well be the bottom two rows of the table. Moving p steps to the right and p steps down leads to the same classifying space (but for $1/2^p$ as many fermion fields), which is a reflection of Bott periodicity, as explained in the text. The number of disconnected components of any such classifying space—i.e., the number of different phases in that symmetry class and dimension—is given by the corresponding π_0, which may be found in Eq. (40). Higher homotopy groups, which classify defects, can be computed using Eq. (39). Table III, given in Appendix A, is the analogous table for charge-conserving Hamiltonians without time-reversal symmetry.

Dimension:	0	1	2	3	4	...
SU(2), T, Q	$\mathbb{Z} \times \frac{O(N)}{O(N/2)\times O(N/2)}$	$U(N/2)/O(N/2)$	$\mathrm{Sp}(N/4)/U(N/4)$	$\mathrm{Sp}(N/8)$	$\mathbb{Z} \times \frac{\mathrm{Sp}(N/8)}{\mathrm{Sp}(N/16)\times \mathrm{Sp}(N/16)}$	...
SU(2), T, Q, χ	$O(N/4)$	$\mathbb{Z} \times \frac{O(N/4)}{O(N/8)\times O(N/8)}$	$U(N/8)/O(N/8)$	$\mathrm{Sp}(N/16)/U(N/16)$	$\mathrm{Sp}(N/32)$	...
No symmetry	$O(2N)/U(N)$	$O(N)$	$\mathbb{Z} \times \frac{O(N)}{O(N/2)\times O(N/2)}$	$U(N/2)/O(N/2)$	$\mathrm{Sp}(N/4)/U(N/4)$	...
T only	$U(N)/\mathrm{Sp}(N/2)$	$O(N)/U(N/2)$	$O(N/2)$	$\mathbb{Z} \times \frac{O(N/2)}{O(N/4)\times O(N/4)}$	...	
T and Q	$\mathbb{Z} \times \frac{\mathrm{Sp}(N/2)}{\mathrm{Sp}(N/4)\times \mathrm{Sp}(N/4)}$	$U(N/2)/\mathrm{Sp}(N/4)$	$O(N/2)/U(N/4)$	$O(N/4)$		
T, Q, χ	$\mathrm{Sp}(N/4)$	$\mathbb{Z} \times \frac{\mathrm{Sp}(N/4)}{\mathrm{Sp}(N/8)\times \mathrm{Sp}(N/8)}$	$U(N/4)/\mathrm{Sp}(N/8)$	$O(N/4)/U(N/8)$		
	⋮				⋱	

In terms of Majorana fermions a_i defined according to $c_j = (a_{2j-1} + ia_{2j})/2$, the symmetry takes the form $a_{2j-1} \to \cos\theta a_{2j-1} + \sin\theta a_{2j}$, $a_{2j} \to -\sin\theta a_{2j-1} + \cos\theta a_{2j}$. However, if a free=fermion Hamiltonian is invariant under the discrete symmetry $c_i \to ic_i$ or, equivalently, $a_{2j-1} \to a_{2j}$, $a_{2j} \to -a_{2j-1}$, then it is automatically invariant under the full $U(1)$ as well, and conserves charge.[27] Thus, we can treat charge conservation as a discrete symmetry Q that is unitary, squares to -1, and commutes with the Hamiltonian (i.e., with the γ matrices and M). Because Q transforms $c_i \to ic_i$, it anticommutes with T. Note further that if a system has time-reversal symmetry, then the product of time reversal T and charge conservation Q is a discrete antiunitary symmetry, QT, which anticommutes with the Hamiltonian and with T and squares to -1. Then QT is defined by a choice of matrix J, analogous to T, as in Eq. (37). If the system is not time-reversal invariant, then charge conservation is a unitary symmetry. It is easier then to work with complex fermions, and the classification of such systems falls into an entirely different sequence, as discussed in Appendix A.

If a system is both time-reversal symmetric and charge conserving, i.e., if it is a time-reversal-invariant insulator, then it may have an additional symmetry that guarantees that the eigenvalues of the Hamiltonian come in $\pm E$ pairs, just as in a superconductor. An example of such a symmetry is the sublattice symmetry of Hamiltonians on a bipartite lattice in which fermions can hop directly from the A sublattice to the B sublattice but cannot hop directly between sites on the same sublattice. In such a case, the system is invariant under a unitary symmetry χ defined as follows. If we block diagonalize χ so that one block acts on sites in the A sublattice and the other on sites in the B sublattice, then we can write $\chi = \mathrm{diag}(k, -k)$, i.e., $a_i(\mathbf{x}) \to -k_{ij}a_j(\mathbf{x})$ for $\mathbf{x} \in A$ and $a_i(\mathbf{x}) \to k_{ij}a_j(\mathbf{x})$ for $\mathbf{x} \in B$. This symmetry transforms the Hamiltonian to minus itself if $k^2 = 1$ or, in other words, if $\chi^2 = 1$. Then χQ is a unitary symmetry that squares to -1 and anticommutes with the Hamiltonian, T, and QT. Hence χQ, too, is defined by a choice of matrix J, as in Eq. (37). We will call such a symmetry a sublattice symmetry χ and a system satisfying this symmetry a "bipartite" system, but the symmetry may have a different microscopic origin.

In an electron system, time reversal ordinarily squares to -1, because the transformation law is $c_\uparrow \to c_\downarrow$, $c_\downarrow \to -c_\uparrow$, as we have thus far assumed in taking $J^2 = -1$. However, it is possible to have a system of fully spin-polarized electrons that has an antiunitary symmetry T that squares to $+1$. (One might object to calling this symmetry time reversal because it does not reverse the electron spins, but T is a natural label because it is a symmetry that is just as good for the present purposes.) Then, because $J^2 = 1$, a choice of J is similar to a choice of a γ matrix. In general, symmetries (37) that square to $+1$ have the same effect on the topology of the space of free-fermion Hamiltonians as adding dimensions because each such J defines a subspace of half the dimension within the eigenspaces of the γ matrices. This is true for systems with $T^2 = 1$.

SU(2) spin-rotation-invariant and time-reversal-invariant insulators (systems with T and Q) effectively fall in this category. The Hamiltonian for such a system can be written in the form $H = h \otimes I_2$, where the second factor is the 2×2 identity matrix acting on the spin index. Then time reversal can be written in the form $T = t \otimes i\sigma_y$, where $t^2 = 1$, and Q can be written in the form $Q = q \otimes I_2$, so that $QT = qt \otimes i\sigma_y$, where $(qt)^2 = 1$. Thus, because the matrix $i\sigma_y$ squares to -1, the symmetries T and QT have effectively become symmetries that square to $+1$. They now move the system through the progression of classifying spaces in the same direction as increasing the dimension, i.e., in the opposite direction to symmetries that square to -1. Thus, SU(2) spin-rotation-invariant and time-reversal-invariant insulators in d dimensions are classified by the same space as systems with no symmetry in $d + 2$ dimensions. However, in a system

that, in addition, has sublattice symmetry $\chi = x \otimes I_2$, we have $(qx)^2 = -1$. Thus, sublattice symmetry is still a symmetry that squares to -1. Because the two symmetries that square to $+1$ (T and QT) have the same effect as increasing the dimension while the symmetry that squares to -1 has the same effect as decreasing the dimension, SU(2) spin-rotation-invariant and time-reversal-invariant insulators with a sublattice symmetry in d dimensions are classified by the same space as systems with no symmetry in $d+1$ dimensions (but with N replaced by $N/4$). Similar considerations apply to superconductors with SU(2) spin-rotational symmetry.

In order to discuss topological defects in the systems discussed here, it is useful to return to the arguments that led to (35). By showing that the space of loops in $O(N/2)/[O(N/4) \times O(N/4)$ is well approximated by $O(N/4)$, we not only showed that $\pi_1(O(N/2)/[O(N/4) \times O(N/4)]) = \pi_0(O(N/4))$ but, in fact, that $\pi_k(O(N/2)/[O(N/4) \times O(N/4)]) = \pi_{k-1}(O(N/4))$ (see Ref. 28). Continuing in the same way, we can approximate the loop space of $O(N/4)$ [i.e., the space of loops in $O(N/4)$] by minimal geodesics from $\mathbb{I}$ to $-\mathbb{I}$: $L'(\lambda) = e^{\lambda A_1}$, where $A_1^2 = -1$. The midpoint of such a geodesic, $L'(\pi/2) = A_1$, again defines a complex structure $A_1 = O^T J O$, where J is given by (16) so that $\pi_k(O(N/4)) = \pi_{k-1}(O(N/4)/U(N/8))$. In a similar way, minimal geodesics in $O(N/4)/U(N/8)$ from A_1 to $-A_1$ can be parametrized by their midpoints A_2, which square to -1 and anticommute with A_1, thereby defining a quaternionic structure, so that the loop space of $O(N/4)/U(N/8)$ is equivalent to $U(N/8)/\mathrm{Sp}(N/8)$ and hence $\pi_k(O(N/4)/U(N/8)) = \pi_{k-1}(U(N/8)/\mathrm{Sp}(N/8))$. Thus, we see that *the passage from one of the classifying spaces to its loop space is the same as the imposition of a symmetry such as time reversal to a system classified by that space*: Both involve the choice of successive anticommuting complex structures. Continuing in this fashion (see Ref. 28), we recover *Bott periodicity*:

$$\begin{aligned}
\pi_k(O(16N)) &= \pi_{k-1}(O(16N)/U(8N)) \\
&= \pi_{k-2}(U(8N)/\mathrm{Sp}(4N)) \\
&= \pi_{k-3}(\mathbb{Z} \times \mathrm{Sp}(4N)/[\mathrm{Sp}(2N) \times \mathrm{Sp}(2N)]) \\
&= \pi_{k-4}(\mathrm{Sp}(2N)) \\
&= \pi_{k-5}(\mathrm{Sp}(2N)/U(2N)) \\
&= \pi_{k-6}(U(2N)/O(2N)) \\
&= \pi_{k-7}(\mathbb{Z} \times O(2N)/[O(N) \times O(N)]) \\
&= \pi_{k-8}(O(N)). \qquad (39)
\end{aligned}$$

The approximations made at each step require that N be in the *stable limit*, in which the desired homotopy groups are independent of N. For instance, $\pi_k(O(N))$ is independent of N for $N > k/2$.

It is straightforward to compute π_0 for each of these groups:

$$\begin{gathered}
\pi_0(O(N)) = \mathbb{Z}_2, \\
\pi_0(O(2N)/U(N)) = \mathbb{Z}_2, \\
\pi_0(U(2N)/\mathrm{Sp}(N)) = 0, \\
\pi_0(\mathbb{Z} \times \mathrm{Sp}(2N)/\mathrm{Sp}(N) \times \mathrm{Sp}(N)) = \mathbb{Z}, \\
\pi_0(\mathrm{Sp}(N)) = 0, \qquad (40) \\
\pi_0(\mathrm{Sp}(N)/U(N)) = 0, \\
\pi_0(U(N)/O(N)) = 0, \\
\pi_0(\mathbb{Z} \times O(2N)/[O(N) \times O(N)]) = \mathbb{Z}.
\end{gathered}$$

Combining (40) with (39), we can compute any of the stable homotopy groups of the above eight classifying spaces. As discussed above, the space of gapped free-fermion Hamiltonians in d dimensions in a given *symmetry class* (determined by the number modulo 8 of symmetries squaring to -1 minus the number of those squaring to $+1$) is homotopically equivalent to one of these classifying spaces. Thus, using (40) with (39) to compute the stable homotopy groups of these classifying spaces leads to a complete classification of topological states and topological defects in all dimensions and symmetry classes, as we now discuss.

Gapped Hamiltonians with a given symmetry and dimension are classified by π_0 of the corresponding classifying space in Table I. Owing to Bott periodicity, the table is periodic along both directions of dimension and symmetry, so that there are eight distinct symmetry classes. Ryu *et al.*[26] denoted these classes using the Cartan classification of symmetric spaces, following the corresponding classification of disordered systems and random matrix theory,[35,36] which was applied to the (potentially gapless) surface states of these systems. In this notation, systems with no symmetry are in class D, those with T only are in DIII, and those with T and Q are in AII. The other five symmetry classes, C, CI, CII, AI, and BDI, arise in systems that have spin-rotational symmetry or a sublattice symmetry. There are actually two more symmetry classes (denoted by A and AIII in the random matrix theory) that lie on a separate 2×2 periodic table, which is less relevant to the present work and will be discussed in Appendix A. In Table II we have listed examples of topologically nontrivial states in physical dimensions 1,2,3 in all eight symmetry classes. To help with the physical understanding of these symmetry classes, we have also listed the physical requirements for the realization of each symmetry class. In each dimension, there are two symmetry classes in which the topological states are classified by integer invariants and two symmetry classes in which the different states are distinguished by $\mathbb{Z}_2$ invariants. In all the cases in which a real material or a well-defined physical model system is known with nontrivial $\mathbb{Z}$ or $\mathbb{Z}_2$ invariant, we have listed a typical example in the table. In some of the symmetry classes, nontrivial examples have not been realized yet, in which case we leave the topological classification $\mathbb{Z}$ or $\mathbb{Z}_2$ in the corresponding position in the table.

In 1D, generic superconductors (class D) are classified by Z_2, of which the nonrivial example is a p-wave superconductor with a single Majorana zero mode on the edge. The time-reversal-invariant superconductors (class DIII) are also classified by Z_2. The nontrivial example is a superconductor in which spin-up electrons pair into a p-wave superconductor and spin-down electrons form another p-wave superconductor that is exactly the time reversal of the spin-up one. Such a superconductor has two Majorana zero modes on the edge that form a Kramers pair and are topologically protected. The two integer classes are bipartite time-reversal-invariant insulators with (CII) and without (BDI) spin-orbit coupling. An example of the BDI class is a graphene ribbon, or equivalently a

TABLE II. Topological periodic table in physical dimensions 1,2,3. The first column contains eight of the ten symmetry classes in the Cartan notation adopted by Schnyder *et al.* (Ref. 26), following Zirnbauer (Refs. 35 and 36). The second column contains the requirements for physical systems which can realize the corresponding symmetry classes. "w/o" stands for "without." SC stands for superconductivity, TRI for time-reversal invariant, and SOC for spin-orbit coupling. The three columns $d = 1,2,3$ list topological states in the spatial dimensions 1,2,3, respectively. 0 means the topological classification is trivial. The labels Z and Z_2 stand for topological states classified by these groups but for which states corresponding to nontrivial elements of $\mathbb{Z}$ or $\mathbb{Z}_2$ have not been realized in realistic materials. The asterisked text stands for topological states for which a well-defined physical model has been proposed but convincing experimental candidate has not been found yet. (See text for more discussions on the realistic materials.)

Symmetry classes	Physical realizations	$d = 1$	$d = 2$	$d = 3$
D	SC	p-wave SC*	$(p + ip)$-SC*	0
DIII	TRI SC	Z_2	$(p + ip)(p - ip)$-SC*	He^3-B
AII	TRI ins.	0	HgTe quantum well	$Bi_{1-x}Sb_x$, Bi_2Se_3, etc.
CII	Bipartite TRI ins.	Carbon nanotube	0	Z_2
C	Singlet SC	0	$(d + id)$-SC*	0
CI	Singlet TRI SC	0	0	Z
AI	TRI ins. w/o SOC	0	0	0
BDI	Bipartite TRI ins. w/o SOC	Carbon nanotube	0	0

carbon nanotube with a zigzag edge.[37,38] The low-energy band structure of graphene and carbon nanotubes is well described by a tight-binding model with nearest-neighbor hopping on a honeycomb lattice, which is bipartite. The integer-valued topological quantum number corresponds to the number of zero modes on the edge, which depends on the orientation of the nanotube. Because carbon has negligible spin-orbit coupling, to a good approximation it can be viewed as a system in the BDI class, but it can also be considered as a system in class CII when spin-orbit coupling is taken into account. In 2D, generic superconductors (class D) are classified by an integer, corresponding to the number of chiral Majorana edge states on the edge. The first nontrivial example was the $p + ip$ wave superconductor, shown by Read and Green[13] to have one chiral Majorana edge state. Nontrivial superconductors in symmetry class D are examples of *topological superconductors*. Some topological superconductors can be consistent with spin-rotation symmetry; singlet superconductors (class C) are also classified by integer, with the simplest physical example a $d + id$ wave superconductor. Similar to the 1D case, the time-reversal-invariant superconductors (class DIII) are classified by Z_2, of which the nontrivial example is a superconductor with $p + ip$ pairing of spin-up electrons and $p - ip$ pairing of spin-down electrons.[26,39,40] The other symmetry class in 2D with a Z_2 classification is composed of time-reversal-invariant insulators (class AII), also known as quantum spin Hall insulators.[41–43] The quantum spin Hall insulator phase has been theoretically predicted[44] and experimentally realized[45] in HgTe quantum wells. In 3D, time-reversal-invariant insulators (class AII) are also classified by Z_2.[21–23] The Z_2 topological invariant corresponds to a topological magnetoelectric response with quantized coefficient $\theta = 0,\pi$.[24] Several nontrivial topological insulators in this class have been theoretically predicted and experimentally realized, including the $Bi_{1-x}Sb_x$ alloy[46,47] and the family of Bi_2Se_3, and Bi_2Te_3, Sb_2Te_3.[48–50] In 3D, time-reversal-invariant superconductors (class DIII) are classified by an integer, corresponding to the number of massless Majorana cones on the surface.[26] A nontrivial example with topological quantum number $N = 1$ turns out to be the B phase of He^3.[26,40,51] The other classes with nontrivial topological classification in 3D are singlet time-reversal-invariant superconductors (CI), classified by an integer, and bipartite time-reversal-invariant insulators (CII), classified by Z_2. Some models have been proposed[52] but no realistic material proposal or experimental realization has been found in these two classes. We would like to note that different physical systems can correspond to the same symmetry class. For example, bipartite superconductors are also classified by the BDI class.

The two remaining symmetry classes [unitary (A) and chiral unitary (AIII)] correspond to systems with charge-conservation symmetry but without time-reversal symmetry, which forms a separate 2×2 periodic table. For the sake of completeness, we carry out the preceding analysis for these two classes in Appendix A.

Topological defects in these states are classified by higher homotopy groups of the classifying spaces. Following the convention of Ref. 27, we name the classifying spaces by $R_q, q = 0,1,2,\ldots,7$, with $R_1 = O(N), R_2 = O(2N)/U(N), \ldots R_7 = U(N)/O(N), R_0 = \mathbb{Z} \times O(2N)/[O(N) \times O(N)]$ in the order of Eq. (40). The symmetries in Table II can be labeled by $p = 0,1,2,\ldots,7$, so that in d dimensions and pth symmetry class, the classifying space is R_{2+p-d}. A topological defect with dimension D ($D < d$) is classified by

$$\pi_{d-D-1}(R_{2+p-d}) = \pi_0(R_{p-D+1}), \tag{41}$$

which is determined by the zeroth homotopy groups in Eq. (40). The important conclusion we obtain from this formula is that the classification of the topological defect is determined by the dimension of the defect D and the symmetry class p, and is *independent* of the spatial dimension d. For p and D, we obtain the same 8×8 periodic table for the classification of topological defects. After the present paper was submitted to the arXiv, this classification scheme for topological defects was independently discussed by Teo and Kane,[53] who also discuss gapless modes at such defects.

In the following we will focus on the 3D system with no symmetry, and discuss the generic cases in Sec. VII. Because a 3D system with no symmetry is classified by

$R_7 = U(N)/O(N)$, pointlike defects in such a system are classified by $\pi_2(U(N)/O(N))$. In the stable limit, $\pi_2(U(N)/O(N)) = \mathbb{Z}_2$. However, we note that, for smaller values of N below the stable limit, the classification is a little different, e.g., $\pi_2(U(2)/O(2)) = \pi_2(U(1) \times S^2) = \mathbb{Z}$. The "eight-band model" in Ref. 20, which we discussed in the strong-coupling limit in the previous section, is an example of this particular "small N" case, which is why the hedgehogs in that model are classified by a winding number $\in \mathbb{Z}$. [In fact, the term hedgehog normally refers to pointlike defects of a field taking values in S^2, which is, therefore, classified by $\pi_2(S^2) = \mathbb{Z}$, i.e., essentially the "eight-band model" of Ref. 20 and the lattice model of Sec. II. In this paper, we use this term more loosely to include pointlike defects classified by $\pi_2(U(N/2)/O(N/2))$ for generic large N.]

IV. EXCHANGING PARTICLES CONNECTED BY RIBBONS IN 3D

In this section, we will take an O(3) nonlinear σ model, i.e., one with target space S^2, as a toy model for our problem. It is essentially the eight-band model discussed in Ref. 20 and in the strong-coupling limit in Sec. II. As noted above, it is the $2N = 8$ limit of the classification reviewed above. It will be more familiar to most readers and easier to visualize than the full problem, which we discuss in the next section. We will give a heuristic explanation of π_1 of the configurations of defects, and will make a few comments about where our toy model goes wrong, compared to the full problem. In the next section, we will undertake a full and careful calculation of π_1 of the configurations of defects of a model with classifying space $U(N)/O(N)$.

A free-fermion Hamitonian with no symmetry, but limited to eight bands, can be expanded about its minimum energy point in the Brillouin zone as

$$H = i\chi(\partial_i \gamma_i + n_i \Gamma_i)\chi. \tag{42}$$

From the considerations in the previous section, we learned that the space of mass terms is S^2, which is why we have written the mass term in the above form with a unit vector $\vec{n} \in S^2$. [More precisely, the space of mass terms is $U(2)/O(2) = U(1) \times S^2$, and the mass term can be written $e^{\theta\gamma_1\gamma_2\gamma_3} n_i \Gamma_i e^{-\theta\gamma_1\gamma_2\gamma_3}$. However, the extra $U(1)$ plays no role here and can be ignored.] In the model of Sec. II, the three components of $\vec{n}$ correspond to dimerization in each of the three directions on the cubic lattice. In Teo and Kane's model they correspond to the real and imaginary parts of the superconducting order parameter and the sign of the Dirac mass at a band inversion.

Now consider pointlike defects in the $\vec{n}$ field, which are classified by $\pi_2(S^2) = \mathbb{Z}$. Defects with winding number ± 1 are positive and negative hedgehogs. For simplicity, we will focus on these; higher winding number hedgehods can be built up from these. (In the real model, as opposed to the toy model, the hedgehogs have a $\mathbb{Z}_2$ classification so there are no higher winding number hedgehogs and, in fact, they do not even have a sign.) As noted by Teo and Kane,[20] the $\vec{n}$ field around a hedgehog can be visualized in a simplified way, following Wilczek and Zee's discussion of the Hopf term in a $(2+1)$-D O(3) nonlinear σ model.[54] The field $\vec{n}$ can be viewed as a map

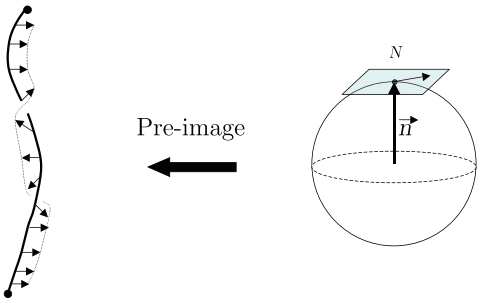

FIG. 6. The preimage of the north pole in the S^2 target space of $\vec{n}$ is a collection of arcs connecting hedgehogs. A fixed tangent vector at the north pole defines a vector field along the arcs, thereby making them framed arcs, which may be viewed as ribbons.

from the physical space where the electrons live, $\mathbb{R}^3$. If we assume that the total winding number is zero (equal numbers of $+$ and $-$ hedgehogs) and that $\vec{n}$ approaches a constant at ∞, we can compactify the physical space $\mathbb{R}^3$ so that it is S^3. The target space of the map is S^2. The preimage of the north pole $N \in S^2$ is a set of arcs and loops. The choice of the north pole N is arbitrary, and any other point on the sphere would be just as good for the following discussion. Let us ignore the loops for the moment and focus on the arcs. Because $\vec{n}$ points in every direction at a hedgehog, the arcs terminate at hedgehogs. In fact, each arc connects a $+1$ hedgehog to a -1 hedgehog. We now pick an arbitrary unit vector in the tangent space of the sphere at N. This vector can be pulled back to S^3 to define a vector field along the arcs, which is clearly normal to the arcs. This is a *framing*, which allows us to define, for instance, a self-winding number for an arc. Intuitively, we can think of a framing as a thickening of an arc into a ribbon. Thus, the field $\vec{n}$ allows us to define a set of framed arcs connecting the hedgehogs—in other words, a set of ribbons connecting the hedgehogs. As the normal vector twists around an arc, the ribbon twists, as shown in Fig. 6. (Although we will draw the ribbons as bands in the physical space, their width should not be taken seriously; they should really be viewed as arcs with a normal vector field.)

Although these ribbons are strongly reminiscent of particle trajectories, it is important to keep in mind that they are not. A collection of ribbons connecting hedgehogs defines a state of the system at an instant of time. Ribbons, unlike particle trajectories, can cross. They can break and reconnect as the system evolves in time. As hedgehogs are moved, the ribbons move with them.

A configuration of particles connected pairwise by ribbons is a seemingly crude approximation to the full texture defined by $\vec{n}$. However, according to the Pontryagin-Thom construction, as we describe in the next section (and explain in Appendix F), it is just as good as the full texture for topological purposes. Thus, we focus on the space of particles connected pairwise by ribbons.

We now consider a collection of such particles and ribbons. For a topological discussion, all that we are interested in about the ribbons is how many times they twist, so we will not draw the framing vector but will, instead, be careful to put kinks into the arcs in order to keep track of twists in the ribbon, as depicted in Fig. 7. The fundamental group of their

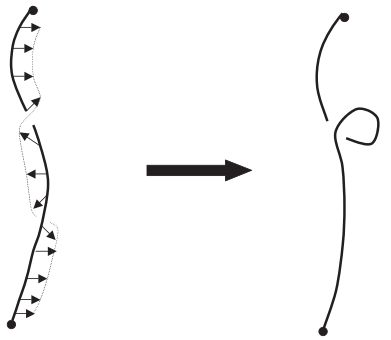

FIG. 7. We will depict framed arcs or ribbons as arcs with twists accounted for by drawing kinks in the arcs, as shown above.

configuration space is the set of transformations that returns the particles and ribbons to their initial configurations, with two such transformations identified if they can be continuously deformed into each other. Consider an exchange of two $+1$ hedgehogs, as depicted in Fig. 8. Although this brings the particles back to their initial positions (up to a permutation, which is equivalent to their initial configuration because the particles are identical), it does not bring the ribbons back to their initial configuration. Therefore, we need to do a further motion of the ribbons. By cutting and rejoining them as shown in Fig. 9(a), a procedure which we call "recoupling," we now have the ribbons connecting the same particles as in the initial configuration. But the ribbon on the left-hand side has a twist in it. So we rotate that particle by -2π in order to undo the twist, as in Fig. 9(b).

Let us use t_i to denote such a transformation, defined by the sequence in Figs. 8, 9(a), and 9(b). The t_i's do not satisfy the multiplication rules of the permutation group. In particular, $t_i \neq t_i^{-1}$. The two transformations t_i and t_i^{-1} are not distinguished by whether the exchange is clockwise or counterclockwise—this is immaterial because a clockwise exchange can be deformed into counterclockwise one—but rather by which ribbon is left with a twist that must be undone by rotating one of the particles.

To see that the operations t_i, defined by the sequence in Figs. 8, 9(a), and 9(b), and t_i^{-1}, defined by the sequence in Fig. 10, are, in fact, inverses, it is useful to note that when they are performed sequentially, they involve two 2π twists of the same hedgehog. In Fig. 9(b), it is the hedgehog on the left-hand side which is twisted; this hedgehog moves to the right-hand side in the first step of Fig. 10 and is twisted again in the fourth step. One should then note that a double twist in a ribbon

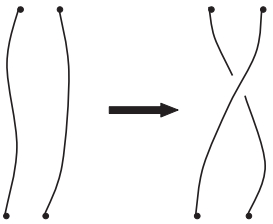

FIG. 8. When two defects are exchanged, the $\vec{n}$ field around them is modified. This is encapsulated by the dragging of the framed arcs as the defects are moved.

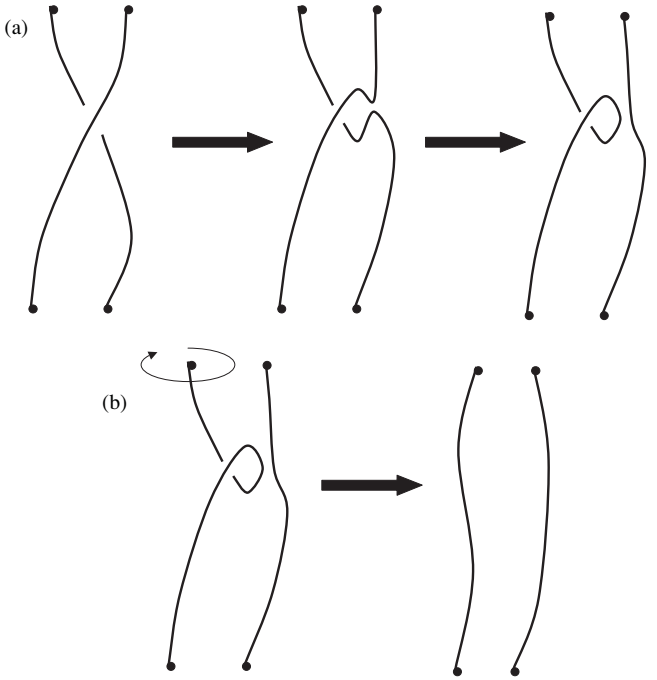

FIG. 9. (a) In order to restore the framed arcs so that they are connecting the same defects, it is necessary to perform a recoupling by which they are reconnected. In order to keep track of the induced twist, it is easiest to perform the recoupling away from the overcrossing. (b) The particle on the left-hand side must be rotated by -2π in order to undo a twist in the framed arc to which it is attached.

can be undone continuously by using the ribbon to "lasso" the defect, a famous fact related to the existence of spin-1/2 and the fact that $\pi_1(\mathrm{SO}(3)) = \mathbb{Z}_2$. This is depicted in Fig. 16 in Appendix E. It will be helpful for our late discussion to keep in mind that t_i not only permutes a pair of particles but also rotates one of them; any transformation built up by multiplying t_i's will enact as many 2π twists as pairwise permutations modulo two.

Thus far we have only discussed the $+1$ hedgehogs. We can perform the similar transformations that exchange -1 hedgehogs. We will not repeat the above discussion for -1 hedgehogs because the discussion would be so similar; furthermore, in the $N \to \infty$ model, which is our main interest, defects do not carry a sign, so they can all be permuted with each other.

We have concluded that $t_i \neq t_i^{-1}$ and, therefore, the group of transformations that bring the hedgehogs and ribbons back

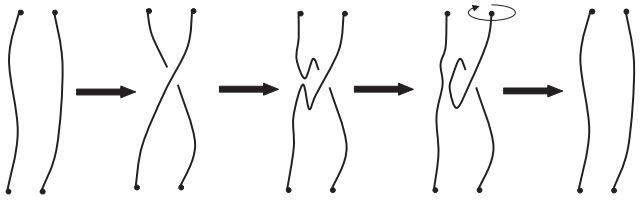

FIG. 10. The sequence of moves that defines t_i^{-1}. [Here, the ith particle is at the top left-hand side and the $(i+1)$th is at the top right-hand side.] This may be contrasted with the sequence in Figs. 8, 9(a), and 9(b), which defines σ_i^1.

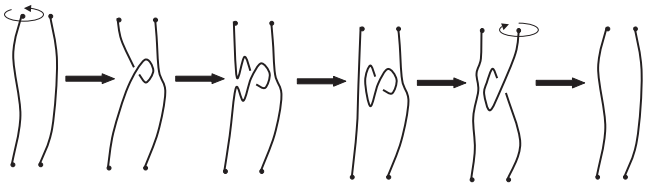

FIG. 11. The sequence of moves that defines x_i: The defect on the left-hand side is rotated by 2π, the twist is transferred to the ribbon on the right-hand side by two recouplings, and then the defect on the right-hand side is rotated by -2π. [Here, the ith defect is at the top left-hand side and the $(i+1)$th is at the top right-hand side.] The defects themselves are not moved in such a process.

to their initial configuration is not the permutation group. This leaves open the question: What is t_i^2? The answer is that t_i^2 can be continuously deformed into a transformation that does not involve moving any of the particles—Teo and Kane's "braidless operations." Consider the transformation x_i depicted in Fig. 11. Defect i is rotated by 2π, the twist is transferred from one ribbon to the other, and defect $i+1$ is rotated by -2π. Because a 4π rotation can be unwound, as depicted in Fig. 16, $x_i^2 = 1$.

Intuitively, one expects that $x_i = t_i^2$ because neither x_i nor t_i^2 permutes the particles, and both of them involve 2π rotations of both particles i and $i+1$. To show that this is, in fact, correct, we need to show that the history in Fig. 11 can be deformed into the sequence of Figs. 8, 9(a), and 9(b) repeated twice. If the history in Fig. 11 is viewed as a "movie" and the sequence of Figs. 8, 9(a), and 9(b) repeated twice is viewed as another movie, then we need a one-parameter family of movies—or a "movie of movies"—which connects the two movies. We will give an example of such a movie of movies shortly. With this example in hand, the reader can verify that $x_i = t_i^2$ by drawing the corresponding pictures, but we will not do so here because this discussion is superseded, in any case, by the next section, where a similar result is shown for the $N \to \infty$ problem by more general methods. We simply accept this identity for now.

We now consider the commutation relation for the x_i's. Clearly, for $|i-j| \geqslant 2$, $x_i x_j = x_j x_i$. It is also intuitive to conclude that

$$x_i x_{i+1} = x_{i+1} x_i, \tag{43}$$

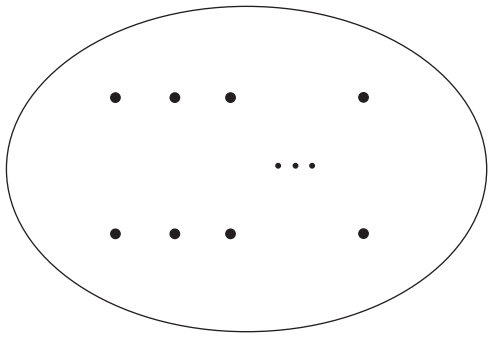

FIG. 13. $B^3 \setminus 2n$ points in standard position. The space $\mathcal{M}_{2n}$ consists of maps from this manifold to $\mathcal{C}$.

because the order in which twists are transferred is seemingly unimportant. However, because this is a crucial point, we verify it by showing in Fig. 12 that the sequence of moves that defines $x_i x_{i+1}$ (a movie) can be continuously deformed into the sequence of moves that defines $x_{i+1} x_i$ (another movie). Such a deformation is a movie of movies; going from left-to-right in Fig. 12 corresponds to going forward in time while going from up to down corresponds to deforming from one movie to another.

Thus, we see that the equivalence class of motions of the defects (i.e., π_1 of their configuration space) has an Abelian subgroup generated by the x_i's. Because $x_i^2 = 1$ and they all commute with each other, this is simply $n-1$ copies of $\mathbb{Z}_2$, or, simply, $(\mathbb{Z}_2)^{n-1}$.

In order to fully determine the group of transformations that bring the hedgehogs and ribbons back to their initial configuration, we need to check that the t_i's generate the full set of such transformations—i.e., that the transformations described above and those obtained by combining them exhaust the full set. In order to do this, we need the commutation relations of the t_i's with each other. Clearly, $t_i t_j = t_j t_i$ for $|i-j| \geqslant 2$ because distant operations that do not involve the same hedgehogs nor the same ribbons must commute. On the other hand, operations involving the same hedgehogs or ribbons might not commute. For instance,

$$t_i x_{i+1} = x_i x_{i+1} t_i. \tag{44}$$

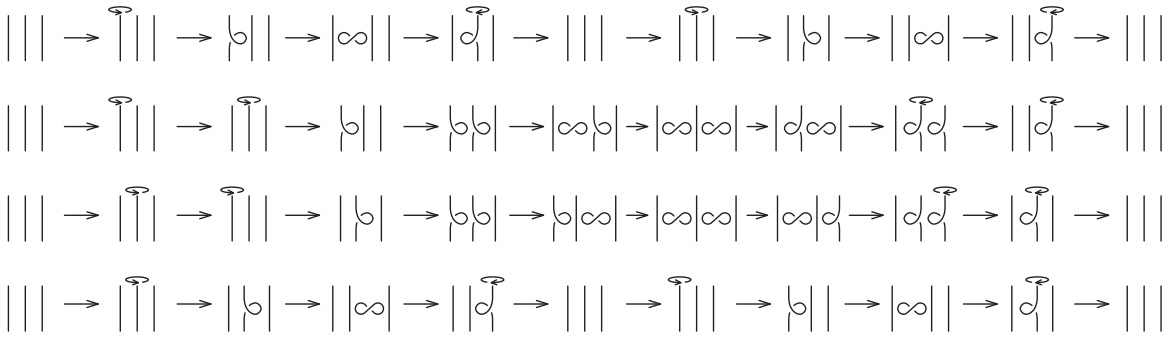

FIG. 12. The sequence of moves that defines $x_i x_{i+1}$ is shown in the top row. The sequence of moves that defines $x_{i+1} x_i$ is shown in the bottom row. The rows in between show how the top row can be continuously deformed into the bottom one. Such a deformation of two different sequences is a movie of movies or a two-parameter family of configurations. Moving to the right-hand side increases the time parameter while moving down increases the deformation parameter that interpolates between $x_i x_{i+1}$ and $x_{i+1} x_i$.

To see why this is true, note that if we perform x_{i+1} first, then defects $i+1$ and $i+2$ are twisted by 2π. However, t_i then permutes i and $i+1$ and twists i by 2π. Thus, the left-hand side permutes i and $i+1$ and only twists $i+2$. The $(i+1)$th hedgehog was twisted by x_{i+1} and then permuted by t_i so that it ended up in the ith position, where it was twisted again in the last step in t_i; two twists can be continuously deformed to zero, so this hedgehog is not twisted at all. The right-hand side similarly permutes i and $i+1$ and only twists $i+2$ by 2π. The reader may find it instructive to flesh out the above reasoning by constructing a movie of movies.

The multiplication rule that we have just described (but not fully justified) is that of a semidirect product, which is completely natural in this context: When followed by a permutation, a transfer of twists ends up acting on the permuted defects. The twists x_i form the group $(\mathbb{Z}_2)^{n-1}$, which we can represent by n-component vectors, all of whose entries are 0 or 1, which satisfy the constraint that the sum of the entries is even. The entries tell us whether a given hedgehog is twisted by 2π or not. In any product of x_i's, an even number of hedgehogs is twisted by 2π. Now consider, for n odd, the group elements given by

$$\sigma_i = x_{n-1}x_{n-3}\cdots x_{i+3}x_{i+1}x_{i-2}x_{i-4}\cdots x_1 t_i \tag{45}$$

for i odd and

$$\sigma_i = x_{n-1}x_{n-3}\cdots x_{i+2}x_i x_{i-1}x_{i-3}\cdots x_1 t_i \tag{46}$$

for i even. From (44), we see that $\sigma_i^2 = 1$. The group element σ_i permutes the ith and $(i+1)$th hedgehogs and twists all of the hedgehogs. Thus, the σ_i's generate a copy of the permutation group S_n. The σ_i's do not commute with the x_i's, however; instead they act according to the semidirect product structure noted above. On the other hand, the situation is a bit different for n even. This may be a surprise because one might expect that n even is the same as n odd but with the last hedgehog held fixed far away. While this is true, exchanging the last hedgehog with the others brings in an additional layer of complexity that is not present for n odd. The construction above, Eqs. (45) and (46), does not work. One of the hedgehogs will be left untwisted by such a construction; because subsequent σ_i's will permute this untwisted hedgehog with others, we must keep track of the untwisted hedgehog and, therefore, the σ_i's will not generate the permutation group. In the even hedgehog number case, the group of tranformations has a $(\mathbb{Z}_2)^{n-1}$ subgroup, as in the odd case, but there is not an S_n subgroup, unlike in the odd case. To understand the even case, it is useful to note that in both cases, every transformation either (a) twists an even number of ribbons, which is the subgroup $(\mathbb{Z}_2)^{n-1}$, (b) performs an even permutation, which is the subgroup A_n of S_n, or (c) twists an odd number of ribbons and performs an odd permutation. Another way of saying this is that the group of transformations is the "even part" of $(\mathbb{Z}_2)^n \rtimes S_n$, the subgroup of $(\mathbb{Z}_2)^n \rtimes S_n$ consisting of those elements whose $(\mathbb{Z}_2)^n$ parity added to their S_n parity is even. In the odd hedgehog number case, this is the semidirect product $(\mathbb{Z}_2)^{n-1} \rtimes S_n$; in the even hedgehog number case, it is not. As we will see in Sec. VI, the difference between the even and odd hedgehog number cases is related to the fact that, for an even number of hedgehogs, the Hilbert space decomposes into even and odd total fermion number parity sectors. By contrast, the situation is simpler for an odd number of hedgehogs, where the parity of the total fermion number is not well defined and the representation is irreducible.

To summarize, we have given some plausible heuristic arguments that the statistics of $+1$ hedgehogs in a model of $2N = 8$ Majorana fermions is governed by a group $E((\mathbb{Z}_2)^n \rtimes S_n)$, the "even part" of $(\mathbb{Z}_2)^n \rtimes S_n$: those elements of $(\mathbb{Z}_2)^n \rtimes S_n$ in which the parity of the sum of the entries of the element in $(\mathbb{Z}_2)^n$ added to the parity of the permutation in S_n is even. (The same group governs the -1 hedgehogs.) Rather than devoting more time here to precisely determining the group for the toy model, we will move on to the problem that is our main concern here, a system of $2N \to \infty$ Majorana fermions. This problem is similar, with some important differences. (1) The target space is no longer S^2 but is, instead, $U(N)/O(N)$. (2) Consequently, the defects do not carry a sign. There is no preferred pairing into $\pm$ pairs; the defects are all on equal footing. All $2n$ of them can be exchanged. (3) The group obtained by computing π_1 of the space of configurations of $2n$ defects then becomes the direct product of the ribbon permutation group $\mathcal{T}_{2n}^r$ with a trivial $\mathbb{Z}$, $\mathcal{T}_{2n} = \mathbb{Z} \times \mathcal{T}_{2n}^r$. The ribbon permutation group $\mathcal{T}_{2n}^r$ is given by $\mathcal{T}_{2n}^r \equiv \mathbb{Z}_2 \times E((\mathbb{Z}_2)^{2n} \rtimes S_{2n})$, where $E((\mathbb{Z}_2)^{2n} \rtimes S_{2n})$ is the "even part" of $(\mathbb{Z}_2)^{2n} \rtimes S_{2n}$.

V. FUNDAMENTAL GROUP OF THE MULTIDEFECT CONFIGURATION SPACE

In Sec. III we concluded that the effective target space for the order parameter of a system of fermions in 3D with no symmetries is $U(N)/O(N)$—which, as is conventional, we will simply call U/O, dropping the N in the large-N limit. This enables us to rigorously define the space of topological configurations, K_{2n}, of $2n$ hedgehogs in a ball, and calculate its fundamental group $\pi_1(K_{2n})$, thereby elucidating Teo and Kane's[20] hedgehog motions and unitary transformations.

We now outline the steps involved in this calculation.

(1) We approximate the space U/O by a *cell complex* (or CW complex), $\mathcal{C}$, a topological space constructed by taking the union of disks of different dimensions and specifying how the boundary of each higher-dimensional disk is identified with a subset of the lower-dimensional disks. This is a rather crude approximation in some respects, but it is sufficient for a homotopy computation.

(2) We divide the problem into (a) the motion of the hedgehogs and (b) the resulting deformation of the field configuration between the hedgehogs. This is accomplished by expressing the configuration space in the following way. Let us call the configuration space of $2n$ distinct points in 3D X_{2n}. (For the sake of mathematical convenience, we will take our physical system to be a ball B^3 and stipulate that the points must lie inside a ball B^3.) Let us denote the space of field configurations by $\mathcal{M}_{2n}$. This space is the space of maps to U/O from B^3 with $2n$ points (at some standard locations) excised, as shown in Fig. 13. The latter space is denoted by $B^3 \backslash 2n$ standard points. Because we will be approximating U/O by $\mathcal{C}$, we can take $\mathcal{M}_{2n}$ to be the space of maps from

$B^3\backslash 2n$ standard points to $\mathcal{C}$ with boundary conditions at the $2n$ points specified below. Then, there is a *fibration* of spaces:

$$\begin{array}{ccc} \mathcal{M}_{2n} & \to & K_{2n} \\ & & \downarrow \\ & & X_{2n} \end{array}$$

(3) We introduce another two fibrations, which further divide the problem into more manageable pieces:

$$\begin{array}{ccc} R_{2n} & \to & K_{2n} \\ & & \downarrow \\ & & Y_{2n} \end{array}$$

$$\begin{array}{ccc} \mathcal{N}_{2n} & \to & Y_{2n} \\ & & \downarrow \\ & & X_{2n} \end{array}$$

The original fibration is kind of a "fiber product" of the two new fibrations. Here, R_{2n} is essentially the space of order parameter textures interpolating between the hedgehogs, and Y_{2n} is the space of configurations of $2n$ points with infinitesimal spheres surrounding each point and maps from each of these spheres to $\mathcal{C}$. $\mathcal{N}_{2n}$ is the space of maps from $2n$ infinitesimal spheres to $\mathcal{C}$, with each one of the spheres surrounding a different one of the $2n$ points (at some standard locations) excised from B^3. We call these order parameter maps from infinitesimal spheres to $\mathcal{C}$ "germs."

(4) Having broken the problem down into smaller pieces by introducing these fibrations, we use the fact that a fibration $F \to E \to B$ induces a long exact sequence for homotopy groups:

$$\cdots \to \pi_i(E) \to \pi_i(B) \to \pi_{i-1}(F) \to \pi_{i-1}(E) \to \cdots.$$

For instance, applying this to the fibration $\mathcal{M}_{2n} \to K_{2n} \to X_{2n}$ leads to the exact sequence $\cdots \to \pi_1(\mathcal{M}_{2n}) \to \pi_1(K_{2n}) \to \pi_1(X_{2n}) \to 1$. It follows that $\pi_1(K_{2n})$ is an extension of the permutation group $S_{2n} = \pi_1(X_{2n})$. By itself, the above long exact sequence is not very helpful for computing any of the homotopy groups involved unless we can show by independent means that two of the homotopy groups are trivial. Then the homotopy groups that lie between the trivial ones in the sequence are tightly constrained.

(5) We directly compute that $\pi_1(\mathcal{N}_{2n}) = (\mathbb{Z}_2)^{2n}$ and $\pi_1(X_{2n}) = S_{2n}$. We show that the homotopy exact sequence then implies that $\pi_1(Y_{2n}) = (\mathbb{Z}_2)^{2n} \rtimes S_{2n}$.

(6) We compute the homotopy groups of R_{2n}, defined by the fibration $R_{2n} \to K_{2n} \to Y_{2n}$. This computation involves a different way from the cell structure of thinking about the topology of a space, called the "Postnikov tower," explained in detail in Appendix E. The basic idea is to approximate a space with spaces with only a few nontrivial homotopy groups. (This is analogous to the cell structure, which has only a few nontrivial homology groups.) The simplest examples of such spaces are Eilenberg-Mac Lane spaces, which only have a single nontrivial homotopy group. The Eilenberg-Mac Lane space $K(A,m)$ is defined for a group A and integer m as the space with homotopy group $\pi_m(K(A,m)) = A$ and $\pi_k(K(A,m)) = 0$ for all $k \neq m$. (The group A must be Abelian for $m > 1$.) Such a space exists and is unique up to homotopy. A space T with only two nontrivial homotopy groups can be constructed through the fibration $K(B,n) \to T \to K(A,m)$. The space T has $\pi_m(T) = A$ and $\pi_n(T) = B$, as may be seen from the corresponding long exact sequence for homotopy groups. Continuing in this fashion, one can construct a sequence of such approximations M_n to a space M. They are defined by $\pi_k(M_n) = \pi_k(M)$ for $k \leqslant n$ and $\pi_k(M_n) = 0$ for $k > n$. They can be constructed iteratively from the fibration $K(A,n) \to M_n \to M_{n-1}$, where $\pi_n(M) = A$.

(7) With $\pi_1(Y_{2n})$, $\pi_2(Y_{2n})$, $\pi_0(R_{2n})$, and $\pi_1(R_{2n})$ in hand, we compute the desired group $\pi_1(K_{2n})$ from the homotopy exact sequence.

We now go through these steps in detail.

Approximating U/O by a cell complex. Depending on microscopic details, gradients in the overall phase of the fermions may be so costly that we wish to consider only configurations in which this overall phase is fixed. We will refer to this as the scenario in which "phase symmetry is broken." In this case, the effective target space is SU/SO, the nonphase factor of $U/O \cong U(1)/O(1) \times SU/SO$. In this case, we simplify matters by replacing SU/SO by $\widetilde{U/O}$, the universal cover of U/O. $\widetilde{U/O}$ is homotopy equivalent to SU/SO, so this substitution is harmless. This substitution results in a reduced configuration space $\widetilde{K}_{2n}$, and we will concentrate first on calculating $\pi_1(\widetilde{K}_{2n})$. In an Appendix C, we show that this reduction essentially makes no difference: $\pi_1(K_{2n}) = \pi_1(\widetilde{K}_{2n}) \times \mathbb{Z}$.

We now define a cell complex $\mathcal{C}$ approximating $\widetilde{U/O}$. In constructing this cell structure, we are not interested in the beautiful homogeneous nature of $\widetilde{U/O}$ but rather only its homotopy type. The homotopy type of a space tells you everything you will need to know to study *deformation classes* of maps either into or out of that space. An important feature of any homotopy type is the list of homotopy groups (but these are by no means a complete characterization in general). For $\widetilde{U/O}$, the homotopy groups are $\pi_i(\widetilde{U/O}) = 0,\mathbb{Z}_2,\mathbb{Z}_2,0,\mathbb{Z},0,0,0,\mathbb{Z}$ for $i = 1,\ldots,9$, and thereafter $\pi_i(\widetilde{U/O})$ cycles through the last eight groups. (For U/O, the first group would be $\mathbb{Z}$.)

Because $\widetilde{U/O}$ is simply connected, but has nontrivial π_2, it is natural in building a cellular model for its homotopy type by beginning with S^2. Because $\pi_2(S^2) = \mathbb{Z}$ and we only need a $\mathbb{Z}_2$ for $\pi_2(\widetilde{U/O})$, we should kill off the even elements by attaching a 3-cell D^3 using a degree-2 map of its boundary 2-sphere to the original S^2. For future reference, take this map to be $(\theta,\phi) \to (2\theta,\phi)$ in a polar coordinate system, where the north pole $N = (\pi,0)$. Similarly, a 4-cell is attached to achieve $\pi_3(\widetilde{U/O}) \cong \mathbb{Z}_2$. The necessity of the 4-cell is proved (Fact 1) below.

The preceding logic leads us to the cell structure:

$$\mathcal{C} = S^2 \bigcup_{\text{degree}=2} D^3 \bigcup_{\text{2Hopf}} D^4 \bigcup \text{cells of dimension} \geqslant 5. \quad (47)$$

Because we are only trying to compute the fundamental group $\pi_1(\widetilde{K}_{2n})$ from our various homotopy long exact sequences, we do not have to figure out the higher cells (dimension $\geqslant 5$) of $\widetilde{U/O}$. We will, however, verify that $\pi_3(\widetilde{U/O})$ is generated by the Hopf map into the base $S^2 \subset \widetilde{U/O}$.

To summarize, we will henceforth assume that the order parameter takes values in the cell complex $\mathcal{C}$. Although $\mathcal{C}$ is

a crude approximation for U/O, it is good enough for the topological calculations which follow.

Dividing the problem into the motion of the hedgehog centers and the deformation of the field configuration. Let us assume that our physical system is a ball of material B^3. Let $n \geqslant 0$ be the number of hedgehog pairs in the system. A configuration in $\widetilde{K}_{2n}$ is a texture in the order parameter, $\Phi(x) : B^3 \to \mathcal{C}$, which satisfies the following boundary conditions at the boundary of B^3 and at the $2n$ hedgehog locations (which are singularities in the order parameter). The order parameter has winding number 0 at the boundary of the ball, ∂B^3, and winding number 1 around each of the hedgehog centers. [Recall that $\pi_2(\mathcal{C}) = \mathbb{Z}_2$, so the winding number can only be 0 or 1].

From its definition, $\widetilde{K}_{2n}$ is the total space of a fibration:

$$\begin{array}{c} \mathcal{M}_{2n} \to \widetilde{K}_{2n} \\ \downarrow \\ X_{2n} \end{array}$$

The above diagram suggests that we should think of the fibration $\mathcal{M}_{2n} \to \widetilde{K}_{2n} \to X_{2n}$ in the following way: Above each point in X_{2n} there is a fiber $\mathcal{M}_{2n}$; the total space formed thereby is $\widetilde{K}_{2n}$. (This is not quite a fiber bundle, because we do not require that there be local coordinate charts in which $\widetilde{K}_{2n}$ is simply the direct product.) Here, X_{2n} is the simply the configuration space of $2n$ distinct points in B^3. We write this formally as $X_{2n} = \prod_{i=1}^{2n} B^3 \setminus$ big diagonal. (The big diagonal consists of $2n$-tuples of points in B^3, where at least two entries are identical.) The space $\mathcal{M}_{2n}$ consists of maps from $B^3 \setminus 2n$ points in a fixed standard position to $\mathcal{C}$ with the prescribed winding numbers given in the preceding paragraph.

Germs of order parameter textures. It is helpful to introduce an intermediate step in the fibration. Define a point in Y_{2n} as a configuration in X_{2n} together with a "germ" of $\Phi(x)$, which we call $\widetilde{\Phi}(x)$, defined only near ∂B^3 and the $2n$ points. The idea behind the germ $\widetilde{\Phi}(x)$ is to forget about the order parameter $\Phi(x)$ except for its behavior in an infinitesimal neighborhood around each hedgehog center and at the boundary of the system. $\widetilde{\Phi}(x)$ must satisfy the same boundary conditions as $\Phi(x)$ itself. We take $\widetilde{\Phi}(x)$ to be constant on ∂B^3 and to have winding number 1 around each of the hedgehog centers. With this definition, we now have the fibration

$$\begin{array}{c} \mathcal{N}_{2n} \to Y_{2n} \\ \downarrow \\ X_{2n} \end{array}$$

where $\mathcal{N}_{2n}$ is the space of (germs of) order parameter textures $\widetilde{\Phi}$ from the neighborhoods of the $2n$ fixed standard points and ∂B^3 to $\mathcal{C}$. We will henceforth replace discussion of germs with the equivalent and simpler concept of maps on $\partial B^3 \cup (\bigcup_{i=1}^{2n} S_i^2)$ where S_i^2 is a small sphere surrounding the ith standard point. Thus,

$$\mathcal{N}_{2n} \subset \text{Maps}\left[\left(\partial B^3 \cup \bigcup_{i=1}^{2n} S_i^2\right) \to \mathcal{C}\right]. \tag{48}$$

We now define Q_{2n} as the ball B^3 with small balls [denoted below by interior (S_i^2)] centered about the hedgehogs deleted:

$$Q_{2n} = \left(B^3 \setminus \bigcup_{i=1}^{2n} \text{interior}\left(S_i^2\right)\right) \tag{49}$$

for fixed standard positions $i = 1, \ldots, 2n$. Then R_{2n} is the space of order parameter textures on Q_{2n}, which satisfy the boundary condition that the winding number is 0 on ∂B^3 and 1 on each of the small spheres. With this definition, we have the fibration

$$\begin{array}{c} R_{2n} \to \widetilde{K}_{2n} \\ \downarrow \\ Y_{2n} \end{array} \tag{50}$$

Given the cell structure $\mathcal{C}$, we can specify the boundary conditions for the order parameter precisely. On ∂B^3, the order parameter is equal to the north pole in S^2. (Recall that $S^2 \subset \mathcal{C}$ is the bottom cell of the structure $\mathcal{C}$, which we are using to approximate U/O.) On each of the spheres S_i^2, the order parameter $\Phi(x)$ defines a map from $S_i^2 \to S^2$, which is the identity map (where, again, S^2 is understood as a subset of the order parameter space $S^2 \subset \mathcal{C}$). This ensures that the order parameter has the correct winding numbers at the boundaries of Q_{2n}. In essence, what we have done in writing Eq. (50) is to break up an order parameter texture containing hedgehogs into (a) the hedgehogs together with the order parameter on infinitesimal neighborhoods around them (i.e., germs) and (b) order parameter textures in the intervening regions between the hedgehogs. The space of configurations (a) is Y_{2n}; the space of configurations (b) is R_{2n}.

The name R_{2n} is for "ribbons." As we saw in Sec. IV, if the order parameter manifold were S^2, we could summarize an order parameter texture by looking at the inverse image of the north pole $N \subset S^2$ and a fixed tangent vector at the north pole. The inverse images form a collection of ribbons. Now, the order parameter manifold is actually (approximated by) $\mathcal{C}$, but the bottom cell in $\mathcal{C}$ is S^2. The effect of the 3-cell is that hedgehogs lose their sign, so there is no well-defined "arrow" running lengthwise along the ribbons. The 4-cell allows the "twist" or framings of ribbons to be altered at will by ± 2.

Long exact sequence for homotopy groups. It is very convenient to use fibrations to calculate homotopy groups. (For those interested in K theory, the last two chapters of Milnor's *Morse Theory*[28] are a must read and exhibit these methods with clarity.) As noted above, fibrations have all the homotopy properties of fiber bundles but are (often) found arising between function spaces where it would be a lot of work—and probably a distraction from important business—to attempt to verify the existence of locally trivial coordinate charts. Operationally, fibrations share with fiber bundles the all-important "homotopy long exact sequence"

$$\begin{array}{c} F \to E \\ \downarrow \\ B \end{array}$$

we have

$$\cdots \to \pi_{i+1}(B) \to \pi_i(F) \to \pi_i(E) \to \pi_i(B) \to \pi_{i-1}(F) \to \cdots.$$

We now compute $\pi_1(Y_{2n})$ from the exact sequence:

$$\pi_2(X_{2n}) \xrightarrow{\partial} \pi_1(\mathcal{N}_{2n}) \to \pi_1(Y_{2n}) \to \pi_1(X_{2n}) \xrightarrow{\partial} \pi_0(\mathcal{N}_{2n}) \tag{51}$$

We can compute two of the homotopy groups in this equation by inspection. $\pi_1(X_{2n})$ is clearly the symmetric group of point exchange:

$$\pi_1(X_{2n}) = S_{2n}. \tag{52}$$

Meanwhile, $\pi_1(\mathcal{N}_{2n})$ amounts to (products of) loops of maps from the S_i^2 to $\mathcal{C}$ and reduces to $2n$ copies of the third homotopy group of $\mathcal{C}$ [and, therefore, to $\pi_3(\widetilde{U/O})$]. Thus, $\pi_1(\mathcal{N}_{2n}) = (\mathbb{Z}_2)^{2n}$:

$$\pi_1(\mathcal{N}_{2n}) = \prod_{i=1}^{2n} \pi_1\big(\mathrm{Maps}\big(S_i^2, \widetilde{U/O}\big)\big) = \prod_{2n \text{ copies}} \pi_3(\widetilde{U/O}) = (\mathbb{Z}_2)^{2n}. \tag{53}$$

To proceed further, we need to evaluate *boundary maps* in the homotopy exact sequence. In Appendix D, we explain boundary maps through the example of the Hopf map. Consider Eq. (51). $\pi_2(X_{2n})$ is generated by the $\binom{2n}{2}$ different two-parameter motions in which a pair of hedgehogs come close together and explore the 2-sphere of possible relative positions around their center of mass. This two-parameter family of motions involves no "rotation" of the maps $\widetilde{\Phi}$, which describe $\pi_1(\mathcal{N}_{2n})$ (i.e., the order parameter configuration in the neighborhood of each hedgehog does not rotate as the hedgehogs are moved), so the leftmost ∂ map in Eq. (51) is zero. Similarly, a simple exchange of hedgehogs produces no twist of the order parameter configuration in the neighborhood of either hedgehog, so the second ∂ map of Eq. (51) is also zero. Thus, we have a short exact sequence:

$$1 \longrightarrow \mathbb{Z}_2^{2n} \xrightarrow{\alpha} \pi_1(Y_{2n}) \xrightarrow{\beta} S_{2n} \longrightarrow 1.$$

To derive this short exact sequence, we used the triviality of the boundary maps noted above and Eqs. (52) and (53) to simplify Eq. (51).

There is a natural group homomorphism s:

$$s : S_{2n} \to \pi_1(Y_{2n}),$$

which associates to each permutation a motion of hedgehogs that permutes the hedgehogs in Y_{2n} but does not rotate the order parameter configurations $\widetilde{\Phi}$ near the hedgehogs. Then $\beta \circ s = id_{S_{2n}}$. In other words, the sequence is *split*:

$$1 \longrightarrow \mathbb{Z}_2^{2n} \xrightarrow{\alpha} \pi_1(Y_{2n}) \underset{s}{\overset{\beta}{\rightleftarrows}} S_{2n} \longrightarrow 1$$

Thus, $\pi_1(Y_{2n})$ is a semidirect product. To determine $\pi_1(Y_{2n})$ completely, it only remains to identify how $s(S_{2n})$ acts on the twist factors $\mathbb{Z}_2^{2n}$ under conjugation. It is quite clear that this action is the only natural one available: $s(p)$ acts on $\mathbb{Z}_2^{2n}$ by applying the permutation p to the $2n$ coordinates of Z_2^{2n}. So, $\pi_1(Y_{2n}) \cong \mathbb{Z}_2^{2n} \rtimes S_{2n}$ with group law,

$$(v, p) \circ (v', p') = (v + p(v'), p \circ p'), \tag{54}$$

where $v \in \mathbb{Z}_2^{2n}$ is a $\mathbb{Z}_2$ vector, $p \in S_{2n}$ a permutation, and $p(v')$ the natural action of S_{2n} on $\mathbb{Z}_2^{2n}$ applied to v'. Note that this is precisely the multiplication rule that we obtained pictorially in Sec. IV.

Computing the homotopy groups of R_{2n}, the space of order parameter textures interpolating between the hedgehogs. Of course, computing $\pi_1(Y_{2n})$ only gets us part of the way home. Our ultimate goal is to compute $\pi_1(\widetilde{K}_{2n})$. Thus, we now turn to the homotopy long exact sequence:

$$\pi_2(Y_{2n}) \xrightarrow{\partial_2} \pi_1(R_{2n}) \to \pi_1(\widetilde{K}_{2n}) \to \pi_1(Y_{2n}) \xrightarrow{\partial_1} \pi_0(R_{2n}).$$

First consider ∂_1. The kernel of ∂_1 is represented by loops in Y_{2n}, which extend to loops in R_{2n}. A loop γ in Y_{2n} is a motion of the hedgehogs together with rotations (about the spheres S_i^2) of $\widetilde{\Phi}$, which brings the system back to its initial configuration. If a loop γ is in kernel of ∂_1, then there is a corresponding loop in the configuration space of ribbons in B^3 (obtained by lifting γ to $\widetilde{K}_{2n}$).

The next steps are to compute $\pi_0(R_{2n})$ and $\pi_1(R_{2n})$. These computations are detailed in Appendix E, where we see that using the cell structure $\mathcal{C}$, which we introduced for $\widetilde{U/O}$, is tricky as a result of the higher cells. Thus, we instead introduce the "Postnikov tower" for $\widetilde{U/O}$, which allows us to make all the calculations we need. We find that $\pi_0(R_{2n}) = \mathbb{Z}_2$ and $\pi_1(R_{2n}) = (\mathbb{Z}_2)^{2n}$.

Thus, $\pi_1(\widetilde{K}_{2n})$ sits in the following exact sequence:

$$\begin{array}{ccccccccc} \pi_2(Y_{2n}) & \xrightarrow{\partial_2} & \pi_1(R_{2n}) & \to & \pi_1(\widetilde{K}_{2n}) & \to & \pi_1(Y_{2n}) & \xrightarrow{\partial_1} & \pi_0(R_{2n}) \\ & & \wr\| & & & & \wr\| & & \wr\| \\ & & (\mathbb{Z}_2)^{2n} & & & & (\mathbb{Z}_2)^{2n} \rtimes S_{2n} & & \mathbb{Z}_2 \end{array}$$

Recall that when we studied $\pi_2(Y_{2n})$, we found [exactly as in the case of $\pi_2(X_{2n})$] that there are $\binom{2n}{2}$ generators corresponding to relative two-parameter motions of any pair of hedgehogs around their center of mass. This can be used to understand the map $\partial_2 : \pi_2(Y_{2n}) \to \pi_2(R_{2n})$. The image of any center-of-mass 2-motion is the "bag" containing the corresponding pair of hedgehogs. Thus, $\mathrm{coker}(\partial_2) \cong \mathbb{Z}_2$ [here, "coker" is the cokernel of ∂_2, which is the quotient $\pi_2(R_{2n})/\partial_2(\pi_2(Y_{2n}))$]; it is $\mathbb{Z}_2^{2n}$ modulo the even sublattice (vectors whose coordinate sum is zero in $\mathbb{Z}_2$). Thus, we have the short exact sequence:

$$\begin{array}{ccccccccc} 1 & \longrightarrow & \mathrm{coker}(\partial_2) & \to & \pi_1(\widetilde{K}_{2n}) & \xrightarrow{\pi} & \ker(\partial_1) & \longrightarrow & 1 \\ & & \cong & & & & & & \\ & & \mathbb{Z}_2 & & & & & & \end{array} \tag{55}$$

The kernel $\ker(\partial_1)$ consists of the part of $\pi_1(Y)$ associated with even (2π) twisting. As shown in Fig. 9, a simple exchange is associated to a total twisting of ribbons by $\pm 2\pi$.

Thus, $\partial_1(v, p) = \sum_{i=1}^{2n} v_i + \mathrm{parity}(p) \in \mathbb{Z}_2$. We use the notation $E(\mathbb{Z}_2^m \rtimes S_m)$ for $\ker(\partial_1)$.

Note: If $m = 2$, $\mathbb{Z}_2^m \rtimes S_m$ is the dihedral group D_4 and its "even" subgroup $\ker(\partial_1) \cong \mathbb{Z}_4$. This shows that for m even, the induced short exact sequence does not split, and the extension is more complicated:

$$1 \longrightarrow \mathbb{Z}_2^{2n-1} \longrightarrow E\big(\mathbb{Z}_2^{2n} \rtimes S_{2n}\big) \longrightarrow S_{2n} \to 1.$$

There is a final step required to solve the extension problem (55) and finish the calculation of $\pi_1(\widetilde{K}_{2n})$. We geometrically

construct a homomorphism $s : \ker(\partial_1) = E(\mathbb{Z}_2^{2n} \rtimes S_{2n}) \to \pi_1(\widetilde{K}_{2n})$, which is a left inverse to the projection.

This will show that $\pi_1(\widetilde{K}_{2n})$ is a semidirect product $\mathbb{Z}_2 \rtimes \ker(\partial_1)$, but because $\mathbb{Z}_2$ has no nontrivial automorphism, the semidirect product is actually direct:

$$\pi_1(\widetilde{K}_{2n}) \cong \mathbb{Z}_2 \times E\left(\mathbb{Z}_2^{2n} \rtimes S_{2n}\right). \tag{56}$$

To construct s, note that all elements of $\ker(\partial_1)$ can be realized by a loop γ of maps into the bottom 2-cell of Eq. (47), S^2. Still confining the order parameter (map) to lie in S^2, such a loop lifts to an arc $\widetilde{\gamma}$ of ribbons representing an arc in $\widetilde{K}_{2n}$. We may choose the lift so that as the ribbons move, they never "pass behind" the $2n$ hedgehogs. For example, we may place the hedgehogs on the sphere of radius $=\frac{1}{2}$ inside the 3-ball B^3 (assumed to have radius $=1$) and then keep all ribbons inside $B^3_{1/2}$. These arcs may be surgered (still as preimages of $N \subset S^2$) so that they return to their original position, except for a possible accumulation of normal twisting $t2\pi$. Because $\gamma \in \ker(\partial_1)$, t must be even. Now, allowing the order parameter (map) to leave S^2 and pass over the 4-cell [of Eq. (47)], attached by 2Hopf : $S^3 \to S^2$, we may remove these even twists. (The 4-cell can introduce small closed ribbons with self-linking $=2$ in a small ball. These small ribbons can be surgered into other ribbons.) This lifts a generating set of $\ker(\partial_1)$ into $\pi_1(\widetilde{K}_{2n})$ as a set theoretic cross section (left inverse to π). But what about relations? Because the entire loop is constant outside $B^3_{\frac{1}{2}}$, the corresponding homology class in $H_2(Q \times I; \mathbb{Z}_2) \cong \pi_1(R)$ is trivial, so s is actually a group homomorphism.

VI. REPRESENTATION THEORY OF THE RIBBON PERMUTATION GROUP

In this section, we discuss the mathematics of the group $\mathcal{T}_m$ and its representation. The purpose of this section is to show that a direct factor of $\mathcal{T}_m$, called the even ribbon permutation group, is a "ghostly recollection" of the braid group and the Teo-Kane representation of the even ribbon permutation group is a projectivized version of the Jones representation of the braid group at a fourth root of unity, i.e., the representation relevant to Ising anyons.

A. Teo-Kane fundamental groups

In Sec. V, we consider only an even number of hedgehogs for physical reasons. In this section, we will include the odd case for mathematical completeness.

The Teo-Kane fundamental group is the fundamental group of the Teo-Kane configuration space K_m. As computed in Sec. V, $\mathcal{T}_m = \pi_1(K_m) \cong \mathbb{Z} \times \mathbb{Z}_2 \times E(\mathbb{Z}_2^m \rtimes S_m)$, where the subgroup $\mathcal{T}_m^r = \mathbb{Z}_2 \times E(\mathbb{Z}_2^m \rtimes S_m)$ is called the ribbon permutation group. Here, $E(\mathbb{Z}_2^m \rtimes S_m)$ is the subgroup of $\mathbb{Z}_2^m \rtimes S_m$ that comprises elements whose total parity in $\mathbb{Z}_2^m$ added to their parity in S_m is even. In the following, we will call the group $G_m = E(\mathbb{Z}_2^m \rtimes S_m)$ the *even* ribbon permutation group because it consists of the part of $\pi_1(Y_m)$ associated with even (2π) twisting. For the representations of the Teo-Kane fundamental groups, we will focus on the even ribbon permutation groups G_m. No generality is lost if we consider only irreducible representations projectively because irreducibles of $\mathbb{Z}$ and $\mathbb{Z}_2$ contribute only overall phases. But for reducible representations, the relative phases from representations of $\mathbb{Z}$ and $\mathbb{Z}_2$ might have physical consequences in interferometer experiments.

The even ribbon permutation group G_m is an index $= 2$ subgroup of $\mathbb{Z}_2^m \rtimes S_m$. To have a better understanding of G_m, we recall some facts about the important group $\mathbb{Z}_2^m \rtimes S_m$. The group $\mathbb{Z}_2^m \rtimes S_m$ is the symmetry group of the hypercube $\mathbb{Z}_2^m$, therefore it is called the hyperoctahedral group, denoted as C_m. C_m is also a Coxeter group of type B_m or C_m (warning: C_m is being used in the previous sentence to denote the hyperoctahedral group and, in this sentence, to denote a family of Coxeter groups), so in the mathematical literature it is also denoted as B_m or BC_m. To avoid confusion with the braid group $\mathcal{B}_m$, we choose to use the hyperoctahedral group notation C_m. The group C_m has a faithful representation as signed permutation matrices in the orthogonal group $O(m)$: matrices with exactly one nonzero entry ± 1 in each row and column. Therefore, it can also be realized as a subgroup of the permutation group S_{2m}, called signed permutations: $\sigma : \{\pm 1, \pm 2, \ldots, \pm m\} \to \{\pm 1, \pm 2, \ldots, \pm m\}$ such that $\sigma(-i) = -\sigma(i)$.

We will denote elements in C_m by a pair (b,g), where $b = (b_i) \in \mathbb{Z}_2^m$ and $g \in S_m$. Recall the multiplication of two elements (b,g) and (c,h) is given by $(b,g) \cdot (c,h) = (b + g.c, gh)$, where $g.c$ is the action of g on c by permuting its coordinates. Let $\{e_i\}$ be the standard basis elements of $\mathbb{R}^m$. To save notation, we will also use it for the basis element of $\mathbb{Z}_2^m$. As a signed permutation matrix e_i introduces a -1 into the ith coordinate x_i. Let s_i be the transposition of S_m that interchanges i and $i+1$. As a signed permutation matrix, it interchanges the coordinates x_i, x_{i+1}. There is a total parity map $\det : C_m \to \mathbb{Z}_2$ defined as $\det(b,g) = \sum_{i=1}^m b_i + \text{parity}(g) \text{mod} 2$. We denote the total parity map as det because in the realization of C_m as signed permutation matrices in $O(m)$, the total parity is just the determinant. Hence G_m, as the kernel of det, can be identified as a subgroup of $SO(m)$. The set of elements $t_i = (e_i, s_i), i = 1, \ldots, m-1$ generates G_m. As a signed permutation matrix, $t_i(x_1, \ldots, x_i, x_{i+1}, \ldots, x_m) = (x_1, \ldots, -x_{i+1}, x_i, \ldots, x_m)$.

Given an element $(b,g) \in C_m$, let $\mathbb{Z}_2^{m-1}$ be identified as the subgroup of $\mathbb{Z}_2^m$ such that $\sum_{i=1}^m b_i$ is even. Then we have the following:

Proposition VI.1. 1. For $m \geqslant 2$, the even ribbon permutation group G_m has a presentation as an abstract group:

$$\langle t_1, \ldots, t_{m-1} | t_i^4 = 1, i = 1, \ldots, m-1,$$
$$\left(t_i t_{i+1}^{-1}\right)^3 = \left(t_i^{-1} t_{i+1}\right)^3 = 1, i = 1, \ldots, m-2 \rangle.$$

This is the set of generators of the group, together with relations that they obey; every element of the group can be written as a product of these generators.

2. The exact sequence

$$1 \to \mathbb{Z}_2^{m-1} \to G_m \to S_m \to 1$$

splits if and only if m is odd.

3. When m is even, a normalized 2-cocycle $f(g,h) : S_m \times S_m \to \mathbb{Z}_2^{m-1}$ for the extension of S_m by $\mathbb{Z}_2^{m-1}$ above can be chosen as $f(g,h) = 0$ if g or h is even and $f(g,h) = e_{g(1)}$ if g and h are both odd.

We briefly give the idea of the proof of Proposition VI.1. For (1), first we use a presentation of C_m as a Coxeter group of

type B_m: $< r_1, \ldots, r_m | r_i^2 = 1, (r_1 r_2)^4 = 1, (r_i r_{i+1})^3 = 1, i = 2, \ldots, m-1 >$. Then the Reidemeister-Schreier method[55] allows us to deduce the presentation for G_m above. For (2), when m is odd, a section s for the splitting can be defined as $s(g) = (0,g)$ if g is even and $s(g) = [(11\cdots 1), g]$ if g is odd. When m is even, that the sequence does not split follows from the argument in Ref. 56. For (3), we choose a set map $s(g) = (0,g)$ if g is even and $s(g) = (e_1, g)$ if g is odd. Then a direct computation of the associated factor set as on p. 91 of Ref. 57 gives rise to our 2-cocycle.

As a remark, we note that there are another two obvious maps from the hyperoctahedral group C_m to $\mathbb{Z}_2$. One of them is the sum of bits in b of (b,g). The kernel of this map is the Coxeter group of type D_m, which is a semidirect product of $\mathbb{Z}_2^{m-1}$ with S_m. The two groups D_m and G_m have the same order, and are isomorphic when m is odd (the two splittings induce the same action of S_m on $\mathbb{Z}_2^{m-1}$), but different when m is even. To see the difference, consider the order 2 automorphism $\phi : C_m \to C_m$ given by $\phi(x) = \det(x)x$. Its restriction is the identity on G_m, but nontrivial on D_m.

B. Teo-Kane unitary transformations

Suppose there are m hedgehogs in B^3. A unitary transformation $T_{ij} = e^{\frac{\pi}{4}\gamma_i\gamma_j}$ of the Majorana fermions is associated with the interchange of the (i,j) pair of the hedgehogs. Interchanging the same pair twice results in the "braidless" operation $T_{ij}^2 = \gamma_i\gamma_j$. The Majorana fermions $\gamma_i, i = 1,2,\ldots,m$ form the Clifford algebra $\mathrm{Cl}_m(\mathbb{C})$. Therefore, the Teo-Kane unitary transformations act as automorphisms of the Clifford algebra,

$$T_{ij} : \gamma \to T_{ij}\gamma T_{ij}^\dagger.$$

The projective nature of the Teo-Kane representation rears its head here already as an overall phase cannot be constrained by such actions. Do these unitary transformations afford a linear representation of the Teo-Kane fundamental group K_m? If so, what are their images? The surprising fact is that the Teo-Kane unitary transformations cannot give rise to a linear representation of the Teo-Kane fundamental group. The resulting representation is intrinsically projective. We consider only the even ribbon permutation group G_m from now on.

To define the Teo-Kane representation of G_m, we use the presentation of G_m by $t_i, i = 1, \ldots, m-1$ in Proposition VI.1. The associated unitary matrix for t_i comes from the Teo-Kane unitary transformation $T_{i,i+1}$. As was alluded above, there is a phase ambiguity of the Teo-Kane unitary matrix. We will discuss this ambiguity more in the next subsection. For the discussion below, we choose any matrix realization of the Teo-Kane unitary transformation with respect to a basis of the Clifford algebra $\mathrm{Cl}_m(\mathbb{C})$. A simple computation using the presentation of G_m in Proposition VI.1 verifies that the assignment of $T_{i,i+1}$ to t_i indeed leads to a representation of G_m. Another verification follows from a relation to the Jones representation in the next subsection. We can also check directly that this is indeed the right assignment for $T_{i,i+1}^2$: $\gamma_i \to -\gamma_i, \gamma_{i+1} \to -\gamma_{i+1}$. In the Clifford algebra $\mathrm{Cl}_m(\mathbb{C})$, γ_i, γ_{i+1} correspond to the standard basis element e_i, e_{i+1}. The element t_i^2 of G_m is $(e_i + e_{i+1}, 1)$. As a signed permutation matrix, t_i^2 sends $(x_1, \ldots, x_i, x_{i+1}, \ldots, x_m)$ to $(x_1, \ldots, -x_i, -x_{i+1}, \ldots, x_m)$, which agrees with the action of $T_{i,i+1}^2$ on γ_i, γ_{i+1}.

To see the projectivity, the interchange of the $(i, i+1)$-pair hedgehogs corresponds to the element $t_i = (e_i, s_i) \in G_m$. Performing the interchange twice gives rise to the element $t_i^2 = (e_i + e_{i+1}, 1)$, denoted as x_i. Because x_i's are elements of a subgroup of G_m isomorphic $\mathbb{Z}_2^{m-1}$, obviously we have $x_i x_{i+1} = x_{i+1} x_i$. On the other hand, $T_{i,i+1}^2 T_{i+1,i+2}^2 = \gamma_i\gamma_{i+1} \cdot \gamma_{i+1}\gamma_{i+2} = \gamma_i\gamma_{i+2}$, and $T_{i+1,i+2}^2 T_{i,i+1}^2 = \gamma_{i+1}\gamma_{i+2} \cdot \gamma_i\gamma_{i+1} = -\gamma_i\gamma_{i+2}$. Because it is impossible to encode the -1 in the x_i's of G_m, the representation has to be projective. Note that an overall phase in T_{ij} will not affect the conclusion. In the next subsection, we will see this projective representation comes from a linear representation of the braid group—the Jones representation at a fourth root of unity and the -1 is encoded in the Jones-Wenzl projector $p_3 = 0$.

To understand the images of the Teo-Kane representation of G_m, we observe that the Teo-Kane unitary transformations $T_{ij} = e^{\frac{\pi}{4}\gamma_i\gamma_j}$ lie inside the even part $\mathrm{Cl}_m^0(\mathbb{C})$ of $\mathrm{Cl}_m(\mathbb{C})$. Therefore, the Teo-Kane representation of G_m is just the spinor representation projectivized to $G_m \subset SO(m)$. It follows that the projective image group of Teo-Kane representation of the even ribbon permutation group is G_m as an abstract group. Recall $\mathrm{Cl}_m^0(\mathbb{C})$ is reducible into two irreducible sectors if m is even, and irreducible if m is odd. When m is even, it is important to know how the relative action of the center $Z(G_m) \cong \mathbb{Z}_2$ of G_m on the two irreducible sectors. The center of G_m is generated by the element $z = [(1\cdots 1), 1]$, whose corresponding Teo-Kane unitary transformation is $U = \gamma_1\gamma_2\cdots\gamma_m$ up to an overall phase. As we show in Appendix H, the relative phase of z on the two sectors is always -1.

VII. DISCUSSION

We now review and discuss the main results derived in this paper. Using the topological classification of free-fermion Hamiltonians,[26,27] we considered a system of fermions in 3D that is allowed to have an arbitrary superconducting order parameter and arbitrary band structure, and is also allowed to develop any other possible symmetry-breaking order such as charge-density wave, etc.—i.e., we do not require that any symmetries are preserved. We argued in Sec. III that the space of possible gapped ground states of such a system is topologically equivalent to $U(N)/O(N)$ for N large [for large N, the topology of $U(N)/O(N)$ becomes independent of N]. By extension, if we can spatially vary the superconducting order parameter and band structure at will with no regard to the energy cost, then there will be topologically stable pointlike defects classified by $\pi_2(U(\mathrm{N})/O(\mathrm{N})) = \mathbb{Z}_2$.

This statement begs the question of whether one actually can vary the order parameter and band structure in order to create such defects. In a given system, the energy cost may simply be too high for the system to wind around $U(N)/O(N)$ in going around such a defect. (This energy cost, which would include the condensation energy of various order parameters, is not taken into account in the free-fermion problem.) If we create such defects, they may be so costly that it is energetically favorable for them to simply unwind by closing the gap over large regions. (The energy cost associated with such an

unwinding depends on the condensation energy of the order parameters involved, which is not included in the topological classification.) Thus, $U(N)/O(N)$ is not the target space of an order parameter in the usual sense because the different points in $U(N)/O(N)$ may not correspond to different ground states with the same energy. However, in Sec. II, we have given at least one concrete model of free fermions with no symmetries in 3D in which the topological defects predicted by the general classification are present and stable. Furthermore, Teo and Kane[20] have proposed several devices in which these defects are simply superconducting vortices at the boundary of a topological insulator.

In order to understand the quantum mechanics of these defects, it is important to first understand their quantum statistics. To do this, we analyzed the multidefect configuration space; its fundamental group governs defect statistics. The configuration space of $2n$ pointlike defects of a system with "order parameter" taking values in $U(N)/O(N)$ is the space that we call K_{2n}. It can be understood as a fibration. The base space is X_{2n}, the configuration space of $2n$ points (which we know has fundamental group S_{2n} in dimension three and greater). Above each point in this base space there is a fiber $\mathcal{M}_{2n}$ which is the space of maps from the ball B^3 minus $2n$ fixed points to $U(N)/O(N)$ with winding number 1 about each of the $2n$ points. K_{2n} is the total space of the fibration. In Sec. V, we found that its fundamental group is $\pi_1(K_{2n}) = \mathbb{Z} \times \mathbb{Z}_2 \times E(\mathbb{Z}_2^{2n} \rtimes S_{2n})$, where $E(\mathbb{Z}_2^{2n} \rtimes S_m)$ is the subgroup of $\mathbb{Z}_2^m \rtimes S_{2n}$ comprising elements whose total parity in $\mathbb{Z}_2^{2n}$ added to their parity in S_{2n} is even.

The fundamental group of the configuration space is the same as the group of equivalence classes of space-time histories of a system with $2n$ pointlike defects. Because these different equivalence classes cannot be continuously deformed into each other, quantum mechanics allows us to assign them different unitary matrices. These different unitaries form a representation of the fundamental group of the configuration space of the system. However, we found in Sec. VI that Teo and Kane's unitary transformations are not a linear representation of $\pi_1(K_{2n})$, but a *projective representation*, which is to say that they represent $\pi_1(K_{2n})$ only up to a phase. Equivalently, Teo and Kane's unitary transformations are an ordinary linear representation of a *central extension* of $\pi_1(K_{2n})$, as discussed in Sec. VI.

This surprise lurks in a seemingly innocuous set of defect motions: those in which defects i and j are rotated by 2π and the order parameter field surrounding them relaxes back to its initial configuration. This has the following effect on the Majorana fermion zero mode operators associated with the two defects:

$$\gamma_i \to -\gamma_i, \quad \gamma_j \to -\gamma_j. \tag{57}$$

One might initially expect that two such motions, one affecting defects i and j and the other affecting i and k, would commute since they simply multiply the operators involved by $-$ signs. However, the unitary operator which generates (57) is[58]

$$U^{ij} = e^{i\theta}\gamma_i\gamma_j. \tag{58}$$

Thus, the unitary operators U^{ij} and U^{ik} do not commute; they anticommute:

$$U^{ij}U^{ik} = -U^{ik}U^{ij}. \tag{59}$$

However, as shown in Fig. 12, the corresponding classical motions can be continuously deformed into each other. Thus, a linear representation of the fundamental group of the classical configuration space would have these two operators commuting. Instead, the quantum mechanics of this system involves a projective representation.

It has recently been proposed that networks[59] of superconducting quantum wires with strong spin-orbit coupling in a magnetic field[60–62] can be used as a platform for topological quantum computation. Such networks support Majorana fermion zero modes at the boundaries between topologically superconducting and nontopological segments. By gating the wires, it is possible to change which parts of the network are topological and which parts are trivial. It is thereby possible to move the Majorana fermion zero modes. Thus far, 2D networks have been the primary focus. In such networks, it is possible to braid the Majorana fermions.[59,63,64] However, as we have seen in this paper, there is no need to restrict ourselves to 2D networks. Exchanging Majorana fermion zero modes in 3D networks can also implement the desired unitary transformations. As we have seen, the precise transformation implemented (i.e., whether we get t_i or t_i^{-1}) depends not on the handedness of the exchange but rather on the precise way in which the system is restored to its initial configuration. In particular, it was determined by which defect was twisted. One version of such a wire network[64] is a direct realization of the strong-coupling model or dimer model of Sec. II (except that the signs of the hopping matrix elements are varied in the dimer model of Ref. 64 rather than fixed in a π-flux pattern, as in Sec. II). A dimer corresponds to a link of the network that Majorana fermions can tunnel, thereby splitting the Majorana zero modes at the two vertices connected by the link. Even wire networks[59] that do not have such a direct relation with dimer models can be related as follows. The transition graph of a dimer configuration is the graph obtained by superimposing on it some fixed reference configuration and erasing those links where the two configurations agree. This leads to a collection of closed loops and open strings bounded by monomers. A configuration of the wire networks of Ref. 59 can be mapped to such a transition graph by identifying the topological segments with the loops and open strings and the nontopological segments with their complement. The ideas of Sec. II then apply.

Projective quasiparticle statistics were first proposed by Wilzcek,[30] who suggested a projective representation of the permutation group in which generators σ_j and σ_k anticommute for $|j-k| \geqslant 2$, rather than commuting. Read[25] criticized this suggestion as being in conflict with locality. We can sharpen Read's criticism as follows. Suppose that one can perform the operation σ_1 by acting on a region of space, called A, containing particles 1 and 2, and one can perform σ_3 by acting on a region called B, containing particles 3 and 4, and suppose that regions A and B are disjoint. Consider the following thought experiment: Let Bob perform operation σ_3 at time $t = 0$ and let Bob then repeat operation σ_3 at time $t = 1$. Let

Alice prepare a spin in the state $(1/\sqrt{2})(|\uparrow\rangle + |\downarrow\rangle)$ at time $t = -1$, and then let Alice perform the following sequence of operations. At time $t = -\epsilon$, for some small ϵ, she performs the unitary operation $|\uparrow\rangle\langle\uparrow| \otimes \sigma_1 + |\downarrow\rangle\langle\downarrow| \otimes I$, where I is the identity operation, leaving the particles alone. At time $t = +\epsilon$, she performs the unitary operation $|\uparrow\rangle\langle\uparrow| \otimes I + |\downarrow\rangle\langle\downarrow| \otimes \sigma_1$. Thus, if the spin is up, she performs σ_1 at time $t = -\epsilon$, while if the spin is down, she does it at time $t = +\epsilon$. Finally, at time $t = 2$, Alice performs the operation σ_1 again. One may then show that, owing to the anticommutation of σ_1 and σ_3, that the spin ends in the state $(1/\sqrt{2})(|\uparrow\rangle - |\downarrow\rangle)$. However, if Bob had not performed any operations, the spin would have ended in the original state $(1/\sqrt{2})(|\uparrow\rangle + |\downarrow\rangle)$. Thus, by performing these interchange operations, Bob succeeds in transmitting information to a spacelike separated region (if A and B are disjoint, and the time scale in the above thought experiment is sufficiently fast, then Alice and Bob are spacelike separated throughout).

Having seen this criticism, we can also see how Teo and Kane's construction evades it. The fundamental objects for Teo and Kane are not particles, but particles with ribbons attached. One may verify that, in every case where operations in Teo and Kane's construction anticommute, the two operations do not act on spatially disjoint regions owing to the attached ribbons. That is, the interchange of particles also requires a rearrangement of the order parameter field.

While this argument explains why a projective representation does not violate causality, it does not really explain why a projective representation actually occurs in this system. Perhaps one clue is the fact that the hedgehogs have long-ranged interactions in any concrete model. Even in the "best-case scenario," in which the underlying Hamiltonian of the system is $U(N)/O(N)$ invariant, there will be a linearly diverging gradient energy for an isolated hedgehog configuration. Thus, there will be a linear long-ranged force between hedgehogs. Consequently, one might adopt the point of view that, as a result of these long-ranged interactions, the overall phase associated with a motion of the hedgehogs is not a purely topological quantity (but will, instead, depend on details of the motion) and, therefore, need not faithfully represent the underlying fundamental group. As one motion is continuously deformed into another in Fig. 12, the phase of the wave function varies continuously from $+1$ to -1 as the order parameter evolution is deformed. It is helpful to compare this to another example of a projective representation: a charged particle in a magnetic field B. Although the system is invariant under the Abelian group of translations, the quantum mechanics of the system is governed by a non-Abelian projective representation of this group (which may be viewed as a linear representation of the "magnetic translation group"). A translation by a in the x direction, followed by a translation by b in the y direction, differs in its action on the wave function from the same translations in the opposite order by a phase abB/Φ_0 equal to the magnetic flux through the area ab in units of the flux quantum Φ_0. If we continuously deform these two sequences of translations into each other, the phase of the wave function varies continuously. For any trajectory along this one-parameter family of trajectories (or movie of movies), the resulting phase of the wave function is given by the magnetic flux enclosed by the composition of this trajectory and the inverse of the initial one. In our model of non-Abelian projective statistics, the phase changes continuously in the same way, but as a result of the evolution of the order parameter away from the defects, rather than as a result of a magnetic field.

An obvious question presents itself: Is there a related theory in which the hedgehogs are no longer confined? Equivalently, could 3D objects with non-Abelian ribbon permutation statistics ever be the weakly coupled low-energy quasiparticles of a system? The most straightforward route will not work: if we had a $U(N)$-invariant system and tried to gauge it to eliminate the linear confining force between hedgehogs, we would find that the theory is sick owing to the chiral anomaly. If we doubled the number of fermions in order to eliminate the anomaly, there would be two Majorana modes in the core of each hedgehog, and their energies could be split away from zero by a local interaction. This is not surprising because ribbon permutation statistics would seem likely to violate locality if the hedgehogs were truly decoupled (or had exponentially decaying interactions). On the other hand, if the hedgehogs were to interact through a Coulomb interaction (or, perhaps, some other power law), they would be neither decoupled nor confined, thereby satisfying the requirements that they satisfy locality and are low-energy particlelike excitations of the system. Elsewhere, we will describe a model that realizes this scenario.[65]

The non-Abelian projective statistics studied in the 3D class with no symmetry can be generalized to arbitrary dimension. As shown in Eq. (41), the classification of topological defects is independent of the spatial dimension. Thus, in any dimension d with no symmetry ($p = 0$), pointlike ($D = 0$) topological defects are classified by $\pi_0(R_{p-D+1}) = \pi_0(R_1) = \mathbb{Z}_2$. Moreover, it can be proved that analogous topological defects in different dimensions not only carry the same topological quantum number, but also have the same statistics. In Sec. V, we have defined the configuration space $\mathcal{M}_{2n}$ which is the space of maps from $B^3 \setminus \bigcup_{i=1}^{2n} B_i^3$ to $R_7 = U/O$, with specific boundary conditions. Now if we consider point defect in the class with no symmetry in 4D, the configuration space $\mathcal{M}_{2n}^{d=4}$ is defined by maps from $B^4 \setminus \bigcup_{i=1}^{2n} B_i^4$ to the classifying space $R_6 = Sp/U$. Noticing that $B^4 \setminus \bigcup_{i=1}^{2n} B_i^4$ is homotopy equivalent to the suspension of $B^3 \setminus \bigcup_{i=1}^{2n} B_i^3$, we obtain that $\mathcal{M}_{2n}^{d=4}$ is equivalent to the space of maps from $B^3 \setminus \bigcup_{i=1}^{2n} B_i^3 \to \Omega(Sp/U)$, where $\Omega(Sp/U)$ is the loop space of Sp/U. Because $\Omega(Sp/U) \simeq U/O$, we obtain $\mathcal{M}_{2n}^{d=4} \simeq \mathcal{M}_{2n}$. Thus we have proved that the configuration space $\mathcal{M}_{2n}$ is independent of the spatial dimension d. On the other hand, the fundamental group of the configuration space X_{2n} of $2n$ distinct points in B^d is independent of d as long as $d > 2$. Consequently, the space K_{2n} defined by the fibration $\mathcal{M}_{2n} \to K_{2n} \to X_{2n}$ is also topologically independent of spatial dimension d for $d > 2$. Thus, the proof we did for $d = 3$ applies to generic dimension, and non-Abelian projective statistics exist in any spatial dimension $d > 3$ for point defects in the no-symmetry class. A similar analysis applies to extended defects with dimension $D > 0$. When the spatial dimension is increased by 1 and the symmetry class remains the same, the classifying space is always changed

from R_{2+p-d} to $R_{2+p-d-1} \simeq \Omega^{-1}(R_{2+p-d})$. Consequently, at least for simple defects with the topology of S^D, the statistics is independent of spatial dimension d as long as d is large enough. For point defects, the "lower critical dimension" is $d = 3$, while for line defects, i.e., $D = 1$, the "lower critical dimension" is at least $d = 4$ because in $d = 3$ we can have braiding between loops.

APPENDIX A: TOPOLOGICAL CLASSIFICATION OF HAMILTONIANS WITH CHARGE CONSERVATION BUT WITHOUT TIME-REVERSAL SYMMETRY

For the sake of completeness, in this Appendix we give the topological classification of free-fermion Hamiltonians with charge conservation but not time-reversal symmetry. We begin with the 0D case. The charge-conservation condition is most transparent when the Hamiltonian is written in terms of complex fermion operators, c_i, $c_i^\dagger$, rather than Majorana fermions:

$$H = \sum_{i,j} h_{ij} c_i^\dagger c_j. \tag{A1}$$

The indices i, j range from 1 to N, the number of bands. As long as there is one c and one $c^\dagger$ in each term, the Hamiltonian will conserve charge. We make no further assumption about the Hamiltonian. As in our discussion in Sec. III, we are only interested in the topology of the space of such Hamiltonians, so two Hamiltonians are considered to be equivalent if they can be continuously deformed into each other without closing the gap. Thus, we can flatten the spectrum and assume that H and, therefore, h_{ij} only has eigenvalues ± 1; any other gapped Hamiltonian can be continuously deformed so that it satisfies this condition. Then, h_{ij} can be written in the form

$$h = U^\dagger \begin{pmatrix} 1 & & & & \\ & \ddots & & & \\ & & 1 & & \\ & & & -1 & \\ & & & & \ddots \\ & & & & & -1 \end{pmatrix} U, \tag{A2}$$

with k diagonal entries equal to $+1$ and $N - k$ diagonal entries equal to -1 for some k. The space of such matrices h_{ij} is equal to the space of matrices U, namely, $U(N)$, modulo those matrices U that commute with the diagonal matrix above, namely, $U(k) \times U(N - k)$. Thus, the space of matrices h_{ij} is topologically equivalent to

$$\mathcal{M}_{2N} = \bigcup_{k=0}^{N} U(N)/[U(k) \times U(N-k)]. \tag{A3}$$

For N sufficiently large, the topology of these spaces cannot depend on k, so we write this simply as $\mathbb{Z} \times U(N)/[U(N/2) \times U(N/2)]$.

Now suppose that we have a 1D system. As in Sec. III, we will consider the Dirac equation that approximates the Hamiltonian in the vicinity of the points in the Brillouin zone at which it becomes small. We write

$$H = \psi^\dagger (i\gamma_1 \partial_1 + M)\psi. \tag{A4}$$

Here, we have suppressed the band index on the fermion operators $\psi^\dagger$ and ψ. Both γ and M are $N \times N$ matrices; γ_1 satisfies $\mathrm{tr}(\gamma_1) = 0$ and $\gamma_1^2 = 1$. Then, the different fermion operators will have the same gap if

$$\{\gamma_1, M\} = 0, \quad M^2 = 1. \tag{A5}$$

Viewed as a linear operator on $\mathbb{C}^N$, γ_1 defines two $N/2$-dimensional subspaces, its eigenvalue $+1$ eigenspace, and its eigenvalue -1 eigenspace. Let us call them X_+ and X_-. Because $\{\gamma_1, M\} = 0$, M is a map from X_+ to X_-. Thus, M is an isometry between two copies of $\mathbb{C}^{N/2}$ and can be viewed as an element of $U(N/2)$. This can be made more concrete by taking, without loss of generality:

$$\gamma_1 = \begin{pmatrix} \mathbb{I} & 0 \\ 0 & -\mathbb{I} \end{pmatrix}, \tag{A6}$$

where $\mathbb{I}$ is the $N/2 \times N/2$ identity matrix. Then, M can be any matrix of the form

$$M = \begin{pmatrix} 0 & U^\dagger \\ U & 0 \end{pmatrix}, \tag{A7}$$

for $U \in U(N/2)$.

Now, consider a 2D system. The Dirac equation takes the form

$$H = \psi^\dagger (i\gamma_j \partial_j + M)\psi, \tag{A8}$$

with $j = 1,2$. As before, γ_1 defines two $N/2$-dimensional subspaces, X_+ and X_-. Then $i\gamma_2 M$ commutes with γ_1 and squares to 1. Thus, it divides X_+ into two spaces, X_+^1 and X_-^2, which are the $+1$ and -1 eigenspaces for $i\gamma_2 M$ (and it similarly divides for X_-). Thus, a choice of M is a choice of linear subspace X_+^1 of X_+ or, in other words,

$$\begin{aligned} M &\in \bigcup_{k=0}^{N} U(N/2)/[U(k) \times U(N/2-k)] \\ &= \mathbb{Z} \times U(N/2)/[U(N/4) \times U(N/4)]. \end{aligned} \tag{A9}$$

Continuing in this way, we derive Table III analogous to Table I but for charge-conserving systems without time-reversal symmetry. Table III has period-2 as the dimension is increased whereas Table I had period-8.

The two rows in Table III correspond to the presence or absence of an additional unitary symmetry, which requires the eigenvalues of the Hamiltonian to come in pairs with equal and opposite energy $\pm E_i$, i.e., a sublattice symmetry, as discussed in Sec. III F. Consider a 0D system described by the Hamiltonian (A1) with such a symmetry. Then there is a unitary matrix U, satisfying

$$\{U, h\} = 0, \quad U^2 = 1. \tag{A10}$$

We can now apply the same logic to U and M that we applied to γ_1 and M when considering 1D systems. Thus, $M \in U(N/2)$. More generally, it is clear that U plays the role of an extra γ matrix, so the row of Table III for systems with sublattice symmetry is just shifted by one from the row of the table for systems without it.

In order to compute the homotopy groups of these classifying spaces, it is useful to follow the logic that we employed in Secs. III D and III F. We approximate the loop space of $U(N)$

TABLE III. The period-2 (in both dimension and number of symmetries) table of classifying spaces for charge-conserving free-fermion Hamiltonians without time-reversal symmetry. The systems have N complex fermion fields in dimensions $d = 0,1,2,3,\ldots$ with no additional symmetries (apart from charge conservation) or with an additional symmetry, such as a sublattice symmetry. Moving p steps to the right and p steps down leads to the same classifying space (but for $1/2^p$ as many fermion fields), which is a reflection of Bott periodicity, as explained in the text. The number of disconnected components of any such classifying space—i.e. the number of different phases in that symmetry class and dimension—is given by the corresponding π_0, which may be found in Eq. (A13). Higher homotopy groups, which classify defects, can be computed using Eq. (A12).

Dimension:	0	1	2	3	⋯
No symmetry	$\mathbb{Z} \times \frac{U(N)}{U(N/2)\times U(N/2)}$	$U(N/2)$	$\mathbb{Z} \times \frac{U(N/2)}{U(N/4)\times U(N/4)}$	$U(N/2)$	⋯
Sublattice symmetry	$U(N/2)$	$\mathbb{Z} \times \frac{U(N/2)}{U(N/4)\times U(N/4)}$	$U(N/4)$	$\mathbb{Z} \times \frac{U(N/4)}{U(N/8)\times U(N/8)}$	⋯

by minimal geodesics from $\mathbb{I}$ to $-\mathbb{I}$: $L(\lambda) = e^{i\lambda A}$, where A is a Hermitian matrix satisfying $A^2 = 1$ so that $L(0) = \mathbb{I}$ and $L(\pi) = -\mathbb{I}$. Any such matrix A divides $\mathbb{C}^N$ into $+1$ and -1 eigenspaces or, in other words, it can be written in the form

$$A = U^\dagger \begin{pmatrix} \mathbb{I}_k & 0 \\ 0 & -\mathbb{I}_{N-k} \end{pmatrix} U, \tag{A11}$$

where $\mathbb{I}_m$ is the $m \times m$ identity matrix. Therefore, $A \in \mathbb{Z} \times \frac{U(N)}{U(N/2)\times U(N/2)}$. Thus, the loop space of $U(N)$ can be approximated by $\mathbb{Z} \times \frac{U(N)}{U(N/2)\times U(N/2)}$. Thus, $\pi_k(U(N)) = \pi_{k-1}(\mathbb{Z} \times U(N)/[U(N/2) \times U(N/2)])$.

To compute homotopy groups of $\mathbb{Z} \times U(N)/[U(N/2) \times U(N/2)]$, consider the homotopy long exact sequence associated to the fibration

$$U(N/2) \to U(N) \to U(N)/U(N/2).$$

It tells us that

$$\cdots \pi_{i-1}(U(N/2)) \to \pi_i(U(N)) \to \pi_i(U(N)/U(N/2)) \cdots.$$

If we are in the stable limit, i.e., for N sufficiently large, then $\pi_{i-1}(U(N/2)) = \pi_i(U(N))$, so $\pi_i(U(N)/U(N/2)) = 0$. Now consider the fibration

$$U(N/2) \to U(N)/U(N/2) \to U(N)/(U(N/2) \times U(N/2)).$$

Then, because $\pi_i(U(N)/U(N/2)) = 0$, the associated homotopy exact sequence is simply

$$0 \to \pi_i(U(N)/[U(N/2) \times U(N/2)]) \to \pi_{i-1}(U(N/2)) \to 0,$$

so $\pi_i(U(N)/[U(N/2) \times U(N/2)]) = \pi_{i-1}(U(N/2))$.

Combining these two relations, we have Bott periodicity for the unitary group:

$$\begin{aligned} \pi_k(U(N)) &= \pi_{k-1}(\mathbb{Z} \times U(N)/[U(N/2) \times U(N/2)]) \\ &= \pi_{k-2}(U(N/2)). \end{aligned} \tag{A12}$$

By inspection, we see that

$$\pi_0(U(N)) = 0, \tag{A13}$$

$$\pi_0(\mathbb{Z} \times U(N)/[U(N/2) \times U(N/2)]) = \mathbb{Z}. \tag{A14}$$

Combining this with Eq. (A12), we learn that the even homotopy groups of $U(N)$ vanish and the odd ones are $\mathbb{Z}$; the reverse holds for $U(N)/[U(N/2) \times U(N/2)]$.

These homotopy groups can be used to classify the different possible phases and topological defects of systems in the symmetry classes and dimensions in Table III. Similar to Table II in Sec. III F, we list in Table IV the nontrivial topological physical systems in the two symmetry classes. In Ref. 26, these were called A and AIII, respectively, following the corresponding classification in random matrix theory.[35,36] In A class (with charge conservation and without sublattice symmetry or time-reversal symmetry) a topological nontrivial state is classified by an integer in 2D, which is the famous quantum Hall system. In the AIII class with sublattice symmetry, in 1D the carbon nanotube or graphene ribbon can be considered as an example with nontrivial edge states. Compared to the requirement of this symmetry class, the carbon nanotube has too high symmetry because time-reversal symmetry is present. An orbital magnetic field can be coupled minimally to the carbon nanotube to get an example system with exactly the required symmetry of AIII class. In 3D there should be an integer classification of the AIII class but no realistic topological nontrivial material is known yet.

APPENDIX B: UNDERSTANDING THE ROLE OF SPATIAL DIMENSION IN THE CLASSIFICATION OF FREE FERMION SYSTEMS

In Sec. III and Appendix A, we have seen that increasing the spatial dimension moves a system through the progression of classifying spaces oppositely to adding symmetries that

TABLE IV. Topological periodic table in physical dimensions 1,2,3 of the complex classes. A and AIII in the first column labels the symmetry classes in the Zirnbauer classification (Refs. 35 and 36). The second column are the requirements to the physical systems that can realize the corresponding symmetry classes. The three columns $d = 1,2,3$ list the topological states in the spatial dimensions 1,2,3 respectively. 0 means the topological classification is trivial. "Z" stands for the topological state that has not been realized in realistic materials.

Symmetry classes	Physical realizations	$d = 1$	$d = 2$	$d = 3$
A	Generic ins.	0	Quantum Hall (GaAs, etc.)	0
AIII	Bipartite ins.	Carbon nanotube	0	Z

square to -1 (but in the same direction as adding symmetries that square to 1). The classifying space for d-dimensional systems is the loop space of the classifying space for $(d+1)$-dimensional systems with the same symmetries. Symbolically,

$$R_{2+p-d} = \Omega(R_{2+p-(d+1)}), \tag{B1}$$

where Ω denotes the loop space and, as in Sec. III, p is the number of symmetries and d is the spatial dimension. Thus, in using Tables I and III, moving one step to the right, which increases the dimension and one step down, which increases the number of symmetries, leaves the classifying space the same.

We explained this in Sec. III and Appendix A by expanding the Hamiltonian about the point(s) in the Brillouin zone where the gap is minimum where it has the form of the Dirac Hamiltonian. Analyzing the space of such Hamiltonians then amounts to analyzing the possible mass terms, namely, the space of matrices which square to -1 and anticommute with the γ matrices and antiunitary symmetry generators. One might worry that this analysis is not completely general because it depends on our ability to expand the Hamiltonian in the form of the Dirac Hamiltonian, and this seems nongeneric. However, Kitaev's texture theorem (unpublished) states that a general gapped free-fermion H canonically deforms to a Dirac Hamiltonian as above without closing the gap, so only these need to be considered.

Another more algebraic approach involves the suspension isomorphism in KR theory. In complex K theory: $KU^{n+d}(X \wedge S^d) \simeq KU^n(X)$, however, for $KR[A]$ with $^-(x_1,\ldots,x_d) = (-x_1,\ldots,-x_d)$, one gets $KR^{n-d}(X \wedge \bar{S}^d) \simeq KO^n(X)$. [There is a similar isomophism in twisted K theory, where $(^-)^2 = -1$.] In (translation-invariant) particle-hole symmetric systems it can be argued via a high-frequency cutoff that momentum space directions correspond not to $\overline{\mathbb{R}}^d$ but actually to $\overline{S}^d$. (Here,

$$\begin{aligned}\frac{i}{4}\sum \gamma_{x_i}^\dagger A_{x_i-x_j}\gamma_{x_j} &= \frac{i}{4}\sum \gamma_{x_i} A_{x_i-x_j}\gamma_{x_j}^\dagger \\ &= -\frac{i}{4}\sum \gamma_{x_j}^\dagger A_{x_i-x_j}\gamma_{x_i} \\ &= -\frac{i}{4}\sum \gamma_{x_i}^\dagger A_{x_i-x_j}\gamma_{x_j},\end{aligned}$$

so reversing a space coordinate introduces a minus sign.)

If translational symmetry is broken to a lattice $\mathbb{Z}^d$ symmetry, then momentum space becomes a d-torus, T^d, and it should replace S^d in the left-hand side of the two isomorphisms above. Fortunately, all K theories are generalized cohomology theories and thus depend only on *stable* homotopy type. Tori have extremely simple stable types:

$$\sum T^d = \sum[\vee_d(S^1) \vee \vee_{\binom{d}{2}}(S^2) \vee \cdots \vee \vee_{\binom{d}{d-1}}(S^{d-1}) \vee S^d], \tag{B2}$$

where $\sum$ denotes suspension. The same formula holds with $(^-)$ above all spaces.

Thus, for lattice-translational symmetry, we may employ

$$KR^{n-d}(X \wedge \bar{T}^d) \simeq \widetilde{KO}^n(X) \oplus_{\binom{d}{d-1}} \widetilde{KO}^{n-1}(X) \oplus_{\binom{d}{d-2}} \cdots \oplus_{\binom{d}{1}} \widetilde{KO}^{n-d+1}(X) \oplus KO^{n-d}(X). \tag{B3}$$

In this Appendix, we want to sketch here a third way of understanding "spatial dimension = de-loop" that is more geometric than either of the alternatives above.

We warn the reader that this section is only a "sketch," so there may be tricky analytic details regarding the precise definition of the controlled spaces that we have overlooked. The math literature[66] in controlled K theory is constructed in a less naive context. We are not sure if there is something essential we are missing.

Let $O_\mathbb{Z}$ be a limiting large orthogonal group with integer ($\mathbb{Z}$) control and a topology (such as compact and open) where sliding a disturbance off to $\pm\infty$ converges to the identity. That is, $O_\mathbb{Z}$ is the set of infinite matrices $\mathcal{O}_{I,J}$ with a finite-to-one map (decapitalizing) $J \mapsto j \in \mathbb{Z}$ such that $|\mathcal{O}_{I,J}| \leqslant e^{-\text{const}|i-j|}$ and $\mathcal{O}^*_{I,J}\mathcal{O}_{I,K} = \delta_{J,K}$ with the following identifications: Any matrix $\mathcal{O}_{I,J}$ with $\mathcal{O}_{I_0,J} \equiv \delta_{I_0,J}$ is equivalent to the matrix with one less row and column obtained by removing the I_0^{th} row and I_0^{th} column.

By changing l, the number of distinct J maps that map to a given j, we can choose any desired constant in the exponential decay $\exp(-\text{const}|i-j|)$. We could also have chosen to study the class of infinite matrices with $\mathcal{O}_{I,J} = 0$ for $|i-j| > 1$; in this case, the matrix $\mathcal{O}_{I,J}$ is a banded matrix, which is nonzero only within distance l of the main diagonal. We refer to the case of exponential decay as "soft control," while we refer to the case that $\mathcal{O}_{I,J} = 0$ for $|i-j| > 1$ as "strict control."

The key claim in this "third" approach is as follows.

Claim. $O_\mathbb{Z} \simeq \frac{O}{O\times O} \times \mathbb{Z} = BO \times Z$ ($\simeq$ denotes weak homotopy type).

We take for $BO \times \mathbb{Z}$ the well-known model of pairs, considered as formal differences, of transverse (not necessarily spanning) subspaces (L_+, L_-) of a d-dimensional real vector space $\mathbb{R}^d$ (with d finite and a limit taken as $d \to \infty$.) The $\mathbb{Z}$ coordinate above is the index $\dim L_+ - \dim L_-$.

Here are the maps: Choose any cut in $\mathbb{Z}$, say, Π_+ projects to J with $j \geqslant 0$ and Π_- projects to J with $j < 0$. Set

$$f : O_\mathbb{Z} \to BO \times \mathbb{Z},$$
$$f(O) = [\ker(\Pi_+ \circ O|_{S_+}), \ker(\Pi_- \circ O|_{S_-})],$$

where $S_{+(-)}$ is the space of basis elements mapping to $[0,L]([-L,-1])$, where $l \gg$ the decay constant for $O_\mathbb{Z}$, and both kernels are regarded as subsets of the span $\mathbb{R}^d$ of elements mapping to $[-L,L]$. Given $(L_+,L_-) \in BO \times \mathbb{Z}$, define $g(L_+,L_-) \in O_Z$ as follows. Think of $L_\pm \subset \mathbb{R}^d$ with P denoting the perpendicular subspace to $\text{span}(L_+,L_-)$. The infinite vector space on which $g(L_+,L_-)$ acts is spanned by a copy of $\mathbb{R}^d$ for each $i \in \mathbb{Z}$. $O = g(L_+,L_-)$ acts as the identity on each $P \times i$, translation by $-1 \in \mathbb{Z}$ on each $L_+ \times i$ and translation by $+1 \in \mathbb{Z}$ on each $L_- \times i$.

Note. The use of the kernel above is correct in the case of strict control. In the case of soft control, we should replace the kernel by the projector onto right singular vectors of $\Pi_+ \circ O|_{S+}$ with singular values of less than or equal to some quantity that is exponentially small in L.

It is immediate that $f \circ g = \text{Id}_{BO\times\mathbb{Z}}$. On the other hand, $g \circ f$ seems to turn a general $O \in O_\mathbb{Z}$ into a very special form (no rotation at all, just various subspaces sliding left and right.) However, we claim that there is a deformation retraction of $O_\mathbb{Z}$ to maps that take this simple form: $r : O_\mathbb{Z} \to \{\text{slides}\} \subseteq O_\mathbb{Z}$.

First, think about a fiberwise O (no sliding) that is X over some $i \in \mathbb{Z}$ and Id over other $j \neq i \in \mathbb{Z}$. Note that

$$\begin{vmatrix} X & 0 \\ 0 & -X \end{vmatrix} \sim \begin{vmatrix} 0 & \mathrm{Id} \\ \mathrm{Id} & 0 \end{vmatrix}$$

via the canonical homotopy

$$\cos\left(\frac{\pi t}{2}\right)\begin{vmatrix} X & 0 \\ 0 & -X \end{vmatrix} + \sin\left(\frac{\pi t}{2}\right)\begin{vmatrix} 0 & \mathrm{Id} \\ \mathrm{Id} & 0 \end{vmatrix}.$$

When d is even (which we may assume) there are further canonical homotopies so that

$$\begin{vmatrix} 0 & \mathrm{Id} \\ \mathrm{Id} & 0 \end{vmatrix} \sim \begin{vmatrix} \sigma_{\mathbb{Z}} & 0 & & \\ 0 & \sigma_{\mathbb{Z}} & & \\ & & \sigma_{\mathbb{Z}} & 0 \\ & & 0 & \sigma_{\mathbb{Z}} \end{vmatrix} \sim |\,\mathrm{Id}\,|$$

Now a "Eilenberg swindle" runs X (canonically) toward $+\infty$.

$$\frac{\mathrm{Id}\ X\ \mathrm{Id}}{(i-1)\ i\ (i+1)} \rightsquigarrow \frac{\mathrm{Id}\ X\ -X\ X\ -X\ \cdots}{i\ (i+1)(i+2)(i+3)(i+4)\cdots} \rightsquigarrow \frac{\mathrm{Id}\ \mathrm{Id}\ \mathrm{Id}\ \mathrm{Id}\ \cdots}{i\ (i+1)(i+2)(i+3)\cdots}$$

Reusing this trick, any fiberwise, though now it is better to slide from the center out to both $\pm\infty$, X can be canonically connected to $\mathrm{Id} \in O_{\mathbb{Z}}$. Similarly, one can (canonically) deform the general $O \in O_{\mathbb{Z}}$ to a sum of three pieces—fixed, left sliding, right sliding—and this is the deformation retraction r written above.

We now promote the (weak) homotopy equivalence $O_{\mathbb{Z}} \simeq BO \times \mathbb{Z}$ to an entire table where the rows are all (weak) homotopy equivalences:

$$\begin{array}{llllll} O_{\mathbb{Z}^3}/U_{\mathbb{Z}^3} & O_{\mathbb{Z}+\mathbb{Z}} & \simeq_2 & O_{\mathbb{Z}}/O_{\mathbb{Z}\times\mathbb{Z}\times\mathbb{Z}} & & U/O \\ \cdots & O_{\mathbb{Z}+\mathbb{Z}}/U_{\mathbb{Z}+\mathbb{Z}} & & O_{\mathbb{Z}} & \simeq_1 & BO\times\mathbb{Z} \\ & \cdots & & O_{\mathbb{Z}}/U_{\mathbb{Z}} & \simeq_3 & O \\ & & & & \cdots & O/U \\ & & & & & \cdots \end{array}$$

Moving diagonally up and left, say, from $\simeq_1$ to $\simeq_2$ seems to be easy: One cuts the control space not at a point but along a codimension 1 hyperplane, in this case the line $y = -\frac{1}{2}$, and finds a pair of locally finite $\mathbb{Z}$-controlled kernels that define an element in $\frac{O_{\mathbb{Z}}}{O_{\mathbb{Z}\times O_{\mathbb{Z}}}} \times \mathbb{Z}$. However, there is one subtle point: The matrices Π_+ and O are both controlled; however, this does not imply that the projector onto the kernel of $\Pi_+ \circ O|_{S_+}$ is also controlled. If we knew that the singular values of $\Pi_+ \circ O|_{S_+}$ had a spectral gap separating the zero singular values (or, in the case of soft control, the singular values that are exponentially small in L) from the rest of the spectrum, then we could show that the projector onto the kernel had soft control, with decay constant set by the gap, but in the absence of knowledge of a gap, this seems to be a difficult technical step.

Moving down the array, say, from $\simeq_1$ to $\simeq_3$, requires "looping" $\simeq_1$. We must check that $\Omega(O_{\mathbb{Z}}) \simeq \frac{O_{\mathbb{Z}}}{U_{\mathbb{Z}}}$, i.e., that the first step in Bott's ladder of eight rungs holds with $\mathbb{Z}$ controls. To do this, one must do a Lie theory in $O_{\mathbb{Z}}$: Find the shortest geodesic arcs from Id to $-\mathrm{Id}$ in $O_{\mathbb{Z}}$, understand which directions they pick out in the Lie algebra $O_{\mathbb{Z}}$ and that their midpoints are $\mathbb{Z}$-controlled complex structures, and finally make the analogs of Bott's index calculations. The initial step is to consider a representative for a "$\mathbb{Z}$-controlled complex structure" (where coordinates are consecutive in $\mathbb{Z}$):

$$J = \mathcal{O}^+ \begin{vmatrix} \ddots & & & & \\ & 0\ 1 & & & \\ & -1\ 0 & & & \\ & & 0\ 1 & & \\ & & -1\ 0 & & \\ & & & \ddots & \end{vmatrix} \mathcal{O}, \quad \mathcal{O} \in O_{\mathbb{Z}},$$

and see that the 1-parameter subgroup $\{e^{t \log \mathcal{O}}\} \subset O_{\mathbb{Z}}$ retains $\mathbb{Z}$ control. This may be checked by writing

$$\log J = \frac{\pi}{2} J,$$

because $J^2 = -I$. This yields $\mathbb{Z}$ controls on $\log J$ and hence on the entire one-parameter subgroup.

One interesting feature of this approach is that we are able to classify different symmetry classes of controlled unitaries on a line. The controlled unitaries $U_{\mathbb{Z}}$ are classified by an integer. This integer is precisely the "flow" described by Kitaev.[15] If the controlled unitary is assumed to be symmetric, it is in the orthogonal group, and again $O_{\mathbb{Z}}$ is classified by an integer. However, if the unitary is chosen to be self-dual, in this case $\frac{U_{\mathbb{Z}}}{Sp_{\mathbb{Z}}}$ has a $\mathbb{Z}_2$ classification. Ryu *et al.*[26] note (see Tables I or IV of that paper) that each of the ten different symmetric spaces can be obtained by considering the exponential of Hamiltonians lying in ten different symmetry classes; for example, given a Hermitian matrix H, the exponential $\exp(iHt)$ is a unitary matrix, while if H is antisymmetric and Hermitian, the exponential $\exp(iHt)$ is an orthogonal matrix. However, the classification of unitaries here implies that there can be an obstruction to writing a controlled unitary as an exponential $\exp(iHt)$ with H of the correct symmetry class and H also controlled.

APPENDIX C: PHASE SYMMETRY UNBROKEN

If the phase symmetry of the order parameter is unbroken (i.e., if we allow gradients in the overall phase), then the effective sigma model target is U/O, not $\widetilde{U/O}$. This means that at every stage of the calculation, an additional circle $\frac{U(1)}{O(1)}$ or $K(\mathbb{Z},1)$ product factor must be added to the target space. This leads to *no* change for $\pi_2(Y)$ or $\pi_1(R)$ [essentially because $\pi_2(\frac{U(1)}{O(1)}) \cong 0$], however, $\pi_1(Y)$ and $\pi_0(R)$ pick up an additional integer, which is the winding number around this circle. Thus, (C1) below,

$$\begin{array}{ccccccccc} \pi_2(Y) & \xrightarrow{\partial_2} & \pi_1(R) & \longrightarrow & \pi_1(\widetilde{K}_{2n}) & \longrightarrow & \pi_1(Y) & \xrightarrow{\partial_1} & \pi_0(R) \\ & & & & \wr\| & & & & \wr\| \\ & & & & \mathbb{Z}_2^{2n} \rtimes S_{2n} & & & & \mathbb{Z}_2 \end{array} \tag{C1}$$

is replaced by (C2),

$$\begin{array}{ccccc} \pi_2(Y^{\text{new}}) & \xrightarrow{\partial_2} & \pi_1(R^{\text{new}}) & \longrightarrow & \pi_1(K_{2n}^{\text{new}}) \\ & & \searrow & & \\ \pi_1(Y^{\text{new}}) & \xrightarrow[\partial_1^{\text{new}}]{} & \pi_0(R^{\text{new}}) & & \\ \wr\| & & \wr\| & & \\ \left(\mathbb{Z}^{2n}\times\mathbb{Z}_2^{2n}\right)\rtimes S_{2n} & & \mathbb{Z}^{2n}\times\mathbb{Z}_2. & & \end{array} \tag{C2}$$

where S_{2n} acts on $\mathbb{Z}^{2n}$ by permuting its standard generating set.

The new $\mathbb{Z}^{2n}$ factor in $\pi_0(R^{\text{new}})$ represents rolling the order parameter around the phase circle as one moves radially into the hedgehog. Similarly, the $\mathbb{Z}^{2n}$ in $\pi_1(Y^{\text{new}})$ comes from wrapping the whole hedgehog around the phase circle as the parameter is advanced. Clearly, the two $\mathbb{Z}^{2n}$'s cancel: $\ker(\partial_1^{\text{new}}) = \ker(\partial_1)$. Thus,

$$\pi_1(K_{2n}) \cong \pi_1(\widetilde{K}_{2n}) \times \mathbb{Z},$$

where the extra factor $\mathbb{Z}$ comes from a base point in B^3 and wraps around the additional circle $\frac{U(1)}{O(1)}$.

APPENDIX D: HOPF MAP—AN EXAMPLE OF BOUNDARY MAPS IN THE HOMOTOPY EXACT SEQUENCE

The Hopf fibration is an example of a fibration (of a fiber bundle, in fact) that arises in several contexts in physics. It consists of a map (the Hopf map) from S^3 to S^2 such that the preimage of each point in S^2 is an S^1. This is familiar from the representation of a vector (e.g., the Bloch sphere) by a spinor (e.g., a two-state system):

$$\mathbf{n} = z^\dagger \sigma z, \tag{D1}$$

where $\sigma = (\sigma_x, \sigma_y, \sigma_z)$ are Pauli matrices and the spinor

$$z = \begin{pmatrix} z_1 \\ z_2 \end{pmatrix} \tag{D2}$$

satisfies $|z_1|^2 + |z_2|^2 = 1$ so that $\mathbf{n}$ is a unit vector. Owing to this normalization condition, the spinor z lives in S^3 while the vector $\mathbf{n}$ lives in S^2. Transforming $z \to e^{i\theta} z$ leaves $\mathbf{n}$ invariant. Thus, the map (D1) maps circles in S^3 to points in S^2, as

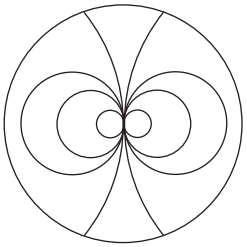

FIG. 14. The circle S^1 starts small, gets large, and becomes small again at the end of the "loop," that is, after it has swung all the way around the sphere S^2.

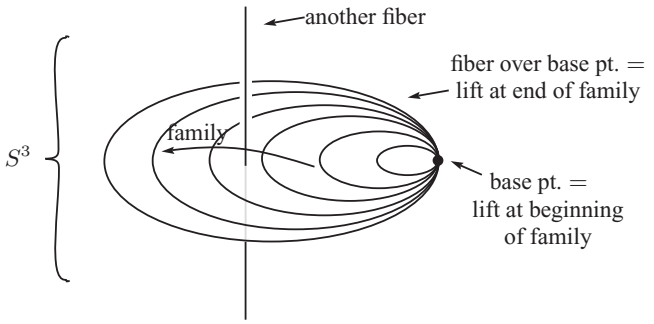

FIG. 15. The lifts of circles S^1 are depicted "upstairs" with respect to the usual picture of Hopf circles filling $\mathbb{R}^3$. The lift at the end of the family is the biggest ellipse in this picture, not a single point, unlike the lift at the beginning of the family. Thus, the loop of circles no longer closes when lifted.

depicted below:

$$\begin{array}{lcll} U(1)\text{ phase} = & S^1 \to S^3 & = \text{normalized states in } \mathbb{C}^2 \\ & \downarrow & \\ & S^2 & = \text{Bloch sphere} \end{array}$$

One context, quite closely related to the present discussion, in which the Hopf map arises is the O(3) nonlinear σ model in $(2+1)$ dimensions. The order parameter field $\mathbf{n}(x)$ is a map from S^3 to S^2 [assuming that $\mathbf{n}(x)$ is constant at infinity, so that space time can be compactified into S^3]. The topological term that can be added to such a model[54] is

$$S_H = -\frac{1}{2\pi}\int d^2x\, d\tau\, \epsilon^{\mu\nu\lambda} A_\mu F_{\nu\lambda}, \tag{D3}$$

where $F_{\nu\lambda} = \partial_\nu A_\lambda - \partial_\lambda A_\nu$ and

$$\epsilon^{\mu\nu\lambda}\partial_\nu A_\lambda \equiv \frac{1}{8\pi}\epsilon^{\mu\nu\lambda}\mathbf{n}\cdot\partial_\nu\mathbf{n}\times\partial_\lambda\mathbf{n}. \tag{D4}$$

This term gives the linking number of skyrmion trajectories in the O(3) nonlinear σ model. To see this, suppose that $\mathbf{n}(\infty) = (0,0,1)$. The preimage of $(0,0,-1)$ (which we may view as the centers of skyrmions) is a set of closed circles, and the Hopf term gives their linking number.

We can use the Hopf map to explain boundary maps in the homotopy exact sequence: $\pi_2(S^2) \xrightarrow[\cong]{\partial} \pi_1(S^1)$:

$$\begin{array}{ccccc} \pi_2(S^2) & \xrightarrow[\cong]{\partial} & \pi_1(S^1) & \longrightarrow & \pi_1(S^3) \\ \wr\| & & \wr\| & & \wr\| \\ \mathbb{Z} & & \mathbb{Z} & & 0. \end{array}$$

which, we see, must be an isomorphism to be consistent with $\pi_1(S^3) \cong 0$. But how is this boundary map defined? We think of a two-sphere S^2 as a loop of circles S^1, as depicted in Fig. 14.

Using the (defining) property of a fibration (see any book on algebraic topology), we may lift this loop of circles S^1 from the base S^2 to the total space S^3. The lifting is perfectly continuous, but it does not give us a sphere. Instead, it gives us a surface with boundary. This boundary is an S^1. What happens is that, at the very end of the loop of circles S^1, the lifting "explodes" the final circle S^1, whose map to the Bloch sphere

is shrinking to a point, into a circle in S^3, as pictured in Fig. 15. In other words, an element of $\pi_2(S^2)$ is lifted to a surface in S^3 whose boundary is a circle. This circle can wind around the fiber S^1, thus defining an element of $\pi_1(S^1)$. This map from an element of $\pi_2(S^2)$ to an element of $\pi_1(S^1)$ is called a *boundary map*, because the element of $\pi_1(S^1)$ is the boundary of the lift to S^3 of the corresponding element of $\pi_2(S^2)$.

APPENDIX E: COMPUTATION OF $\pi_0(R_{2n}),\pi_1(R_{2n})$ USING THE "POSTNIKOV TOWER" FOR $\widetilde{U/O}$

In this Appendix, we compute the homotopy groups $\pi_0(R_{2n}),\pi_1(R_{2n})$.

Recall that the homotopy classes of maps from a 3-manifold M^3 to S^2 can be understood in terms of the ribbons that are the (framed) inverse image of the north pole $N \subset S^2$. Such ribbons serve as generators for the path components of Maps$(M^3 \to S^2)$ and the relations are "framed cobordisms," that is, imbedded surfaces $(S; r_0, r_1) \subset (M^3 \times [0,1]; M \times 0, M \times 1)$, where S is a surface "coborder" between initial and final ribbons r_0 and r_1. S, like the ribbons themselves, has a normal framing which restricts to the oriented ribbon directions of both r_0 and r_1. This is a special case of what, in topology, is called the Pontryagin-Thom construction (PTC) (see Appendix F for more details).

Of course, there is more to $\widetilde{U/O}$ than the bottom S^2. Let us look next at the influence of the 3-cell D^3 on R_{2n}. Whereas $S^2 \setminus N$ is already contractible, to make $S^3 \bigcup_{\deg 2} D^3$ contractible, we must remove a diameter $\delta \subset D^3$ whose endpoints are glued to N. Making our maps f transverse to $\delta \subset D^3$ (and not just $N \subset S^2$ as would be ordinarily done in the PTC) we see that the ribbons (and their framed cobordisms) are now subject to a "singularity" at the f preimages of the origin $O \subset D^3$. The singularity is very mild: It is simply a point on the ribbon where the orientation (induced by comparing orientations on M^3 and S^2) longitudinally along the ribbon r_0 changes direction. The upshot is that the generators for $\pi_0(R_{2n})$ now consist of ribbons with no longitudinal arrows assigning a direction along the ribbon. [These generating ribbons are, of course, subject to the boundary condition that there are exactly $2n$ arc endpoints meeting each hedgehog exactly once at its marked point $f^{-1}(N)$.] Closed loops of ribbons may also arise. Because all maps from a 3-manifold deform into these lowest cells, $S^2 \bigcup_{\deg 2} D^3 \subset \widetilde{U/O}$, all generators of $\pi_0(R_{2n})$ are of this form.

Finding the relations defining $\pi_0(R_{2n})$ requires looking at maps of a four manifold $[Q \times I, \partial(Q \times I)]$ into $\widetilde{U/O}$. To study these by a variant of the PTC, we would need to take into account all cells up to dimension 4, $sk^4(\widetilde{U/O})$, the "4-skeleton." Similarly, a full analysis of $\pi_1(R_{2n})$ would require looking at $sk^5(\widetilde{U/O})$.

Fact E.1. $\pi_3(S^2 \bigcup_{\deg 2} D^3) \cong \mathbb{Z}_4$ and is generated by the Hopf map $h : S^3 \to S^2$.

Proof. The Whitehead exact sequence reads

$$H_4(X) \longrightarrow \Gamma(\pi_2(X)) \longrightarrow \pi_3(X) \xrightarrow{\text{Hurewicz}} H_3(X),$$

where Γ is Whitehead's quadratic functor. It is known that $\Gamma(\mathbb{Z}_2) \cong \mathbb{Z}_4$. If $X = S^2 \bigcup_{\deg 2} D^3$, the outer integral homology groups vanish, so $\pi_3(X) \cong \mathbb{Z}_4$ as claimed.

To see that the generator $g \in \pi_3(X)$ deforms to S^2, make it transverse to the origin $O \subset D^3$. Because D^3 is attached to S^2 with positive degree, the signed sum of inverse images $g^{-1}(O) = 0$. These may be paired and then removed by building a framed cobordism (see the PTC Appendix F) from $g^{-1}(O)$ to $\emptyset$ inside $S^3 \times [0,1]$. The map g' associated to the $S^3 \times 1$ level avoids $O \subset D^3$ and so may be radially deformed into S^2. ∎

Consequence E.2. $sk^4(\widetilde{U/O}) = S^2 \bigcup_{\deg 2} D^3 \bigcup_{2\text{Hopf}} D^4$

Proof. Consider the commutative diagram:

$$\begin{array}{ccccc} & & & & SO \\ & & & & \downarrow \text{fiber} \\ S^3 & \cong & SU(2) & \longrightarrow & SU \\ \text{Hopf map} \downarrow & & \text{coset} \downarrow & & \delta \downarrow \text{coset} \\ S^2 & \cong & \frac{SU(2)}{SO(2)} & \longrightarrow & \frac{SU}{SO} \end{array}$$

Applying the π_3 functor, we obtain

$$\begin{array}{ccc} \mathbb{Z} & \xrightarrow{\cong} & \mathbb{Z} \\ \downarrow \cong & & \downarrow \text{epimorphism} \\ \mathbb{Z} & \xrightarrow{\text{epimorphism}} & \mathbb{Z}_2 \end{array}$$

From the homotopy exact sequence of

$$\begin{array}{ccc} SO & \to & SU \\ & & \downarrow \\ & & \frac{SU}{SO} \cong \widetilde{U/O}, \end{array}$$

we can see that

$$\begin{array}{ccccccc} \pi_3(SO) & \xrightarrow{\times 2} & \pi_3(SU) & \longrightarrow & \pi_3(\frac{SU}{SO}) & \longrightarrow & \pi_2(SO) \\ \wr\| & & \wr\| & & \wr\| & & \wr\| \\ \mathbb{Z} & & \mathbb{Z} & & \mathbb{Z}_2 & & 1 \end{array}$$

and we conclude that δ is an epimorphism. Thus, the Hopf map, which is order 4 in X, needs a 4-cell to be attached in order to make it order 2 in $\widetilde{U/O}$. ∎

We will not need this, but for the curious, $sk^5(\widetilde{U/O})$ requires one additional 5-cell that maps degree 2 over the 4-cell.

As remarked, studying maps *into* cell structures becomes laborious. Homotopy theory works best when studying maps *out of* cell structures and into fibrations. So, let us introduce the two-stage Postnikov tower for $\widetilde{U/O}$.

The notation $K(\pi,n)$ is used for any connected space (generally infinite dimensional) that has only a single nontrivial homotopy group, $\pi_n(K(\pi,n)) = \pi$. It is easy to show that the homotopy type of $K(\pi,n)$ is unique. At the next stage of complexity come spaces Z with two nontrivial homotopy groups, say, $\pi_m(Z) = A$ and $\pi_n(Z) = B$, $m < n$. Such spaces

(for simplicity we now assume $m \geqslant 2$) have a homotopy type determined by the total space T of a fibration called a *two-stage Postnikov Tower*:

$$\begin{array}{ccc} K(n,B) & \longrightarrow & T \\ \text{(fiber)} & & \downarrow \\ & & K(m,A)\ \text{(base)} \end{array}$$

To completely specify how the fibration twists and the homotopy type of T we need to specify the "k" invariant $k \in H^{n+1}(K(m,A);B)$.

The space $K(m,A)$ classifies cohomology in the sense that for any space S, the homotopy classes of maps $[S,K(m,A)]$ naturally biject with $H^m(S;A)$. [There is a "fundamental" class $\iota \in H^m(K(m,A);A)$ so that for $f : S \to K(m,A)$ we associate $f^*\iota \in H^m(S;A)$.] Thus, the k invariant is really a map:

$$k : K(m,A) \to K(n+1,B),$$

and T is the pullback of the path loop fibration over $K(n+1,B)$:

$$\begin{array}{ccc} \Omega K(n+1,B) = K(n,B) & \longrightarrow & \text{pt.} \\ & & \downarrow \\ & & K(n+1,B) \end{array}$$

$$\begin{array}{ccc} K(n,B) & & K(n,B) \\ \downarrow & & \downarrow \\ T & \longrightarrow & \text{pt.} \\ \downarrow & & \downarrow \\ K(m,A) & \xrightarrow{k} & K(n+1,B) \end{array}$$

where we have denoted the contractible space of paths in $K(n+1,B)$ starting at its base point by its homotopy model, a single point, pt.

For spaces with many homotopy groups, the Postnikov tower can be continued iteratively.

In our case, $\pi_i(\widetilde{U/O}) = 0,\mathbb{Z}_2,\mathbb{Z}_2,0$ for $i = 1,2,3,4$, so a two-stage tower is adequate for computing $\pi_i(R)$ for $i = 0,1$. Thus, our model T for $\widetilde{U/O}$ is now a fibration:

$$\begin{array}{ccc} K(\mathbb{Z}_2,3) & \longrightarrow & T \\ & & \downarrow \\ & & K(\mathbb{Z}_2,2) \end{array}$$

Similar to the previously computed cell structure of $\widetilde{U/O}$, the cells of $K(\mathbb{Z}_2,2)$ through dimension $\leqslant 3$ are the same. But for $K(\mathbb{Z}_2,2)$, the 4-cell kills the Hopf map and the 5-cell is now degree 4 over the 4-cell. The cell complex for $K(\mathbb{Z}_2,2)$ begins as follows:

$$\begin{array}{ccccccccccc} C_5 & \longrightarrow & C_4 & \longrightarrow & C_3 & \longrightarrow & C_2 & \longrightarrow & C_1 \\ \wr\| & & \wr\| & & \wr\| & & \wr\| & & \wr\| \\ \mathbb{Z} & \xrightarrow{\times 4} & \mathbb{Z} & \xrightarrow{0} & \mathbb{Z} & \xrightarrow{\times 2} & \mathbb{Z} & \longrightarrow & 0 \end{array}$$

The $\mathbb{Z}_2$ cohomology is then the homology of the hom sequence of this chain complex into $\mathbb{Z}_2$:

$$\mathbb{Z}_2 \xleftarrow{0} \mathbb{Z}_2 \xleftarrow{0} \mathbb{Z}_2 \xleftarrow{0} \mathbb{Z}_2 \longleftarrow 0.$$

Thus, one finds that $H^4(K(\mathbb{Z}_2,2);\mathbb{Z}_2) \cong \mathbb{Z}_2$, so there are only two possible fibrations (up to homotopy type) as above, the product $K(\mathbb{Z}_2,2) \times K(\mathbb{Z}_2,3)$ and a "twisted product." Fact E.1 says that $\pi_3(T)$ actually comes by composing the Hopf map into the (2-sphere inside the) base $K(\mathbb{Z}_2,2)$. This is clearly false for the product where that composition would factor through $\pi_3(K(\mathbb{Z}_2,2)) \cong 1$. This shows that the model T for $\widetilde{U/O}$ has nontrivial k invariant.

If X is a space and

$$\begin{array}{ccc} F & \to & E \\ & & \downarrow \\ & & B \end{array}$$

is a fibration, then there is a corresponding fibration of the space of maps:

$$\begin{array}{ccc} \mathcal{M}(X,F) & \to & \mathcal{M}(X,E) \\ & & \downarrow \\ & & \mathcal{M}(X,B) \end{array}$$

(We now use the usual comma instead of "$\to$" in the notation for map spaces.) This is our main tool; it enables us to tear apart maps into T into maps into $K(\mathbb{Z}_2,2)$ and $K(\mathbb{Z}_2,3)$, which are easy things to compute, namely, cohomology groups. A small wrinkle is that because of the boundary conditions we will study relative maps and end up with relative cohomology groups, but these are also easily computed.

So, let us now return to the computation of $\pi_0(R_{2n})$. We study the fibration:

$$\begin{array}{ccc} R3 & \to & R \\ & & \downarrow \\ & & R2 \end{array}$$

where R is our original R_{2n} (the subscript $n \geqslant 0$ is suppressed). $R2$ is the space Maps$(Q \to K(\mathbb{Z}_2,2))$ with rigid boundary conditions [from ∂Q to $S^2 \subset K(\mathbb{Z}_2,2)$] analogous to R but with maps to T replaced with maps to its base space $K(\mathbb{Z}_2,2)$. Similarly, $R3$ is Maps$(Q \to K(\mathbb{Z}_2,3))$ with ∂Q mapping to the base point of $K(\mathbb{Z}_2,3)$. We have from the homotopy exact sequence:

$$\begin{array}{ccccccc} \pi_1(R2) & \xrightarrow{\partial_1} & \pi_0(R3) & \to & \pi_0(R) & \to & \pi_0(R2) \\ & & \wr\| & & \wr\| & & \\ & & H^3(Q,\partial Q;\mathbb{Z}_2) & & H^2(Q,\partial Q;\mathbb{Z}_2) \cong H_1(Q;\mathbb{Z}_2) & & \\ & & \wr\| & & \nearrow \cong 1 & & \\ & & \mathbb{Z}_2 & & \text{Poincare duality} & & \end{array}$$

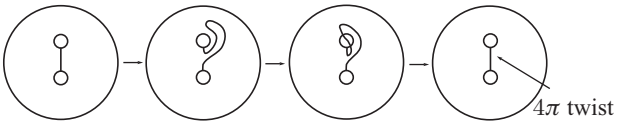

FIG. 16. By pulling a ribbon over a hedgehog and "lassoing" it, a 4π twist is performed.

The boundary map is always zero for product fibrations, but in this case, it is potentially affected by the k invariant (coming from the k invariant of T).

Following the usual procedure, ∂_1 may be understood as the "twist" (mod 2) in a ribbon induced by the "lasso move" shown in Fig. 16, which is well known to be 4π.

Because 4π is an even multiple of 2π, ∂_1 is in fact zero and $\pi_0(R) \cong \mathbb{Z}_2$. The two components can, on the level of framed ribbons, be identified with a total twisting of ribbons being an *even* or *odd* multiple of 2π.

$\pi_1(R)$ may be similarly computed:

$$\begin{array}{ccccccc}
\cdots & \longrightarrow & \pi_1(R3) & \longrightarrow & \pi_1(R) & \longrightarrow & \pi_1(R2) \longrightarrow \cdots \\
 & & \wr\| & & & & \wr\| \\
 & & H^3(Q\times I, \partial(Q\times I);\mathbb{Z}_2) & & & & H^2(Q\times I, \partial(Q\times I);\mathbb{Z}_2) \\
 & & \wr\| & \longleftarrow \text{Poincare duality} \longrightarrow & & & \wr\| \\
 & & H^1(Q\times I;\mathbb{Z}_2) & & & & H_2(Q\times I;\mathbb{Z}_2) \\
 & & \wr\| & & & & \wr\| \\
 & & 1 & & & & \mathbb{Z}_2^{2n}
\end{array}$$

Thus, $\pi_1(R) \cong \mathbb{Z}_2^{2n}$. Intuitively, $\pi_1(R)$ is represented by 2D "bags" or homology classes that a loop of ribbons, defining an element of $\pi_1(R)$, sweeps out in $Q \times I$.

APPENDIX F: PONTRYAGIN-THOM CONSTRUCTION

Homotopy classes $[M^d, S^k]$ may be studied geometrically. The idea is to make any map $f : M^d \to S^k$ transverse to a base point $N \in S^k$. Then $f^{-1}(N)$ is a $(d-k)$-dimensional submanifold K of M^d equipped with a framing of its normal bundle obtained by pulling back a fixed normal k frame to N. This construction is reversible: Given a submanifold with normal framing $K^{d-k} \subset M$, there is a map $f : M^d \to S^k$ that wraps an ϵ neighborhood η of K over S^k by using polar coordinates around the north pole N and the framing to send each normal $D^k_\epsilon \subset \eta$ degree $= 1$ over S^k and sends the rest of $M \setminus \eta$ to the south pole in S^k.

This discussion can be relativized. A homotopy $F : M \times [0,1] \to S$, $F|_{M\times 0} = f$, $F|_{M\times 1} = g$ yields by inverse image $\overline{K}$ of N a "framed cobordism" from $K_0 \subset M \times 0$ to $K_1 \subset M \times 1$, that is, a manifold $\overline{K}^{d-k+1} \subset M \times [0,1]$ with a normal k framing that restricts at 0(1) to $K_{0(1)}$ and its normal k framing.

The maps to S^k that are produced from a framed submanifold may seem extreme and unrepresentative because most points map to the south pole. However, the beauty of the construction is that, because $S^k \setminus N$ is contractible, no real choice (up to homotopy) exists for the part of the map that avoids N. Thus we have the following:

Fact F.1. The space of maps $\mathcal{M}(M^d, S^k)$ is (at least weakly) homotopy equivalent to the space of framed submanifolds $\{L^{d-k} \subset M^d\}$ (provided both are given reasonable topologies).

Fact F.2. Fact F.1 holds in a relative setting, e.g., the $\{\text{space of homotopies}\} \overset{\text{weakly}}{\simeq} \{\text{space of framed cobordisms}\}$. For example, merely on the level of π_0, this says that "homotopy classes of maps (M^d, S^k) are in 1-1 correspondence with framed cobordism classes of framed submanifolds $K^{d-k} \subset M^d$."

This basic PTC may be generalized to maps (N^d, M^k) whenever we can identify a "spine" $X \subset M^k$ so that $M \setminus X$ is contractible. One then studies $f^{-1}(X)$ [actually f^{-1}(a germ of X) corresponding to the old framing data] instead of $f^{-1}(N)$. For this approach to be practical, X and its neighborhood have to be fairly simple. In this extended setting, one must also keep track of the maps $f| : [f^{-1}(X)] \to X$ because this is no longer unique.

APPENDIX G: MULTIPLICATION TABLE FOR $\pi_1(K_{2n})$

We have shown $\mathcal{T}_{2n} = \pi_1(K_{2n}) \cong \mathbb{Z} \times \mathbb{Z}_2 \times G_{2n}$ and a short exact sequence (SES):

$$1 \longrightarrow G_{2n} \longrightarrow \mathbb{Z}_2^{2n} \rtimes S_{2n} \xrightarrow{\text{total parity}} \mathbb{Z}_2 \longrightarrow 1$$

Thus, we have another SES:

$$1 \longrightarrow \mathbb{Z}_2^{2n-1} \longrightarrow G_{2n} \underset{s}{\rightleftarrows} S_{2n} \longrightarrow 1$$

with a merely set theoretic section s. However, using s (line 3.5 of Ref. 57) we can write the multiplication table out for G_{2n}, hence $\pi_1(K_{2n})$ in terms of a twisted 2-cocycle f on S_{2n}:

$$(a,g)(b,h) = [a + g \cdot b + f(g,h), gh], \tag{G1}$$

where $a \in \mathbb{Z}_2^{2n}$, $g,h \in S_{2n}$. g acts on $\mathbb{Z}_2^{2n-1}$ by including $\mathbb{Z}_2^{2n-1} \subset \mathbb{Z}_2^{2n}$ as the "even" vectors and letting g permute the factors of $\mathbb{Z}_2^{2n}$. It only remains to determine a twisted cocycle $f \in H^2(S_{2n}; \mathbb{Z}_2^{2n-1})$, where the action of S_{2n} on $\mathbb{Z}_2^{2n-1}$ is as above. The cohomology class represented by f is nonzero because the exact sequence does not split. As a check, we know (line 3.10 in Ref. 57) that f should obey

$$g(f(h,k)) - f(gh,k) + f(g,hk) - f(g,k) = 0. \tag{G2}$$

Claim. $f(g,h) = 0$ if g or h is even and $f(g,h) = e_{g(1)}$ if g and h are both odd, where $e_{g(1)}$ is the $g(1)$th standard generator of $\mathbb{Z}_2^{2n}$.

APPENDIX H: "GHOSTLY RECOLLECTION" OF THE BRAID GROUP

To promote the Teo-Kane representation to a linear representation of the braid group $\mathcal{B}_m$, we have the freedom to introduce an overall Abelian phase to each $T_{i,j}$. There are several different choices related to different physical systems. For our purpose here, any choice suffices. The different choices lead to different linear images of the braid groups as the braid generator matrix has different orders.

The Ising topological quantum field theory (TQFT) can be realized using the Kauffman bracket by choosing $A = ie^{-\frac{2\pi i}{16}}$. The braid group representation from a TQFT is not well defined as a matrix representation because in general we do not have a canonical choice of the basis vectors.

In the Kauffman bracket formulation of the Ising TQFT, bases of representation spaces can be constructed using linear combinations of Temperley-Lieb (TL) diagrams or trivalent graphs. Then the representation of the braid groups is given by the Kauffman bracket, interpreted as a map from $\mathcal{B}_m$ to units of TL algebra.

The Temperley-Lieb-Jones algebra $\mathrm{TL}_m(A)$ at the above chosen A is isomorphic to the Clifford algebra. Therefore the γ matrices $\{\gamma_i\}$ can be represented by TL generators $\{U_i\}$. In terms of the γ matrices, the Jones representation in Kauffman bracket normalization is

$$\rho_A(\sigma_i) = e^{-\frac{3\pi i}{8}} e^{-\frac{\pi}{4}\gamma_i\gamma_{i+1}}.$$

The Jones original representation from von Neumann algebra is

$$\rho_A^J(\sigma_i) = e^{\frac{\pi i}{4}} e^{-\frac{\pi}{4}\gamma_i\gamma_{i+1}}.$$

We will also refer to the $T_{i,i+1}$ representation of the braid group

$$\rho_A^\gamma(\sigma_i) = e^{-\frac{\pi}{4}\gamma_i\gamma_{i+1}}$$

as the γ-matrix representation.

The ratio of the two distinct eigenvalues of the braid generator is $-i$, independent of the overall Abelian phase. The orders of the braid generator matrices in the three normalizations are 16,4,8, respectively. In the following, we will focus on the Jones representation.

Let $q = A^{-4} = i$, then the Kauffman bracket is $\rho_A(\sigma_i) = \langle\sigma_i\rangle = A + A^{-1}U_i$, where U_i's are the TL generators. For convenience, we introduce the Jones generators of the TL algebras $e_i = \frac{U_i}{d}, d = \sqrt{2}, i = 1,\ldots,m-1$. These e_i's should not be confused with the basis element e_i's of $\mathbb{R}^m$. The TL algebra in terms of e_i's is

$$e_i^\dagger = e_i, \quad e_i^2 = e_i, \quad e_i e_{i\pm1} e_i = \frac{1}{d^2} e_i.$$

The Jones representation is $\rho_A^J(\sigma_i) = -A\rho_A(\sigma_i) = -1 + (1+q)e_i$. Let $x_i\langle\sigma_i^2\rangle$. Then we have $x_i^2 = 1$, $x_i x_j = x_j x_i$ if $|i-j| > 1$, and $x_i x_{i+1} = -x_{i+1}x_i$. The -1 in the relation $x_i x_{i+1} = -x_{i+1}x_i$ is from the Jones-Wenzl projectors $p_3 = 0$. By a simple calculation, the Jones-Wenzl projector p_3 in terms of $\{e_i, e_{i+1}\}$ is $p_3 = 1 + 2(e_i e_{i+1} + e_{i+1}e_i - e_i - e_{i+1})$, and $x_i x_{i+1} + x_{i+1}x_i = 2p_3$.

Note that $\{x_i = 1 - 2e_i, i = 1,\ldots,m-1\}$ generate $\mathrm{TL}_m(A)$. Write x_i in terms of γ matrices, we have $x_i = \sqrt{-1}\gamma_i\gamma_{i+1}$, which identifies $TL_m(A)$ with the even part $\mathrm{Cl}_m^0(\mathbb{C})$ of $\mathrm{Cl}_m(\mathbb{C})$. On the other hand, if we set $v_i = (\sqrt{-1})^{i-1}x_i\cdots x_1, i = 1,\ldots,m-1$, a direct computation shows that $v_i^\dagger = v_i, v_i v_j + v_j v_i = 2\delta_{i,j}$. Therefore, $\{v_i, i = 1,\ldots,m-1\}$ form the Clifford algebra $\mathrm{Cl}_{m-1}(\mathbb{C})$. Of course, the two different realizations $\mathrm{TL}_m(A)$ as Clifford algebras are just the well known isomorphism $\mathrm{Cl}_m^0(\mathbb{C}) \cong \mathrm{Cl}_{m-1}\mathbb{C})$.

To identify the image of the Jones representation, we use the exact sequence $1 \to \mathrm{PB}_m \to \mathcal{B}_m \to S_m \to 1$. The image of the pure braid group PB_m is generated by $\{x_i\}$. As an abstract group, the group can be presented with generators $x_i, i = 1,\ldots,x_{m-1}$ and relations $x_i^2 = 1$, $x_i x_j = x_j x_i$ if $|i-j| > 1$, and $x_i x_{i+1} = -x_{i+1}x_i$. This group, called the nearly-extra-special 2-group in Ref. 67 and denoted as E_{m-1}^1, is of order $2^m m!$. Consequently, the image $\tilde{G}_m$ of the Jones representation of $\mathcal{B}_m$ fits into the exact sequence $1 \to E_{m-1}^1 \to \tilde{G}_m \to S_m \to 1$. If we projectivize this sequence, we have $1 \to \mathbb{Z}_2^{m-1} \to G_m \to S_m \to 1$. (This sequence splits if and only if m is odd.) In this sense, the ribbon permutation group is a "ghostly recollection" of the braid group.

The center $Z(E_{m-1}^1)$ of E_{m-1}^1 is $\mathbb{Z}_2 = \{\pm1\}$ if m is even, and $\mathbb{Z}_2 \times \mathbb{Z}_2 = \{\pm1, \pm x_1x_3\cdots x_{m-1}\}$ if m is odd. The representation of E_{m-1}^1 is faithful, but when m is even, none of the irreducible sector is faithful because the central element $\pm x_1x_3\cdots x_{m-1}$ acts by ±1, too. The action of x_i on the two irreducible sectors are the same for $i = 1,2,\ldots,m-2$ and differs only on x_{m-1}, which is ±1. When projectivized, note that the element $\alpha = (11\cdots1) \in \mathbb{Z}_2^m$, as an element in $\mathbb{Z}_2^{m-1}$, is invariant under the action of S_m, hence the projective image of each irreducible sector is isomorphic to $\mathbb{Z}_2^{m-2}$.

As comparison, we mention the related result in Ref. 25. The Jones representation there is in the γ-matrix normalization. The pure braid generators are of order 4. Hence the pure braid group image is a variant E_{m-1}^{-1} of E_{m-1}^1. The generators of the two groups are related by the change of x_i to $-\sqrt{-1}x_i$. A presentation of E_{m-1}^{-1} with generators $x_i, i = 1,\ldots,x_{m-1}$ has relations $x_i^2 = -1$, $x_i x_j = x_j x_i$ if $|i-j| > 1$, and $x_i x_{i+1} = -x_{i+1}x_i$. The center $Z(E_{m-1}^{-1})$ is more complicated: $\mathbb{Z}_2$ if m is odd, and $\mathbb{Z}_2 \times \mathbb{Z}_2$ if $m = 4k+1$ and $\mathbb{Z}_4$ if $m = 4k+3$. When m is even, the image of each irreducible sector is identified as the lifting of G_m to $\mathrm{Spin}(m)$.[25] It follows from the above discussion, the linear image of the Jones representation in γ-matrix normalization fits into the exact sequence $1 \to \mathbb{Z}_4 \times E_{m-1}^1 \to \mathbb{Z}_8 \times \tilde{G}_m \to \mathbb{Z}_2 \times S_m \to 1$, where $\tilde{G}_m$ is the image of $\mathcal{B}_m$ above.

[1] J. M. Leinaas and J. Myrheim, Nuovo Cimento B **37**, 1 (1977).
[2] F. Wilczek, Phys. Rev. Lett. **48**, 1144 (1982).
[3] F. A. Bais, Nucl. Phys. B **170**, 32 (1980).
[4] G. A. Goldin, R. Menikoff, and D. H. Sharp, Phys. Rev. Lett. **54**, 603 (1985).
[5] J. Fröhlich and F. Gabbiani, Rev. Math. Phys. **2**, 251 (1990).
[6] A. Y. Kitaev, Ann. Phys. (NY) **303**, 2 (2003).
[7] C. Nayak, S. H. Simon, A. Stern, M. Freedman, and S. Das Sarma, Rev. Mod. Phys. **80**, 1083 (2008).
[8] G. Moore and N. Read, Nucl. Phys. B **360**, 362 (1991).
[9] C. Nayak and F. Wilczek, Nucl. Phys. B **479**, 529 (1996).
[10] S.-S. Lee, S. Ryu, C. Nayak, and M. P. A. Fisher, Phys. Rev. Lett. **99**, 236807 (2007).
[11] M. Levin, B. I. Halperin, and B. Rosenow, Phys. Rev. Lett. **99**, 236806 (2007).
[12] P. Bonderson and J. K. Slingerland, Phys. Rev. B **78**, 125323 (2008).
[13] N. Read and D. Green, Phys. Rev. B **61**, 10267 (2000).
[14] D. A. Ivanov, Phys. Rev. Lett. **86**, 268 (2001).
[15] A. Y. Kitaev, Ann. Phys. (NY) **321**, 2 (2006).
[16] L. Fu and C. L. Kane, Phys. Rev. Lett. **100**, 096407 (2008).

[17] J. D. Sau, R. M. Lutchyn, S. Tewari, and S. Das Sarma, Phys. Rev. Lett. **104**, 040502 (2010).
[18] S. Doplicher, R. Haag, and J. E. Roberts, Commun. Math. Phys. **23**, 199 (1971).
[19] S. Doplicher, R. Haag, and J. E. Roberts, Commun. Math. Phys. **35**, 49 (1974).
[20] J. C. Y. Teo and C. L. Kane, Phys. Rev. Lett. **104**, 046401 (2010).
[21] J. E. Moore and L. Balents, Phys. Rev. B **75**, 121306 (2007).
[22] L. Fu, C. L. Kane, and E. J. Mele, Phys. Rev. Lett. **98**, 106803 (2007).
[23] R. Roy, Phys. Rev. B **79**, 195322 (2009).
[24] X.-L. Qi, T. L. Hughes, and S.-C. Zhang, Phys. Rev. B **78**, 195424 (2008).
[25] N. Read, J. Math. Phys. **44**, 558 (2003).
[26] A. P. Schnyder, S. Ryu, A. Furusaki, and A. W. W. Ludwig, Phys. Rev. B **78**, 195125 (2008).
[27] V. Lebedev and M. Feigel'man (eds.), Advances in Theoretical Physics: Landau Memorial Conference, Chernoyolovka, Russia, 22–26 June 2008, AIP Conf. Proc. 1134; A. Kitaev, e-print arXiv:0901.2686.
[28] J. Milnor, *Morse Theory* (Princeton University Press, Princeton, NJ, 1963).
[29] N. D. Mermin, Rev. Mod. Phys. **51**, 591 (1979).
[30] F. Wilczek, e-print arXiv:hep-th/9806228.
[31] D. S. Rokhsar and S. A. Kivelson, Phys. Rev. Lett. **61**, 2376 (1988).
[32] S. Ryu, C. Mudry, C. Y. Hou, and C. Chamon, Phys. Rev. B **80**, 205319 (2009).
[33] C. Nayak, Phys. Rev. B **62**, 4880 (2000).
[34] M. Stone, C.-K. Chiu, and A. Roy, e-print arXiv:1005.3213.
[35] M. R. Zirnbauer, J. Math. Phys. **37**, 4986 (1996).
[36] A. Altland and M. R. Zirnbauer, Phys. Rev. B **55**, 1142 (1997).
[37] M. Fujita, K. Wakabayashi, K. Nakada, and K. Kusakabe, J. Phys. Soc. Jpn. **65**, 1920 (1996).
[38] K. Nakada, M. Fujita, G. Dresselhaus, and M. S. Dresselhaus, Phys. Rev. B **54**, 17954 (1996).
[39] R. Roy, e-print arXiv:cond-mat/0608064.
[40] X.-L. Qi, T. L. Hughes, S. Raghu, and S.-C. Zhang, Phys. Rev. Lett. **102**, 187001 (2009).
[41] C. L. Kane and E. J. Mele, Phys. Rev. Lett. **95**, 226801 (2005).
[42] C. L. Kane and E. J. Mele, Phys. Rev. Lett. **95**, 146802 (2005).
[43] B. A. Bernevig and S. C. Zhang, Phys. Rev. Lett. **96**, 106802 (2006).
[44] B. A. Bernevig, T. L. Hughes, and S. C. Zhang, Science **314**, 1757 (2006).
[45] M. König, S. Wiedmann, C. Brüne, A. Roth, H. Buhmann, L. Molenkamp, X.-L. Qi, and S.-C. Zhang, Science **318**, 766 (2007).
[46] L. Fu and C. L. Kane, Phys. Rev. B **76**, 045302 (2007).
[47] D. Hsieh, D. Qian, L. Wray, Y. Xia, Y. S. Hor, R. J. Cava, and M. Z. Hasan, Nature (London) **452**, 970 (2008).
[48] H. Zhang, C.-X. Liu, X.-L. Qi, X. Dai, Z. Fang, and S.-C. Zhang, Nat. Phys. **5**, 438 (2009).
[49] Y. Xia, L. Wray, D. Qian, D. Hsieh, A. Pal, H. Lin, A. Bansil, D. Grauer, Y. Hor, R. Cava, and M. Hasan, Nat. Phys. **5**, 398 (2009).
[50] Y. L. Chen, J. G. Analytis, J.-H. Chu, Z. K. Liu, S.-K. Mo, X. L. Qi, H. J. Zhang, D. H. Lu, X. Dai, Z. Fang, S. C. Zhang, I. R. Fisher, Z. Hussain, and Z.-X. Shen, Science **325**, 178 (2009).
[51] R. Roy, e-print arXiv:0803.2868.
[52] A. P. Schnyder, S. Ryu, and A. W. W. Ludwig, Phys. Rev. Lett. **102**, 196804 (2009).
[53] J. C. Y. Teo and C. L. Kane, Phys. Rev. B **82**, 115120 (2010).
[54] F. Wilczek and A. Zee, Phys. Rev. Lett. **51**, 2250 (1983).
[55] W. Magnus, A. Karrass, and D. Solitar, *Combinatorial Group Theory: Presentations of Groups in Terms of Generators and Relations* (Dover, Mineola, NY, 2004) (reprint of the 1976 second edition).
[56] V. F. R. Jones, *Geometric Methods in Operator Algebras (Kyoto, 1983)*, Vol. 123 of *Pitman Res. Notes Math. Ser.* (Longman Sci. Tech., Harlow, 1986), pp. 242–273.
[57] K. S. Brown, *Cohomology of Groups*, Vol. 87 of *Graduate Texts in Mathematics* (Springer, New York, 1982).
[58] We note that neither Teo and Kane's arguments (Ref. 20) nor ours determine the phase θ. In a 2D system of anyons, it is not an arbitrary phase. For instance, in a system of Ising anyons, θ must be equal to $\pi/8$. Any value of θ which is not a 16th root of unity necessarily implies that the theory has additional structure and, therefore, additional particle types.
[59] J. Alicea, Y. Oreg, G. Refael, F. von Oppen, and M. P. A. Fisher, e-print arXiv:1006.4395.
[60] R. Lutchyn, J. D. Sau, and S. Das Sarma, e-print arXiv:1002.4033.
[61] Y. Oreg, G. Refael, and F. von Oppen, e-print arXiv:1003.1145.
[62] J. D. Sau, S. Tewari, R. Lutchyn, T. Stanescu, and S. Das Sarma, e-print arXiv:1006.2829.
[63] D. J. Clarke, J. D. Sau, and S. Tewari, e-print arXiv:1012.0296.
[64] J. D. Sau, D. J. Clarke, and S. Tewari, e-print arXiv:1012.0561.
[65] M. H. Freedman *et al.* (unpublished).
[66] J. Roe, *Index Theory, Coarse Geometry, and Topology of Manifolds*, Vol. 90 of *CBMS Regional Conference Series in Mathematics* (Conference Board of the Mathematical Sciences, Washington, D.C., 1996), pp. x+100.
[67] J. M. Franko, E. C. Rowell, and Z. Wang, J. Knot Theory Ramifications **15**, 413 (2006).